NEW TRENDS IN ENGINEERING

SELÇUK UNIVERSITY INTERNATIONAL

TECHNOLOGY AND INNOVATION

STUDENT SYMPOSIUM

24-27 NOVEMBER 2022 KONYA

EDITORS

Prof. Dr. Süleyman NEŞELİ

Asst. Prof. Dr. Hakan TERZİOĞLU

NEW TRENDS IN ENGINEERING

EDITORS

Prof. Dr. Süleyman NEŞELİ

Asst. Prof. Dr. Hakan TERZİOĞLU

NEW TRENDS IN ENGINEERING

EDITORS

Prof. Dr. Süleyman NEŞELİ
Asst. Prof. Dr. Hakan TERZİOĞLU

tablet kitabevi

T.C. KÜLTÜR BAKANLIĞI
YAYINCI SERTİFİKASI: 46644

EBOOK ISBN: 978-605-5447-74-8

Konya Aralık - 2022

CONTENTS

CHAPTER 1

STUDENT PERFORMANCE MODELING APPROACHES: A REVIEW OF EDUCATIONAL DATA MINING STUDIES

Esma ÖZEL[1]
[1]Selcuk University, Konya/Turkey
ORCID: 0000-0001-9806-3883

Onur İNAN[2]
[2]Selcuk University, Konya/Turkey
ORCID: 0000-0003-4573-7025

Hakan TERZİOĞLU[3]
[3]Selcuk University, Konya/Turkey
ORCID: 0000-0001-5928-8457

INTRODUCTION

Computer and network technologies have facilitated the rapid storage of data, which has led to millions of data being generated every day. This growing data set requires analyzing and transforming into information with help of powerful and versatile tools. This need brings Data Mining (DM) to come to the fore. Discovering the structures and patterns in big and complicated datasets is mainly what DM is for. Gartner Inc. defined DM comprehensively as "Data mining is the process of discovering meaningful correlations, patterns, and trends by sifting through large amounts of data stored in repositories. Data mining employs pattern recognition technologies, as well as statistical and mathematical techniques." (Inc., 2022).

Talking about big data, educational institutions are home to various complex raw data. In an educational environment, continuous monitoring of student or educator activities is required to provide quality education. However, with big amounts of data in educational databases, this aim is hard to achieve, so big data and data mining technology emerge to solve these problems. Educational Data Mining (EDM) definition is in use for DM applications in the education is recognized as.

In EDM, there are various objectives to achieve, for example, improving learning quality by guiding educators and students, and a better understanding of the learning process. Using data repositories, EDM strives to modify the practice to benefit learners through the integration of data and theory. Many different data and their relationships are available in educational institutions to use all types of data mining techniques. The education sector benefits from the conversion of educational data into useful information. Prediction of student performance provides responsible educators with practical teaching approaches, thereby helping to strengthen the education sector. The following objectives are intended to be achieved through this study:

1. To find out which tools are preferred in reviewed EDM studies.
2. Determining which DM methods are used to predict student performance.
3. To identify commonly selected keywords for EDM studies.
4. To take a glance at the datasets used.
5. Determining the most accurate DM method to predict student performance.

In section II we presented the background of the EDM process; in section III we presented the methodology of the review process of the studies; in section IV we discussed the results, and the conclusion and future work is presented in section V.

LITERATURE REVIEW

Data mining in the education sector is predominantly used to predict, group, model, and monitor various learning activities using techniques such as classification, clustering, association rules, statistics, and visualization (Aldowah, Al-Samarraie, & Fauzy, 2019). EDM is a process for addressing important educational questions using DM techniques applied to specific datasets originating from educational environments (Romero & Ventura, 2013). In Romero and Ventura's review (2013) on EDM, they figured out a cycle (Figure 1) about how DM in educational environments is applied. The items in EDM lifecycle have educational systems as source of data; ie traditional classrooms, e-Learning environments, data mining tools and methods; ie Python, Weka, RapidMiner, etc. and classification, clustering and directions of meaningful information gained are students, educators and responsible administrators.

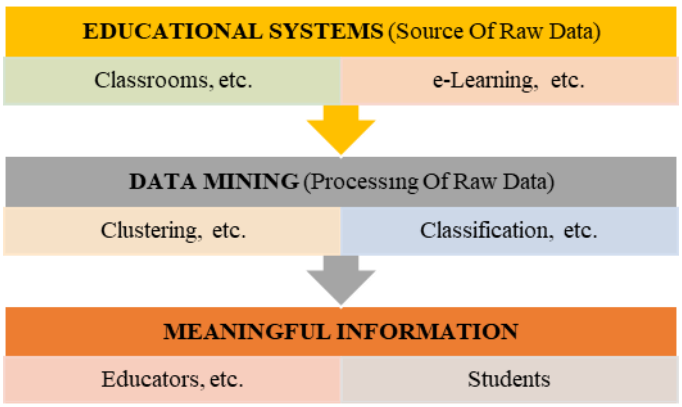

Figure 1: Phases of EDM

It is possible to reach many studies using Machine Learning (ML) methods in the field of education, and these studies have played a key role in identifying the deficiencies and errors in the field and giving advice to learners and teachers. N. D. Lynn and A.W.R. Emanuel (2021)

reviewed the EDM studies between 2010 to 2020 and sorted them by their overall prediction accuracy. According to the results, the best performer method was the Decision Trees (DT) with an accuracy of (98%), following Naïve Bayes (NB) with an accuracy of (97%) (Lynn & Emanuel, 2021). A. Tekin and Z. Öztekin (2018) reviewed the EDM studies in Türkiye between 2006 and 2016, and they concluded that the data analysis methods in these studies were mostly classification and clustering (TEKİN & ÖZTEKİN, 2018). A. Peña-Ayala (2014), reviewed and summarized 240 EDM related studies, and they discussed functionalities of them by strengths, weaknesses, opportunities, and threats (Peña-Ayala, 2014). K. Akgün and M. Bulut Özek (2020), studied 102 EDM related articles and find out the most frequently used DM techniques were decision trees and artificial neural networks (Akgün & Bulut Özek, 2020). A.Khan and S.K. Ghosh (2021) studied on 140 papers related to student performance in classroom learning and the study found out that the early prediction before course commencement is in need of more work (Khan & Ghosh, 2021). H. Aldowah et al. (2019) reviewed and compared the 402 EDM studies between 2000 and 2017 and found out computer-supported visualization analytics (CSVA) is under-researched in the educational field (Aldowah et al., 2019). A.M. Shahiri and W. Husain (2015) reviewed the EDM studies with an analytic method, so they addressed improvements needed in higher education in Malaysia (Shahiri & Husain, 2015).

RESEARCH METHODOLOGY

An analysis of existing studies about predicting student performance is conducted using a review protocol. The review protocol has three phases; planning, conducting, and reporting the analysis (Kitchenham et al., 2010; Lynn & Emanuel, 2021). This review aims to find answers for research questions, determine the tools used in researches and find out the most convenient and reliable method for predicting student performance (Lynn & Emanuel, 2021). Figure 2 gives a glance of the review methodology used in this paper.

The research questions

In this study; to determine appropriate research questions, we followed the Kitchenham steps. Kitchenham steps consist three viewpoints; they are, population, intervention, and outcomes steps (Kitchenham et al., 2010). In our work; population; university or high school students, intervention; student performance modelling approaches with data mining methods and the tools used, outcomes and results; chosen prediction method and prediction accuracy. This study addressed the following research questions;

Q1. Which method is the most suitable one for student performance prediction according to common methods?

Q2. Which tools are preferred in reviewed EDM studies?

Q3: What are commonly used methods in reviewed EDM studies?

Q4. What are commonly selected keywords in reviewed EDM studies?

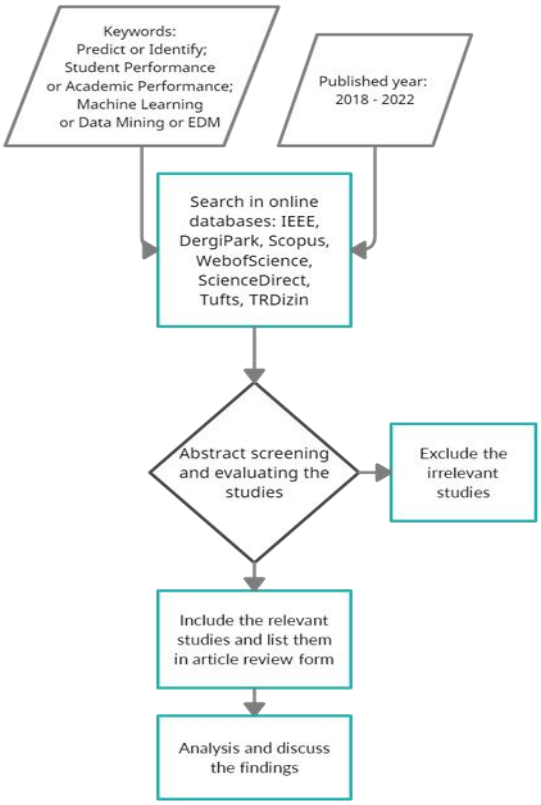

Figure 2: Review Methodology

The research strategy

IEEE Xplore, Dergipark, Web of Science, TR Index, Science Direct, Tufts, and Scopus indexing engines were used in the review of the studies (Table 1). As date range last five years is specified. In literature search process "educational data mining", "classification", "student performance", "prediction algorithm", "learning analytics", "data mining", "decision trees", "academic performance" keywords and their different combinations were searched respectively and the results were filtered by research subject areas. Also conference proceedings were searched related to EDM and finally repetitive studies were eliminated.

Table 1: Databases used in review process.

Database Name	Number of Accessed Studies
TR Dizin	32
Dergipark	25
Scopus	46
Web of Science	44
IEEE	45
Science Direct	29
Tufts	25

Inclusion/Exclusion Criteria

In this study, an "Article Review Form" developed by the researchers was used to record the searched publications. Studies in Table 1 were rearranged according to inclusion/exclusion criteria and the relevant details were recorded in the article review form. Inclusion/exclusion criteria have been determined as follows:

a. Is it an open-access article?
b. Is it in Turkish or English language?
c. Is it a review paper?
d. Did it publish between 2018 and 2022 (last five years)?
e. Is it an EDM or ML study?
f. Does it include the research keywords or combinations?
g. Does it include the studied factors?

Studies that do not include any of the data mining tasks (classification, estimation, association rules, clustering), which are literature surveys, which do not focus on predicting student performance which do not specify the tools used in the study, and which are repetitive studies, which are not available in full-text were left out from the research. As a result, the analysis consists of 44 research articles given in Table 2.

Table 2: EDM studies included in the research.

#	Main Purpose	Study
1	to use DM and ML algorithms on actual student data sets	(Abdar, Zomorodi-Moghadam, & Zhou, 2018; Abe, 2019; Al Breiki, Zaki, & Mohamed, 2019; Alharthi, 2021; Fernandes et al., 2019; Houndayi, Houndji, Zohou, & Ezin, 2020; Jalota & Agrawal, 2019; Qazdar, Er-Raha, Cherkaoui, & Mammass, 2019; Ramaswami, Susnjak, Mathrani, Lim, & Garcia, 2019; Singh & Pal, 2020; Yavuz & Hatice, 2019)
2	to predict student success with semi-supervised classification methods	(Karlos, Kostopoulos, & Kotsiantis, 2020; Satı, 2018)
3	to apply different classification algorithms	(Adebayo & Chaubey, 2019; Nand, Chand, & Reddy, 2021; Rosado, Payne, & Rebong, 2019; Sharma, 2019; Yaacob, Nasir, Yaacob, & Sobri, 2019)
4	to predict student performance including behavioral features with data mining methods	(Ajibade, Ahmad, & Shamsuddin, 2019; Dabhade et al., 2021; Güre, Şevgin, & Kayri, 2022; Sana, Siddiqui, & Arain, 2019)
5	to predict student success including demographic and socioeconomic features with educational data mining methods	(ABBASOĞLU, 2020; Waheed et al., 2020)
6	to apply clustering techniques for	(Al-Hagery, Alzaid, Alharbi, & Alhanaya, 2020; Mohamed Nafuri, Sani, Zainudin, Rahman, & Aliff, 2022)

	analyzing the student data	
7	to apply a hybrid model to predict student performance	(Alshanqiti & Namoun, 2020; Hassan, Ahmad, & Anuar, 2020; Injadat, Moubayed, Nassif, & Shami, 2020; Karthikeyan, Thangaraj, & Karthik, 2020; Mutrofin, Maisarah, Widodo, Ginardi, & Fatichah, 2020; Siddaiah & PM, 2022; Zhao et al., 2020)
8	to predict student performance with supervised ML algorithms	(Bhutto, Siddiqui, Arain, & Anwar, 2020; Hashim, Awadh, & Hamoud, 2020; Pimentel, Ospina, & Ara, 2021; YILDIZ & Börekci, 2020)
9	to find best algorithm to classify and to find important features on success	(FİLİZ & Ersoy, 2020; Peerbasha & Surputheen, 2021)
10	to predict student final grade using personal characteristics	(Ha, Loan, Giap, & Huong, 2020; Ma'sum, 2022; Sravani & Bala, 2020; Yağcı, 2022)

RESULTS AND DISCUSSION

The review results will be held in subtitles as following; datasets used in reviewed studies, tools used for data mining, commonly used keywords in the studies, conventional methods used for predicting student performance respectively.

Datasets used in the studies reviewed

Within the scope of the research, the frequency of use of the sample levels preferred by the researchers at the point of data collection is shown in Figure 3. University students (31 studies) and high school students (13 studies) are the source of datasets in reviewed papers. The number of samples in these datasets varies from 85 data to 5 million data.

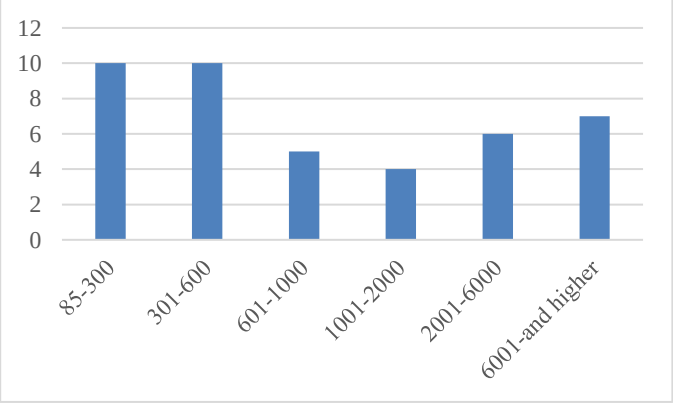

Figure 3: Number of student samples in the datasets.

DM tools used in the studies reviewed

Various DM tools are accessible for filtering the relevant data, fitting a predictive model, analyzing the relationship, mining algorithms, and visualizing the results (Slater et al., 2017). In this study, we face nine different data mining tools (Table 3). Researchers used Python (18)

(Orange, Jupyter, Scikit, etc.) and WEKA (13) mostly, followed by R (5), RapidMiner (3), SPSS (1), Mathematica (1), H2O (1), XAPI (1) and KNIME (1) respectively.

Table 3: Tools used for data mining in reviewed EDM studies.

Year	Python	WEKA	R	Others
2018		(Abdar et al., 2018; Satı, 2018)		
2019	(Qazdar et al., 2019; Ramaswami et al., 2019)	(Al Breiki et al., 2019; Jalota & Agrawal, 2019; Sana et al., 2019; Sharma, 2019)	(Yavuz & Hatice, 2019)	(Abe, 2019; Adebayo & Chaubey, 2019; Ajibade et al., 2019; Fernandes et al., 2019; Rosado et al., 2019; Yaacob et al., 2019)
2020	(Alshanqiti & Namoun, 2020; Bhutto et al., 2020; FİLİZ & Ersoy, 2020; Hassan et al., 2020; Houndayi et al., 2020; Karlos et al., 2020; Mutrofin et al., 2020; Singh & Pal, 2020; YILDIZ & Börekci, 2020; Zhao et al., 2020)	(ABBASOĞLU, 2020; Ha et al., 2020; Hashim et al., 2020; Karthikeyan et al., 2020)	(Injadat et al., 2020; Sravani & Bala, 2020)	(Al-Hagery et al., 2020; Waheed et al., 2020)
2021	(Alharthi, 2021; Dabhade et al., 2021; Peerbasha & Surputheen, 2021)	(Nand et al., 2021)	(Pimentel et al., 2021)	
2022	(Ma'sum, 2022; Mohamed Nafuri et al., 2022; Siddaiah & PM, 2022; Yağcı, 2022)		(Güre et al., 2022)	

There are a handful of programming languages perfectly suited to data manipulation and feature engineering by data scientists. In this regard, Python is considered by many to be particularly useful. It is easier to manage context-dependent or temporal characteristics in Python than in Excel or Google Sheets. Furthermore, Python can handle unusual and specialized data formats, such as the JSON files produced by online learning platforms(Slater et al., 2017). Python has a lot of libraries to use; Scikit-learn for ML, NumPy for mathematical expressions, Orange for data visualization, and Pandas for data preparation(Stančin & Jović, 2019). Weka is also a preferred tool in EDM by researchers because it has a vast set of classification, clustering, and association mining algorithms (Slater et al., 2017). It could be difficult for an educationalist with having constricted understanding of data mining to use DM tools that are not directly for educational purposes.

Keywords used in the studies reviewed

The keywords chosen by the authors within the scope of our research and their frequency of use are given in Table 4. As the table shows, the EDM keyword became the most commonly preferred keyword by researchers to specify the field of study, followed by ML, Prediction, Classification, and others.

Table 4: Preferred keywords and their frequency of use.

Keyword	Count	%
Educational Data Mining	22	15,1
Student Performance	9	6,2
Machine Learning	21	14,4
Data Mining	13	8,9
Classification	14	9,6
Prediction	15	10,3
Regression	12	8,2
Academic Performance	7	4,8
Decision Tree	8	5,5
E-Learning	2	1,4
Naive Bayes	5	3,4
Algorithm	10	6,8
Neural Network	4	2,7
Learning Analytics	4	2,7

DM Methods used in the studies reviewed

Data mining techniques are divided into two titles, Predictive Methods (PM) and Descriptive Methods (DM). Clustering (a DM) and prediction (a PM) have become popular methods among other DM methods. Types of clustering include k-means, x-means, DBSCAN, fuzzy clustering, etc. algorithms. Types of prediction include classification algorithms which are a widely preferred technique to detect student behaviors and to predict student performance.

We saw that various classification techniques like Artificial Neural Network (ANN), Support Vector Machine (SVM), Decision Tree (DT), Naïve Bayes (NB), Random Forest (RF), XGBoost, k-Nearest Neighbors (k-NN), etc. were used to predict student performance in reviewed articles.

In the examined studies, the graph showing the intensity of use of the classification algorithms in data mining by researchers is given in Figure 4 and their percentages are given in Figure 5.

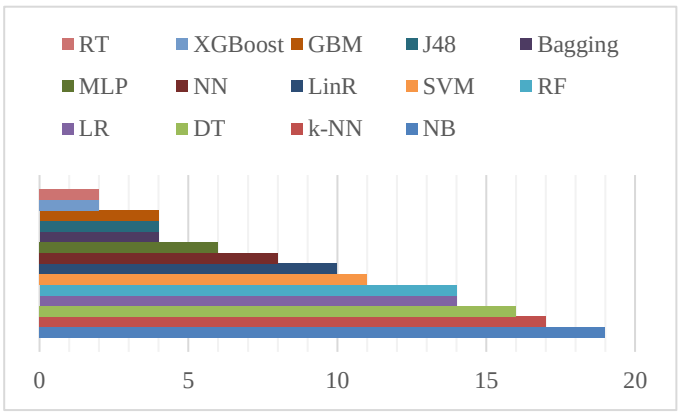

Figure 4: Trending DM algorithms used

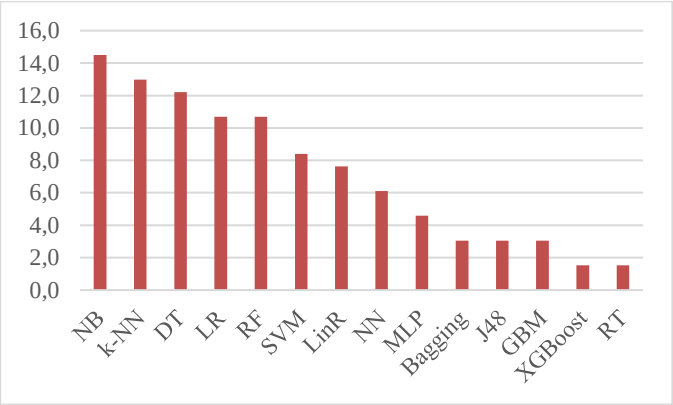

Figure 5: Percentages of DM algorithms used.

In these EDM studies, we face eight categories of applications that have been researched mostly. Some of them provide information to instructors or students by analyzing educational data (Abdar et al., 2018; Abe, 2019; Al Breiki et al., 2019; Alharthi, 2021; Fernandes et al., 2019; Houndayi et al., 2020; Jalota & Agrawal, 2019; Qazdar et al., 2019; Ramaswami et al., 2019; Singh & Pal, 2020; Yavuz & Hatice, 2019), some of them reveal student characteristics (ABBASOĞLU, 2020; Ajibade et al., 2019; Dabhade et al., 2021; Güre et al., 2022; Ha et al., 2020; Ma'sum, 2022; Sana et al., 2019; Sravani & Bala, 2020; Waheed et al., 2020; Yağcı, 2022), and some study relationships between students and educational environments (Alshanqiti & Namoun, 2020; FİLİZ & Ersoy, 2020; Hassan et al., 2020; Injadat et al., 2020; Karthikeyan et al., 2020; Mutrofin et al., 2020; Peerbasha & Surputheen, 2021; Siddaiah & PM, 2022; Zhao et al., 2020).

Prediction accuracy is determined by the characteristics that are used during the prediction process. Due to the influence of studied attributes on the prediction accuracy, the Artificial Neural Network method produced the best results in most of the researches.

In reviewed articles, researchers reached the best scores within their specific research by using ANN, RF, SVM, and DT mostly. The other methods with high prediction accuracy are given in Figure 6.

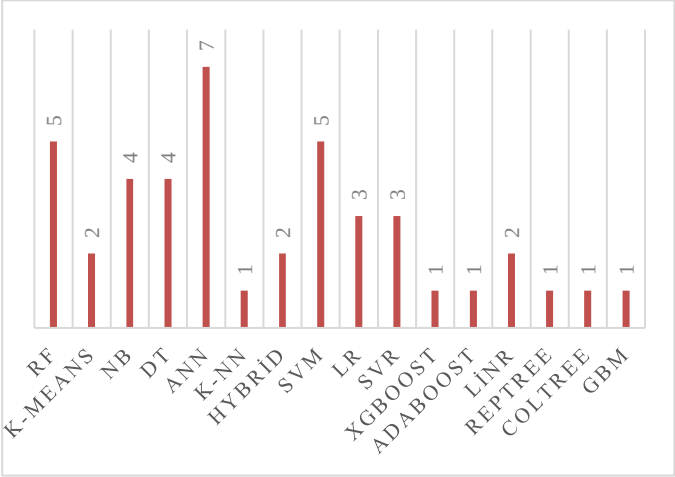

Figure 6: Percentage of Methods with Best Accuracy

CONCLUSION AND FUTURE WORK

According to the results, we can say the literature reviews and the studies in the field of the application of EDM are balanced. Today, with the developing educational technologies, the concept of academic success comes to the fore. In the examined studies, it was clear that studies on academic success were noticeably high. When articles are reviewed according to the year of publication, the studies conducted in this field in recent years have increased gradually. The analyzed studies show that students' behavioral features got a great impact on academic performance.

Among various techniques used in EDM, classification is one of the most common techniques used by most researchers. Other DM techniques of regression, clustering, statistics, association rule, and visual data mining have big numbers of users as well. However, some techniques such as correlation and hybrid models were not used that much because of faced difficulties while determining attributes necessary to adapt.

Several studies were conducted by looking at the data and finding the patterns after the study has been concluded. Experiments with varying conditions are scarcely reported. In future work, interested parties can use the data results in this paper as a starting point for their studies in the field of educational data mining. Also use of different hybrid methods to improve the accuracy of results gained is recommended. Furthermore, to use datasets directly gathered from students about students' neural activity and state of mind could be analyzed and used in EDM to understand students' learning process better and so their academic performance.

REFERENCES

Abbasoğlu, B. (2020). Ortaokul Öğrencilerinin Akademik Başarılarının Eğitsel Veri Madenciliği Yöntemleri Ile Tahmini. *Veri Bilimi, 3*(1), 1-10.

Abdar, M., Zomorodi-Moghadam, M., & Zhou, X. (2018). *An Ensemble-Based Decision Tree Approach For Educational Data Mining.* Paper Presented At The 2018 5th International Conference On Behavioral, Economic, And Socio-Cultural Computing (Besc).

Abe, K. (2019). *Data Mining And Machine Learning Applications For Educational Big Data In The University.* Paper Presented At The 2019 Ieee Intl Conf On Dependable, Autonomic And Secure Computing, Intl Conf On Pervasive Intelligence And Computing, Intl Conf On Cloud And Big Data Computing, Intl Conf On Cyber Science And Technology Congress (Dasc/Picom/Cbdcom/Cyberscitech).

Adebayo, A. O., & Chaubey, M. S. (2019). Data Mining Classification Techniques On The Analysis Of Student's Performance. *Gsj, 7*(4), 45-52.

Ajibade, S.-S. M., Ahmad, N. B. B., & Shamsuddin, S. M. (2019). *Educational Data Mining: Enhancement Of Student Performance Model Using Ensemble Methods.* Paper Presented At The Iop Conference Series: Materials Science And Engineering.

Akgün, K., & Bulut Özek, M. (2020). Eğitsel Veri Madenciliği Yöntemi İle İlgili Yapılmış Çalışmaların İncelenmesi: İçerik Analizi. *Uluslararası Eğitim Bilim Ve Teknoloji Dergisi*. Doi:10.47714/Uebt.753526

Al-Hagery, M. A., Alzaid, M. A., Alharbi, T. S., & Alhanaya, M. A. (2020). Data Mining Methods For Detecting The Most Significant Factors Affecting Students' Performance. *Int. J. Inf. Technol. Comput. Sci.(Ijitcs), 12*(5), 1-13.

Al Breiki, B., Zaki, N., & Mohamed, E. A. (2019). *Using Educational Data Mining Techniques To Predict Student Performance.* Paper Presented At The 2019 International Conference On Electrical And Computing Technologies And Applications (Icecta).

Aldowah, H., Al-Samarraie, H., & Fauzy, W. M. (2019). Educational Data Mining And Learning Analytics For 21st Century Higher Education: A Review And Synthesis. *Telematics And Informatics, 37,* 13-49.

Alharthi, H. (2021). *Machine Learning Techniques To Predict Academic Performance Of Health Sciences Students.* Paper Presented At The 2021 20th International Symposium On Distributed Computing And Applications For Business Engineering And Science (Dcabes).

Alshanqiti, A., & Namoun, A. (2020). Predicting Student Performance And Its Influential Factors Using Hybrid Regression And Multi-Label Classification. *Ieee Access, 8*, 203827-203844.

Bhutto, E. S., Siddiqui, I. F., Arain, Q. A., & Anwar, M. (2020). *Predicting Students' Academic Performance Through Supervised Machine Learning.* Paper Presented At The 2020 International Conference On Information Science And Communication Technology (Icisct).

Dabhade, P., Agarwal, R., Alameen, K. P., Fathima, A. T., Sridharan, R., & Gopakumar, G. (2021). Educational Data Mining For Predicting Students' Academic Performance Using Machine Learning Algorithms. *Materials Today: Proceedings, 47*, 5260-5267. Doi:Https://Doi.Org/10.1016/J.Matpr.2021.05.646

Fernandes, E., Holanda, M., Victorino, M., Borges, V., Carvalho, R., & Van Erven, G. (2019). Educational Data Mining: Predictive Analysis Of Academic Performance Of Public School Students In The Capital Of Brazil. *Journal Of Business Research, 94*, 335-343.

Filiz, E., & Ersoy, Ö. (2020). Educational Data Mining Methods For Timss 2015 Mathematics Success: Turkey Case. *Sigma Journal Of Engineering And Natural Sciences, 38*(2), 963-977.

Güre, Ö. B., Şevgin, H., & Kayri, M. (2022). Examination Of Variables Affecting Science Success Of Eighth Grade Students Using Ordinal Logistic Regression Method. *Journal Of Social Sciences Of Mus Alparslan University, 10(2)* 781-797.

Ha, D. T., Loan, P. T. T., Giap, C. N., & Huong, N. T. L. (2020). An Empirical Study For Student Academic Performance Prediction Using Machine Learning Techniques. *International Journal Of Computer Science And Information Security (Ijcsis), 18*(3), 21-28.

Hashim, A. S., Awadh, W. A., & Hamoud, A. K. (2020). *Student Performance Prediction Model Based On Supervised Machine Learning Algorithms.* Paper Presented At The Iop Conference Series: Materials Science And Engineering.

Hassan, H., Ahmad, N. B., & Anuar, S. (2020). Improved Students' Performance Prediction For Multi-Class Imbalanced Problems Using Hybrid And Ensemble Approach In Educational Data Mining. *Journal Of Physics: Conference Series, 1529*(5), 052041. Doi:10.1088/1742-6596/1529/5/052041

Houndayi, I. B., Houndji, V. R., Zohou, P. J., & Ezin, E. C. (2020, 2020//). *Amonai: A Students Academic Performances Prediction System.* Paper Presented At The E-Infrastructure And E-Services For Developing Countries, Cham.

Inc., G. (2022). Data-Mining. Retrieved From Https://Www.Gartner.Com/En/Information-Technology/Glossary/Data-Mining

Injadat, M., Moubayed, A., Nassif, A. B., & Shami, A. (2020). Systematic Ensemble Model Selection Approach For Educational Data Mining. *Knowledge-Based Systems, 200*, 105992.

Jalota, C., & Agrawal, R. (2019). *Analysis Of Educational Data Mining Using Classification.* Paper Presented At The 2019 International Conference On Machine Learning, Big Data, Cloud And Parallel Computing (Comitcon).

Karlos, S., Kostopoulos, G., & Kotsiantis, S. (2020). Predicting And Interpreting Students' Grades In Distance Higher Education Through A Semi-Regression Method. *Applied Sciences, 10*(23), 8413.

Karthikeyan, V. G., Thangaraj, P., & Karthik, S. (2020). Towards Developing Hybrid Educational Data Mining Model (Hedm) For Efficient And Accurate Student Performance Evaluation. *Soft Computing, 24*(24), 18477-18487.

Khan, A., & Ghosh, S. K. (2021). Student Performance Analysis And Prediction In Classroom Learning: A Review Of Educational Data Mining Studies. *Education And Information Technologies, 26*(1), 205-240.

Kitchenham, B., Pretorius, R., Budgen, D., Brereton, O. P., Turner, M., Niazi, M., & Linkman, S. (2010). Systematic Literature Reviews In Software Engineering–A Tertiary Study. *Information And Software Technology, 52*(8), 792-805.

Lynn, N., & Emanuel, A. (2021). *Using Data Mining Techniques To Predict Students' Performance. A Review.* Paper Presented At The Iop Conference Series: Materials Science And Engineering.

Ma'sum, M. A. (2022, 22-22 Jan. 2022). *Predicting Student Achievement Before Final Exam: A Regression-Based Approach.* Paper Presented At The 2022 2nd International Conference On Information Technology And Education (Icit&E).

Mohamed Nafuri, A. F., Sani, N. S., Zainudin, N. F. A., Rahman, A. H. A., & Aliff, M. (2022). Clustering Analysis For Classifying Student Academic Performance In Higher Education. *Applied Sciences, 12*(19), 9467.

Mutrofin, S., Maisarah, M., Widodo, S., Ginardi, R. V. H., & Fatichah, C. (2020). Application Of A Combination Between Principal Component Analysis And Logistic Regression Based On Support Vector Machine On Educational Data Mining With Overlapping Data Problem. *Iop Conference Series: Materials Science And Engineering, 874*(1), 012018. Doi:10.1088/1757-899x/874/1/012018

Nand, R., Chand, A., & Reddy, E. (2021, 23-25 Oct. 2021). *Data Mining Students' Performance In A Higher Learning Environment.* Paper Presented At The 2021 3rd Novel Intelligent And Leading Emerging Sciences Conference (Niles).

Peerbasha, S., & Surputheen, M. M. (2021). Prediction Of Academic Performance Of College Students With Bipolar Disorder Using Different Deep Learning And Machine Learning Algorithms. *International Journal Of Computer Science & Network Security, 21*(7), 350-358.

Peña-Ayala, A. (2014). Educational Data Mining: A Survey And A Data Mining-Based Analysis Of Recent Works. *Expert Systems With Applications, 41*(4), 1432-1462.

Pimentel, J., Ospina, R., & Ara, A. (2021). Learning Time Acceleration In Support Vector Regression: A Case Study In Educational Data Mining. *Stats, 4*, 682-700. Doi:10.3390/Stats4030041

Qazdar, A., Er-Raha, B., Cherkaoui, C., & Mammass, D. (2019). A Machine Learning Algorithm Framework For Predicting Students Performance: A Case Study Of Baccalaureate Students In Morocco. *Education And Information Technologies, 24*(6), 3577-3589. Doi:10.1007/S10639-019-09946-8

Ramaswami, G., Susnjak, T., Mathrani, A., Lim, J., & Garcia, P. (2019). Using Educational Data Mining Techniques To Increase The Prediction Accuracy Of Student Academic Performance. *Information And Learning Sciences, 120*(7/8), 451-467.

Romero, C., & Ventura, S. (2013). Data Mining In Education. *Wires Data Mining And Knowledge Discovery, 3*(1), 12-27. Doi:Https://Doi.Org/10.1002/Widm.1075

Rosado, J. T., Payne, A. P., & Rebong, C. B. (2019). Emineprove: Educational Data Mining For Predicting Performance Improvement Using Classification Method. *Iop Conference Series: Materials Science And Engineering, 649*(1), 012018. Doi:10.1088/1757-899x/649/1/012018

Sana, S., Siddiqui, I. F., & Arain, Q. A. (2019). Analyzing Students' Academic Performance Through Educational Data Mining. *3c Tecnología: Glosas De Innovación Aplicadas A La Pyme, Edición Especial, 8*(1), 402-421. Doi:Http://Dx.Doi.Org/10.17993/3ctecno.2019.Specialissue2.402-421

Satı, N. U. (2018). Semi-Supervised Classification In Educational Data Mining: Students' Performance Case Study. *International Journal Of Computer Applications, 179*(26), 13-17.

Shahiri, A. M., & Husain, W. (2015). A Review On Predicting Student's Performance Using Data Mining Techniques. *Procedia Computer Science, 72*, 414-422.

Sharma, T. (2019). Educational Data Mining-Students Performance Prediction. *International Journal For Research In Applied Science And Engineering Technology, 7*, 454-467. Doi:10.22214/Ijraset.2019.8063

Siddaiah, S. K., & Pm, D. M. S. (2022). Technique To Predict Student Performance Through Ensemble Learning Algorithm In E-Learning Environment. *Available At Ssrn 4054489*.

Singh, R., & Pal, S. (2020). Machine Learning Algorithms And Ensemble Technique To Improve Prediction Of Students Performance. *Ijatcse, 9*(3).

Slater, S., Joksimovi, X, Sre, X, Ko, . . . Gasevic, D. (2017). Tools For Educational Data Mining: A Review. *Journal Of Educational And Behavioral Statistics, 42*(1), 85-106. Retrieved From Http://Www.Jstor.Org/Stable/26447650

Sravani, B., & Bala, M. M. (2020). *Prediction Of Student Performance Using Linear Regression.* Paper Presented At The 2020 International Conference For Emerging Technology (Incet).

Stančin, I., & Jović, A. (2019, 20-24 May 2019). *An Overview And Comparison Of Free Python Libraries For Data Mining And Big Data Analysis.* Paper Presented At The 2019 42nd International Convention On Information And Communication Technology, Electronics And Microelectronics (Mipro).

Tekin, A., & Öztekin, Z. (2018). Eğitsel Veri Madenciliği İle İlgili 2006-2016 Yillari Arasinda Yapilan Çalişmalarin İncelenmesi. *Eğitim Teknolojisi Kuram Ve Uygulama, 8*(2), 108-124.

Waheed, H., Hassan, S.-U., Aljohani, N. R., Hardman, J., Alelyani, S., & Nawaz, R. (2020). Predicting Academic Performance Of Students From Vle Big Data Using Deep Learning Models. *Computers In Human Behavior, 104*, 106189.

Yaacob, W. F. W., Nasir, S. A. M., Yaacob, W. F. W., & Sobri, N. M. (2019). Supervised Data Mining Approach For Predicting Student Performance. *Indones. J. Electr. Eng. Comput. Sci, 16*(3), 1584-1592.

Yağcı, M. (2022). Educational Data Mining: Prediction Of Students' Academic Performance Using Machine Learning Algorithms. *Smart Learning Environments, 9*(1), 11. Doi:10.1186/S40561-022-00192-Z

Yavuz, O. B., & Hatice, C. (2019). Educational Data Mining: A Tutorial For The Rattle Package In R. *International Journal Of Assessment Tools In Education, 6*(No. 5-Special Issue), 20-36. Doi:Https://Dergipark.Org.Tr/En/Pub/Ijate/Issue/43543/627361

Yildiz, M., & Börekci, C. (2020). Predicting Academic Achievement With Machine Learning Algorithms. *Journal Of Educational Technology And Online Learning, 3*(3), 372-392.

Zhao, L., Chen, K., Song, J., Zhu, X., Sun, J., Caulfield, B., & Mac Namee, B. (2020). Academic Performance Prediction Based On Multisource, Multifeature Behavioral Data. *Ieee Access, 9*, 5453-5465.

CHAPTER 2

METAL FOAM AND APPLICATION ON HEAT EXCHANGER

B.S. Dyah Hayu ROSYIDAH[1]
[1]Selcuk University, Konya/Turkey
ORCID: 0000-0003-3754-4047

Ahmet Ali SERTKAYA[2]
[2]Selcuk University, Konya/Turkey
ORCID: 0000-0002-9884-445X

INTRODUCTION

Metal foam is celled structured of random permeable cells with metal ligament as an interconnector. Nickel, aluminum, copper, steel, ceramics, and metal alloys are the common base material. An open cell has 12 until 14 pentagonal or hexagonal surfaces. There are several parameters to characterize metal foam. The average diameter of open cells is denoted by dp and defined as the pore diameter. Meanwhile, the ligaments' average diameter is referred as the strut diameter and denoted by df. The number of pores per inch of metal foam or PPI has range from 5 until 100. The void space volume measured by the weight and sample volume is explained as the porosity ε with values around 80%– 99%.

The advantages of metal foam material, such as large specific surface area, low density, stiffness, and its mechanical strength, sustain it as extensively used material in industry. In automotive industry, metal foam is popular as sound damper, crashes energy absorber, and exhaust gas design. Aerospace industry has utilized metal foam as aircraft clamp, bearing support, and aircraft wing design.

The thermal properties of metal foam have supported its applications for heat exchanger,

electronic cooling, and dry-cooling. The metal foam's thermal conductivity and high permeability attract large attention of researchers to improve
the heat transfer technology on recent years (Antohe et al, 1997). For increasing the heat exchanger surface area, the porous media utilization or the base fluid properties can be transformed by using nanofluids (Habibishandiz et al., 2022).
The world energy demand is predicted increasing around 1.3% per year up to 2040 aligned with the industrial process requirement and society demand (The International Energy Agency, 2019). Thus, the energy conservation area and great efficient technology appeal high attention. For the thermal application, the heat conversion tools have to be light and compact also perform in a high efficiency.
Nowadays the applications of metal foam in various fields are increased rapidly. The experimental researches of metal foam heat transfer verified the metal foam ability as heat exchanger. Bhattacharya and Calmidi (2000) determined the hydraulic characteristics of metal foam through their experimental study. Nield et al. (2017) conducted a prediction formula to calculate metal foam effective thermal conductivity.
This study reviews the performance of meal foam in heat transfer technologies. It is focused in three applications which are compact heat exchanger, solar thermal tool and thermal energy storage.
Metal foam includes to the porous material. Henry Darcy, a French civil engineer (Nield et al., 2017), expressed the first equation to describe the fluids velocity of porous media on 1856. Surely as a kind of porous media, metal foam's penetration complies the Darcy's law (Kim et al., 2016). The Darcy model examined the fluid flow in porous media and discovered a proportional relation between the pressure drop and velocity. There is a lack of The Darcy model which ignores the solid boundary on fluid flow. The Darcy Brinkman model rose by Brinkman (1949) is expressed the penetration in porous media with considering the solid boundary wall effect. When metal foam is compared to soil, it has a greater permeability generating a higher velocity. The inertial effect of quadratic term is considered by Forchheimer model (1901). The Darcy-Brinkman-Forchheimer model is extensively used for fluid flow numerical studies on metal foam. Wang et al (2020) presented the elaborate review for the four models mentioned. Table 1 below contains a summary of the metal foam models equations.

Table 1 : The Porous Media Flow Models

Flow Model	Equation
Darcy model	$\frac{\Delta p}{L} = \frac{\mu}{K}u$
Darcy-Brinkman model	$\frac{\Delta p}{L} = \frac{\mu}{K}u + \frac{\mu}{\varepsilon}\nabla^2 u$
Darcy-Forchheimer model	$\frac{\Delta p}{L} = \frac{\mu}{K}u - \frac{c_F \rho}{\sqrt{K}}u^2$
Darcy-Brinkman-Forchheimer model	$\frac{\Delta p}{L} = \frac{\mu}{K}u + \frac{\mu}{\varepsilon}\nabla^2 u - \frac{c_F \rho}{\sqrt{K}}u^2$

Δ_p is pressure drop; K is metal foam permeability; c_F is coefficient of inertia.

The fluid and porous were assumed as homogeneous and isotropic phases by neglecting the heat convection from the foam ligament and fluid on the beginning metal foam studies (Nield et al., 2017). For describing the heat conduction between porous and boundary, the effective thermal conductivity, denoted by k_{eff}, was suggested. The eq. (1) shows a formula of the effective thermal conductivity, denoted by k_{eff}, which is discovered by Nield et al. [5]. It is a weighted arithmetic mean of solid and fluid phases.

$$k_{eff} = (1-\varepsilon)k_s + \varepsilon k_f \tag{1}$$

where k_s denotes the foam ligament thermal conductivity and k_f denotes the fluid thermal conductivity. The result is the maximum rate of the real effective thermal conductivity value. Local thermal equilibrium (LTE) model handles the heat transfer for metal foams having low thermal conductivity ligament material. The local thermal equilibrium (LTE) model will be shown in eq. (2) in term q is the internal volumetric heat source.

$$\left(\rho c_p\right)\frac{\partial T}{\partial t} + \left(\rho c_p\right)_f u \times \nabla T = \nabla\left(k_{eff}\,\nabla\, T\right) + q \tag{2}$$

Isfahani et al. (2019) suggested the use of local thermal equilibrium (LTE) model when the fluid thermal conductivity is less than 10. The local thermal equilibrium (LTE) model is easier to apply numerically than the local thermal non equilibrium (LTNE) model because it only solves one energy equation for both solid and fluid phases.

While the ratio of fluid thermal conductivity and foam ligament decreases, the thermal transfer in metal foam will be dominated by heat convection between solid and fluid phase. Due to the local thermal equilibrium (LTE) model neglect the difference temperature between solid and liquid, for this condition LTE does not work. The local thermal non-equilibrium (LTNE) model is established by two coupled energy equations, as shown in eq s. (3) and (4) below.

$$(1-\varepsilon)\left(\rho c_p\right)\frac{\partial T_s}{\partial t} = (1-\varepsilon)\nabla(k_s \nabla T_s) + (1-\varepsilon)q_s + \left(T_f - T_s\right)h_{sf} \tag{3}$$

$$\varepsilon\left(\rho c_p\right)\frac{\partial T_s}{\partial t} + \left(\rho c_p\right)u\nabla T = \varepsilon\nabla\left(k_f \nabla T_f\right) + (1-\varepsilon)q_f + \left(T_s - T_f\right)h_{sf} \tag{4}$$

where h_{sf} refers to the interfacial convective heat transfer coefficient, T_s denotes the local solid temperature and T_f is the local fluid temperature.

Many previous studies for high thermal conductivity metal foams used local thermal non-equilibrium (LTNE) model to calculate heat convection energy equation. The thermal conductivity ratio of fluid and solid $\left(k_f/k_s\right)$ was a key parameter for determining the LTNE effect, as Lu et al. (2006) and Zhao et al. (2004) concluded in macro channel filled with metal foam. Xu et al. (2000) merged the LTE and LTNE models to present an analytical study of thermal convection in metal foam, then the results showed that the LTE model estimated heat transfer in metal foam with a relative deviation less than 20% under the value of ε > 95% or $\left(k_f/k_s\right)$ > 0.148.

The random cells of metal foam are assumed as regular three-dimensional mincro-structures. It is considered its morphology such as two-dimensional hexagonal structure (Zhao et al., 2004), cubic cell model (Nield et al., 2017), three-dimensional dodeca-hedron unit cell (Calmidi et al., 2000), three-dimensional tetrakaidecahedron unit cell (Boomsma et al., 2003), and Kelvin cell mode (Boomsma et al., 2001) to define the metal foam physical properties. The volume-averaged semi-empirical equations are able to be used for simulating the metal foam flow and

thermal characteristics by macroscopic approach based on those ideal micromodels. However, it neglects the pore scale details. For simulating the intricate metal foam geometry, generally the microscopic approaches are needed.

On current decades, researchers have used ideal cell models to build metal foam periodic cell structures. Boomsma et al. (2003) investigated the flow characteristics of metal foam using the 14-sided tetrakaidecahedron cell (Kelvin model). The wall effects that cause flow resistance should be taken into account in volume-average simulations. The body-centered cubic (BCC) model was used by Krishnan et al. (2008) to perform direct simulations of heat transfer and flow in metal foam, the BBC unit cell is a tetrakaidecahedron with a low surface-area-to-volume ratio. The interconnection and shape of the cell structure would change in morphology as pore diameter and porosity varied. The variations could not be described in detail by the constant ideal cell model. The cell geometry of metal foam is modeled as a real structure using 3D tomographic scan technology. Furthermore, the detail is performed in random cells.

Ranut et al. (2014, 2015) used high-resolution X-ray micro-tomography to create a 3D structure of metal foams. Three types of metal foam with PPIs (the number of pores per inch of metal foam) of 10, 20, and 30 were shown. The results confirmed that the flow in metal foam followed the Darcy-Forchheimer law, with the effective heat conductivity determined by foam ligaments due to fluid distribution's marginal effects.

As previously stated, the direct numerical simulation on metal foam describes the wall effects, interfacial heat transfer coefficient, and variations in foam shape in detail at the expense of a massive computation. In future work, direct numerical simulation based on a real foam model will provide more accurate microstructure and physical parameters.

COMPACT HEAT EXCHANGERS

The heat exchangers are widely used in various fields, as examples for transportation, power generation, refrigeration, cooling system, and the oil and gas processing. On recent years, the technology development is rapidly running to comply the global sustainability challenges. This condition triggers the researches to provide the advanced heat exchanger design. High performance heat exchangers specifically employ the high surface area which offers heat flow efficiency.

A compact heat exchanger is an equipment which designed to transfer heat efficiently from one medium to another. The minimum surface area of compact heat exchanger is 300 m2 per volume. It has high heat transfer coefficient up to 5000 W/m2K. Other parameters, it is characterized by laminar flow and small flow passage. The application of metal foam, both full or partial mode, is suitable to maximize the thermal performance of compact heat exchanger. Figure 1 is shown the application of metal foam in heat compact heat exchanger. Aluminum foam is recently used to wrap the heat exchanger as shown in Figure 2.

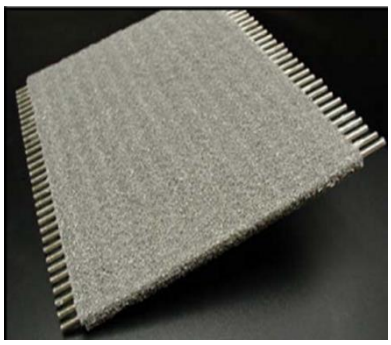

Figure 1: The lightweight metal foam heat exchanger

Figure 2: The aluminum foam for heat exchanger

This study reviews the thermal performances of simple heat exchanger types, which are plate and tube heat exchanger, also the tube in tube heat exchanger as more complicated heat exchanger type. Kim et al. (2015) implemented a plate-foam heat exchanger filled with 6101 aluminum-alloy foam. The modified j-factor and Nusselt number correlations were aimed to define the heat transfer rate.

$$j = \frac{U}{\rho c_p u} Pr^{2/3} = 13.73(Re_H^{-0.489} Da^{0.451}) \quad (5)$$

$270 \leq Re_H \leq 2050$

$$Nu = 0.0159\left(Re_H^{0.426} Pr^{1/3} Da^{-0.787}\right) \quad (6)$$

$1000 \leq Re_H \leq 3000$

Where Re_H denotes Reynolds number based on the value of channel height H. Below is expressed the correlation with friction factor.

$$f = \frac{(\Delta p/L)H}{\rho u^2} = \frac{1}{Re_H.Da} + \frac{0.105}{Da^{1/2}} = \frac{1}{Re_K} + 0.105 \quad (7)$$

Where Re_K refers to the value of Reynolds number based on the permeability $K^{0.5}$.

If the rate of tube side's thermal resistance is greater than the shell side, the tube heat exchangers are fully filled with metal foam. Lu et al. (2006) conducted a series of analytical studies on a wide range of applications, including tube and tube-in-tube heat exchangers filled with metal foam. The thermal-hydrodynamic properties of high porosity open-cell metal foam filled tubes were determined by Lu et al. (2006). The research revealed that the overall Nusselt number of the metal-foam filled tube increases as the relative density. The metal foam application is able to increase the heat transfer supremely with the expense of higher pressure drop.

An investigation about the thermal performance of a tube-in-tube heat exchanger filled with

metal foam in both inner and outer tubes did by Zhao et al. (2004). Their research tested the morphological effects of metal foam on overall heat transfer and the result showed that the thermal performance of metal foam heat exchangers can be more excellent than the conventional finned heat exchangers. Du et al. (2010) used the LTNE model for accomplishing conjugated heat transfer in a tube-in-tube heat exchanger simulation. According to the result, an optimal range of inner tube diameter to outer tube diameter ratio is 0.6-0.7. Tzeng (2007) conducted additional research on aluminum foam heat sinks with and without conductive pipe. The application of open cells aluminum foam on heat exchanger have been done by Sertkaya et al. (2012) and the design is shown in Figure 3.

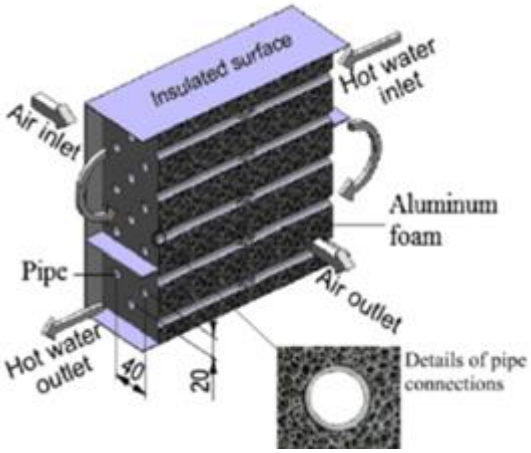

Figure 3: The open cells aluminum foam heat exchanger (Sertkaya et al., 2012)

There are many complex numerical studies by the growth of Darcy-Brinkman-Forchheimer and the local thermal non equilibrium models. Buonomo et al. (2018) and Huisseune et al. (2014) did a numerical analysis on a single array of circular tubes embedded with metal foam. Buonomo et al. (2018) tested the optimal foam thickness was 5 times of the tube diameter. In contrast from regular channel filled with metal foam, the Colburn j-factor increases with decreasing of pore density and increasing the porosity. Huisseune et al. (2015) proved the heat transfer rate of the foamed heat exchangers was up to 6 times greater than the bare tube bundle at the same fan power for air velocity in range of 1.2–3.2 m/s. However, the louvered fin heat exchanger excelled all foamed heat exchangers.

As previously discussed, compact heat exchangers fully embedded in metal foam can significantly improve heat transfer rate with the expense of significant pressure drop. The performance evaluation criterion of heat exchangers fully embedded with metal foam is lower than the finned heat exchangers. Thus the optimizing of metal foam configuration is needed.

Beside fully filled by metal foam, the heat exchanger with partially filled metal foam is expeditious technology to gain both heat transfer and pressure drop. Both positive and negative sides are achieved to improve the heat transfer while minimizing the pressure drop. Wrapped the porous media outside the tubular heat exchanger is an example for its application.

The porous media wrapped around the cylinder modifies the onset of vortex shedding, resulting in a change in thermal properties. Therefore, to decrease the flow resistance in tubular heat exchangers, the metal foam is wrapped around the tube. Due to the buoyancy and viscous effects, the wake of a bare circular cylinder is periodic, with vortex shedding at Reynolds numbers greater than 40. The buoyancy effect causes negative vorticity on the cylinder's downstream side. As a result of the fluid penetrating into the porous area from the front stagnation point to a

specific angle, the heat and mass transfer rate increased. The downstream heat transfer process was dominated by conduction.

The value of angle fabric porous was found by Sobera et al. (2003), which is 50°. The critical values were taken by the thickness and permeability of the porous layer. If the conditions pass the critical value, the heat conduction will dominate the heat transfer because the velocity in porous media is low. If the conditions blow the critical values, the heat convection will dominate the heat transfer because it occurs in both porous media and clear area.

Odabaee et al. (2012) thoroughly evaluated the performance of a cylinder wrapped in metal foam using the first and second laws of thermodynamics. Porosity was used to represent thermal conductivity, permeability was used to represent penetration ability, and metal foam thickness was used to represent heat transfer area. Regarding bare cylinder as the benchmark, the comparisons of the area goodness factor for different cylinders revealed that the increase of permeability induced the heat transfer per unit of pressure drop at the cost of an increase of pressure drop.

Metal foam thickness had a critical value for heat transfer per unit of pressure drop. Heat transfer per unit of pressure drop increased slightly above the critical value. The phenomenon was demonstrated by calculating the total entropy generation rate.

Tube bundles, one of the most well-known types of heat exchangers, have been used in a various industrial application. Metal foam is able to provide a larger specific surface area than commercial fins due to its compactness. As previously discussed, metal foam fully filled in gaps of tube bundle results in significant heat transfer enhancement at the expense of significant pressure drop.

The pressure drop could be reduced by reducing recirculation and vortices in the layout of metal foam as an interconnector in an in-line tube bundle. However, the improvement in heat transfer was not significant (Ramana et al., 2010).

There are two separated parts of fluid in the tube bundle wrapped with metal foam. The first fluid developed a zigzag flow, and the second penetrated the metal foam area. It is not same with the single cylinder wrapped in metal foam, the front and rear tubes influence the wake with vortex shedding.

METAL FOAM FOR SOLAR THERMAL EQUIPMENTS

The solar thermal equipment is defined into two types which are concentrating and non-concentrating. Overall metal foam is used to improve the solar thermal equipment efficiency due to its high thermal performance.

Non concentrating solar collectors use in intermediate low temperature. One of commonly application of non-concentrating solar collectors in industry is the flat plate solar collector. However, the solar energy flux density distribution is not even, and convection between the fluid and radiant absorber plate is inefficient. The application of metal foam was investigated for designing heat advanced device in solar collector pipe or channel.

Jouybari et al. (2017) tested the effects of two parameters in a thin flat-plate solar collector fully filled with metal foam which are radiation and the foam shape. Evidently, the radiation gives prominent effect than the shape of foam. At a constant Darcy number range, the increase of pressure drop is neglected. The experimental results also showed the Nusselt number increased up to 82% by the application of porous material.

A series of study of convective heat transfer in flat plate solar collector filled by metal foam, with three different methods such as numerical, analytical, and fin-analysis method, was done by Xu et al (2014). The metal foam channel performs great properties both in thermal performance and flow resistance ability. This study discovered when the porosity raised until 95%, thus the local thermal non-equilibrium effect could be neglected.

For more complicated case involving the combination of conduction-convection-radiation energy equation, the homotopy perturbation method can be used to solve the case based on a semi-analytical approach (Denghan et al., 2015). Overall, the applications of fully filled metal foam on flat plate solar collectors offer better thermal performance but in the other side sacrifice the huge value of pressure drop.

Concentrating solar collector offers thermal energy at higher temperature than the flat plate solar collector. This kind of solar collector centralizes the solar energy before converted process into heat. The direct volumetric solar absorption collector utilizes porous material with ability to receive up to 1500°C temperatures. A ceramic porous absorber is researched by Chavez and Chaza (1991) and the result indicates the significant lost on radiative heat at the rate of temperature 730°C.

The experimental study of SiC foam with 0.785 porosity value and 30 pore per inch pore density was did by Pitz-Paal et al. (1997). An experimental study was also done by Albanakis et al. (2009) to compare the heat transfer performance in various materials, such as copper, nickel, nickel alloy, inconel, and aluminum. The experimental results detect nickel and inconel porous media stand out among other materials.

Zaversky et al. (2018) investigated ceramic foam volumetric receivers experimentally and numerically. The analysis revealed that the thermal performance was determined by the parameters of the first layer. Notably, the foam thickness had a minor impact on thermal performance and should not exceed 30 mm. The volumetric receiver performed better in terms of thermal performance as pore density and porosity were reduced. These characteristics were also discovered in a numerical study conducted by Wu et al. (2011). The correlation between the porosity effects, the extinction coefficient, and thermal conductivity are described by inverse relation. The result defines that the concentrated solar irradiance can penetrate deeper into the foam due to decreased pore density and increased porosity. Solar absorption dominates the heat transfer process.

The Monte Carlo ray tracing (MCRT) and finite volume method (FVM) are combined to gain a better understanding of solar absorption in foams. The increase of porosity raises the solid phase temperature of foam at the fluid outlet surface (Wang et al. 2013). Some studies on the thermal and flow characteristics of SiC and ceramic foam were also carried out to lay the groundwork for volumetric receiver design (Zaversky et al., 2018).

A parabolic through is the most well-known concentrating solar collector. Jamal-Abad et al. (2017) inserted copper foam into an absorber tube with a porosity of 0.9 and a pore density of 30 PPI. The results demonstrated that thermal performance was improved, particularly at lower flow rates.

One type of linear concentrating solar collector is the parabolic trough collector. Jamal-Abad et al. (2017) inserted copper foam into an absorber tube with a porosity of 0.9 and a pore density of 30 PPI. The results demonstrated that thermal performance was improved, particularly at

lower flow rates.

Valizade et al. (2020) compared full-copper and semi-copper foams arrangements of direct absorption parabolic through collectors. In contrast to the volumetric receiver, the solar absorbed by glass receiver and metal tube with metal foam functioned as a tubular heat exchanger. For improving the absorption ability and the thermos-physical effectiveness, the increase of pore density and the decrease of porosity are influential parameters. In this experiment, the full copper foam arrangement successfully improved the thermal efficiency up to 171.21%. Meanwhile, the semi copper arrangements improved up to 119,6%. Because of the shape of the light spot reflected from the multi-mirror, solar receivers with multi-dish collectors are commonly used in parabolic dish concentrator systems.

METAL FOAM FOR THERMAL ENERGY STORAGE

Thermal energy storage uses to relocate the renewable energy sources before distributing period which is most commonly used on solar thermal systems. It is able to be used for improving the compatibility of heating and air conditioning systems with electrical power supplies. Aligned with the rising of renewable energy source trend on recent years, the researches for supporting the advanced thermal energy storage are needed.

Sensible heat storage has the simplest method and the most developed technology for commercial industry because cheap and less danger materials. This system converts solar energy into sensible heat in a storage media, typically solid or liquid, and releases it as needed. Low thermal capacity is a weakness of sensible heat storage depending on its material.

Latent heat storage stores energy in phase change material (PCM). When the phase transition occurs, the thermal energy is stored at constant temperature. Zhou and Zhao (2011) presented the comparison of heat transfer properties of phase change materials embedded by metal foam and expanded graphite. Metal foam had higher heat transfer rate based on the continuous matrix. For providing an advanced thermal energy storage in the future, further understanding about the impacts of metal foam properties is a must.

Siahpush et al. (2008) found the copper foam with 95% porosity increased the effective thermal conductivity values from 0.423 up to 3.06 W (m K)-1 in experimental and analytical study of phase change heat transfer using porous foam. Another previous study discovered the use of metal foams with smaller porosities and higher pore densities are able to increase the heat transfer rate even more based on the experimental results of different metal foam samples (Tian et al., 2011).

An aluminium foam experiment with 9 pores per inch and 0.9137 porosity did by Chen et al. (2014). The numerical result carried out the heat conduction dominated the melting of phase change material which indicated the increasing of flow resistance in the domain by the implementation of metal foam. Meanwhile, the convection did not have a significant influence. For the optimal thermal energy storage design, the flow resistance should be reduced as minimum as possible. Sundarram et al. (2014) discovered that the phase change period increased due to the smaller pore size at a constant porosity. The transportable electronic devices had high heat generation with slight convective cooling. For this kind device, the effect of pore sixe and porosity also influenced by the heat generation and cooling system.

A shell tube as latent heat thermal energy storage was tested by Liu et al. (2013). The experiment method provided the high temperature fluid in tube, and phase change materials located in shell

side embedded with metal foam. The melting period decreased but the pores density increased from 10 up to 30. The pores density increased from 30 PPI to 60 PPI and the melting period lengthened. It showed that the pores density had reached a critical value, which caused the heat convection being the dominant process during the melting period.

The effect of metal foam ligaments ratio and phase change material heat conductivities on phase transition process is presented by Mesalhy et al. (2005). The linier relation between the ratio of metal foam ligaments and phase change material heat conductivities is detected. It is also discovered the use of high porosity and thermal conductivity metal foam material is the best way to improve the response of phase change material storage.

Shirbani et al. (2022) used Lattice Boltzmann method to observe the effects of various metal foam pore arrangements for increasing the phase change material. According to this study, the metal foam pore size and structure are the important parameters to determine the melting time. The closed cell metal foams are able to minimize the melting time by improving the heat transfer rate.

CONCLUSION AND FUTURE WORK

This paper observed the application of metal foam for heat transfer technologies. It is concluded that metal foam is suitable for optimizing heat exchanger technologies due to the characteristics. This review is focused on three main applications of metal foam on advanced heat exchanger, solar thermal equipment, and thermal energy storage.

On a macroscopic scale, the heat transfer laws for flow properties in metal foam are already defined. From its appearance, metal foam is surely confirmed as porous material. The microstructure properties of metal foam such as pore density, permeability, and porosity are proved for optimizing the heat transfer performance.

Metal foam embedded partially on heat exchanger is ideal way to minimize the pressure drop. The flow and temperature fields are affected by the interaction of the porous area and the fluid space area. For providing the advanced heat exchanger design, the relation between heat transfer improvement and pressure drop as the impacts of metal foam must be known first.

Metal foam is able to use for solar thermal collectors by integrating it with the radiation properties. The experimental effects of metal foam for non-concentrating solar collectors are reviewed in this paper. Evidently, the radiation gives prominent effect than the shape of foam. Meanwhile, the application of metal foam on concentrating solar collector causes domination term in directly receiving the solar thermal energy for solar energy absorber. The previous studies observed the effects of metal foam application on sensible heat storage and latent heat storage. It is proved that metal foam is able to improve the response of phase change material storage. Overall, metal foam offers the advanced thermal storage design for the future technology.

REFERENCES

A. Bhattacharya et al. Thermophysical properties of high porosity metal foams Int J Heat Mass Transf.2002.

A. Sertkaya, K. Altınısık, K. Dincer, Experimental investigation of thermal performance of aluminum finned heat exchangers and open-cell aluminum foam heat exchangers, Exp Therm Fluid Sci, 36 (2012), pp. 86-92.

Albanakis C, Missirlis D, Michailidis N, et al. Experimental analysis of the pressure drop and heat transfer through metal foams used as volumetric receivers under concentrated solar radiation. Exp Thermal

Antohe B V, Lage J L, Price D C, et al. Experimental determination of permeability and inertia coefficients of mechanically compressed aluminum porous matrices. J Fluids Eng, 1997, 119: 404–412.

Boomsma K, Poulikakos D. On the effective thermal conductivity of a three-dimensionally structured fluid-saturated metal foam. Int J Heat Mass Transfer, 44: 827–836, 2001.

Boomsma K, Poulikakos D, Ventikos Y. Simulations of flow through open cell metal foams using an idealized periodic cell structure. Int J Heat Fluid Flow, 24: 825–834 40, 2003.

Brinkman H C. A calculation of the viscous force exerted by a flowing fluid on a dense swarm of particles. Appl Sci Res, 1949, 1:27.

Buonomo B, di Pasqua A, Ercole D, et al. Numerical investigation on aluminum foam application in a tubular heat exchanger. Heat Mass Transfer, 2018, 54: 2589–2597

Buonomo B, Pasqua A, Ercole D, et al. Numerical investigation on a heat exchanger in aluminum foam. Energy Procedia, 2018, 148: 782– 789.

Calmidi V V, Mahajan R L. Forced convection in high porosity metalfoams. J Heat Transfer, 2000, 122: 557–565.

Chen Z, Gao D, Shi J. Experimental and numerical study on melting of phase change materials in metal foams at pore scale. Int J Heat Mass Transfer, 72: 646–655, 2014.

Dae Yeon Kim, Tae Hong Sung, Kyung Chun Kim, Application of metal foam heat exchangers for a high-performance liquefied natural gas regasification system. Volume 105, Pages 57-69, 15 June 2016.

Dehghan M, Rahmani Y, Domiri Ganji D, et al. Convection-radiation heat transfer in solar heat exchangers filled with a porous medium: Homotopy perturbation method versus numerical analysis. Renew Energy, 2015, 74: 448–455.

Du Y P, Qu Z G, Zhao C Y, et al. Numerical study of conjugated heat transfer in metal foam filled double-pipe. Int J Heat Mass Transfer, 53: 4899–4907, 2010.

Forchheimer P. Wasserbewegung durch boden. Z Ver Deutsch Ing,1901, 45: 1782–1788

Huisseune H, De Schampheleire S, Ameel B, et al. Evaluation of the thermal hydraulic performance of round tube metal foam heat ex-changers for HVAC applications. In: Proceedings of the International Heat Transfer Conference. Kyoto, 2014.

Huisseune H, De Schampheleire S, Ameel B, et al. Comparison of metal foam heat exchangers to a finned heat exchanger for low reynolds number applications. Int J Heat Mass Transfer, 2015, 89: 1–9.

Jamal-Abad M T, Saedodin S, Aminy M. Experimental investigation on a solar parabolic trough collector for absorber tube filled with porous media. Renew Energy, 107: 156–163, 2017.

Jouybari H J, Saedodin S, Zamzamian A, et al. Effects of porous material and nanoparticles on the thermal performance of a flat plate solar collector: An experimental study. Renew Energy, 2017, 114: 1407–1418.

Krishnan S, Garimella S V, Murthy J Y. Simulation of thermal transport in open-cell metal foams: Effect of periodic unit-cell structure. J Heat Transfer, 130: 024503, 2008.

Liu Z, Yao Y, Wu H. Numerical modeling for solid-liquid phase change phenomena in porous media: Shell-and-tube type latent heat thermal energy storage. Appl Energy, 112: 1222–1232, 2013.

Lu W, Zhao C Y, Tassou S A. Thermal analysis on metal-foam filled heat exchangers. Part i: Metal-foam filled pipes. Int J Heat Mass Transfer, 2006, 49: 2751–2761

Mesalhy O, Lafdi K, Elgafy A, et al. Numerical study for enhancing the thermal conductivity of phase change material (PCM) storage using high thermal conductivity porous matrix. Energy Convers Manage, 46: 847–867, 2005.

M. Habibishandiz, M.Z.Saghir. A critical review of heat transfer enhancement methods in the presence of porous media, nanofluids, and microorganisms, Volume 30, 101267, May 2022.
M. Shirbani, M. Siavashi, M. Hosseini, M. Bidabadi. Improved thermal energy storage with metal foam enhanced phase change materials considering various pore arrangements: a pore-scale parallel lattice Boltzmann solution, J. Energy Storage 52 (2022) 104744.
Nield D A, Bejan A. Convection in Porous Media. Cham: Springer, 2017.
Odabaee M, Hooman K. Metal foam heat exchangers for heat transfer augmentation from a tube bank. Appl Thermal Eng, 2012, 36: 456–463.
Pitz-Paal R, Hoffschmidt B, Böhmer M, et al. Experimental and numerical evaluation of the performance and flow stability of different types of open volumetric absorbers under non-homogeneous irradiation. Sol Energy, 1997, 60: 135–150.
Ramana P V, Narasimhan A, Chatterjee D. Experimental investigation of the effect of tube-to-tube porous medium interconnectors on the thermohydraulics of confined tube banks. Heat Transfer Eng, 2010, 31: 518–526.
Ranut P, Nobile E, Mancini L. High resolution microtomography-based CFD simulation of flow and heat transfer in aluminum metal foams. Appl Thermal Eng, 69: 230–240, 2014.
Ranut P, Nobile E, Mancini L. High resolution X-ray microtomography-based CFD simulation for the characterization of flow permeability and effective thermal conductivity of aluminum metal foams. Exp Thermal Fluid Sci, 2015, 67: 30–36.
S.N. Roohani Isfahani, M.R. Salimpour, E. Shirani, Numerical study and sensitivity analysis on convective heat transfer enhancement in a heat pipe partially filled with porous material using LTE and LTNE methods, Heat TransferAsian Research 48 (8) (2019) 4342–4353.
Siahpush A, O'Brien J, Crepeau J. Phase change heat transfer en-hancement using copper porous foam. J Heat Transfer, 130: 082301, 2008.
Sobera M P, Kleijn C R, Van den Akker H E A, et al. Convective heat and mass transfer to a cylinder sheathed by a porous layer. AIChE J, 2003, 49: 3018–3028.
Sundarram S S, Li W. The effect of pore size and porosity on thermal management performance of phase change material infiltrated mi-crocellular metal foams. Appl Thermal Eng, 64: 147–154, 2014.
The International Energy Agency. World energy outlook 2019. https://www.iea.org/reports/world-energy-outlook-2019.
Tian Y, Zhao C Y. A numerical investigation of heat transfer in phase change materials (PCMs) embedded in porous metals. Energy, 36: 5539–5546, 2011.
Tzeng S C. Spatial thermal regulation of aluminum foam heat sink using a sintered porous conductive pipe. Int J Heat Mass Transfer, 2007, 50: 117–126.
Valizade M, Heyhat M M, Maerefat M. Experimental study of the thermal behavior of direct absorption parabolic trough collector by applying copper metal foam as volumetric solar absorption. Renew Energy, 145: 261–269, 2020.
Wang F, Shuai Y, Tan H, et al. Heat transfer analyses of porous media receiver with multi-dish collector by coupling MCRT and FVM method. Sol *Energy, 93: 158–168*, 2013.
Wang H, Guo L J, Chen K. Theoretical and experimental advances on heat transfer and flow characteristics of metal foams. Sci China Tech Sci, 63: 705–718, 2020.
Wu Z, Caliot C, Flamant G, et al. Coupled radiation and flow modeling in ceramic foam volumetric solar air receivers. Sol Energy, 2011, 85: 2374–2385
Xu H, Gong L, Huang S, et al. Non-equilibrium heat transfer in metal-foam solar collector with no-slip boundary condition. Int J Heat Mass Transfer, 2014, 76: 357–365 138.
Xu Y, Chung D D L. Increasing the thermal conductivity of boron nitride and aluminum nitride particle epoxy-matrix composites by particle surface treatments. Composite Interfaces, 2000, 7: 243– 256.

Zaversky F, Aldaz L, Sánchez M, et al. Numerical and experimental evaluation and optimization of ceramic foam as solar absorber— single-layer vs multi-layer configurations. Appl Energy, 2018, 210: 351–375

Zhao C Y, Kim T, Lu T J, et al. Thermal transport in high porosity cellular metal foams. J Thermophys Heat Transfer, 18: 309–317, 2004.

Zhou D, Zhao C Y. Experimental investigations on heat transfer in phase change materials (PCMs) embedded in porous materials. Appl Thermal Eng, 31: 970–977, 2011.

CHAPTER 3

MONOCOQUE CHASSIS

Melike EROĞLU[1],
Selcuk University, Konya/Turkey
ORCID: 0000000180850301

Ömer Cem GÖKDOĞAN[2]
Selcuk University, Konya/Turkey
ORCID: 0000000250911588

Süleyman NEŞELİ[3]
[3]Selçuk Üniversitesi, Konya/Turkey
ORCID: 0000-0003-1553-581X

Gökhan YALÇIN[4]
[4]Konya Technical Universty, Konya/ Turkey
ORCID: 0000-0003-4491-0228

INTRODUCTION

The part where the parts, including the bodywork, are gathered in one spot is the chassis. The construction of the chassis, which has many mathematical calculations, is actually not so simple. As well as its rigidity, sprain angles are given great importance. At the same time, when the chassis is exposed to any force, it must provide the resistance to meet it. One of the most important features of the chassis is to absorb most of the resistance during an accident and minimize damage. In terms of cost, one-piece chassis are cheaper and have been used in mass production vehicles in previous years.

[1] The driving position of the driver in the vehicle is very important for ergonomics. Due to the narrow layout of the vehicle, drivers have serious problems with steering control. It is important that the driver is comfortable in the harsh conditions of the competition.

The driver's driving position and steering are important. For this reason, care must be taken in the design of the chassis so that the driver can feel safe in the cockpit and have a spacious space.

5 BASIC LOAD CONDITIONS	
1	Bending condition (Bending)
2	Torsion
3	Combined bending and bending state
4	Lateral loads
5	Longitudinal loads (Longitudinal)

Although rigidity seems to be important in chassis design, it must first provide high strength, inertia, weldability, and be suitable for bending and cutting functions. It also needs to absorb forces from any direction. Stresses are expected to be homogeneously distributed rather than accumulating at a certain point on the chassis. If the weight-rigidity balance is not achieved, the performance of the vehicle decreases. One of the most important points when designing the chassis is to eliminate the loads that the vehicle is exposed to while it is static and dynamic and to make the appropriate design. These loads are given in the table below.

CHASSIS

We can call the chassis basically the body or skeleton that serves to hold the parts of the car together. Of course, it is not limited to these, but it is one of the elements that affect the handling. The most important example of this is the force on the vehicle when the vehicles enter the corner. When you turn right while driving at a certain speed, we feel that we are sliding left in the car, this force is felt not only by us but also by the chassis of the car. This feeling in the frame will come back to us as a sprain. That's why the chassis we designed is designed in monocoque to be both force-resistant and lightweight in weight. A monocoque chassis is basically a frameless chassis, also known as a unit chassis. There are no joints in the monocoque chassis. But the conventional chassis has bolted or welded connections. It is the section where all the parts are

assembled, which meets the impact violence at the time of the accident, and which minimizes the severity of the accident by breaking through the necessary breaking points. A chassis must be durable, lightweight, rigid and have few parts.

Since vehicle classes are in different areas and tasks, the carrier chassis parts are also structurally separated from each other. The types of chassis are shown below.

CHASSIS TYPES

1. Parallel arm chassis
2. Ladder Type Chassis
3. X Type Cross Arm Chassis
4. Single Arm Platform Type Chassis
5. Fork Sleeve Chassis
6. Monocoque Chassis

Parallel Arm Chassis

It is the type of chassis commonly used in trucks and buses. It consists of two parallel arms and crossbars connected to these two arms. The arms are usually made in the press with U, square, rectangular and circular sections. Sleepers and superstructure; it is attached to the chassis arms with welding, rivet and bolts.

Ladder Type Chassis

The ladder chassis, named for its resemblance to a ladder, is one of the oldest, simplest, and most frequently used lower body, separate chassis/chassis designs. It consists of two symmetrical beams, profiles or channels that run along the length of the car and are connected by several transverse transverse links.

X Type Cross Arm Chassis

As the name suggests, it has the shape of x. This type of chassis is usually lightweight.

3.4.Single Arm Platform Type Chassis

It is a chassis type that is often preferred in automobiles.

Fork Sleeve Chassis

It is advantageous in terms of its use. In cars, there are protrusions that extend to the front. They are usually designed to transport the engine and engine elements.

Monocoque chassis

Monocoque type chassis design is a design method made to support and protect the outer body against incoming influences. The fact that the chassis is whole allows the mechanical elements to function as the main structural element to which it is attached. There are also semi-monocoque designs.

The word monocoque, as its name suggests, is a term of French origin meaning "one shell" or "one body". When we look at the history of the monocoque, we see that it was first used for

boats, and it is known for the fact that it carries both pulling and compression forces in the shell, as well as the absence of an inner frame that carries a load. Monocoque bodies do not have a lot of beams and mixed mixed structures. The beams in monocoque bodies are mostly used to shape and align the body. The main beams consist of surface and partition walls. Although monocoque bodies are resistant to any impact, they immediately undergo deformation (deformity) and corrosion (wear, rust.) when there is a depression or crush on the surface. At the same time, production costs are less. It provides flexibility in design and has a wide range of uses. Monocoque bodies are able to absorb (suck, destroy) sudden impacts.

The vehicle chassis designed for the International Teknofest "Efficiency Challenge" Electric Vehicle Races is designed as a monocoque chassis. Apart from being lightweight, the most important reason for choosing a monocoque chassis is that it is more durable and flexible compared to chassis combined with welding or bolt connection. Thanks to this flexible structure, it prevents the stresses that may occur from gathering at a point and can spread the stresses throughout the body. The length of the chassis is 3367 mm and the width is 1253 mm. The thickness of the channels is 98 mm, the height is 92 mm and the distances between the channels are 6 mm.

The material used is glass fiber, which is the same material as the shell due to the fact that it is monocoque. Fiberglass material is not easily deformed with its durability and is therefore preferred.

Glass fiber material characteristics:

- It is highly resistant to corrosion.
- It is not affected by heat or cold.
- There is no fluid permeability.
- Its shape does not deteriorate and resists impacts.
- It is suitable for production in different shapes and colors.
- It is a lightweight material.
- Thanks to its fiberglass properties, it can be easily shaped.
- It does not mold or rust.

• It is a health-friendly material and can be used in all areas.

• Thanks to its durability, it has a long service life.

At the same time, the monocoque chassis has more advantages than the aluminum frame. Monocoque design can provide us better ground clearance. They are also always lighter than traditional ones, and weight has always been an important factor in the automotive industry. Figure 1, Figure 2 and Figure 3 show a render image of the monocoque chassis.

Figure 1: Monocoque chassis render image

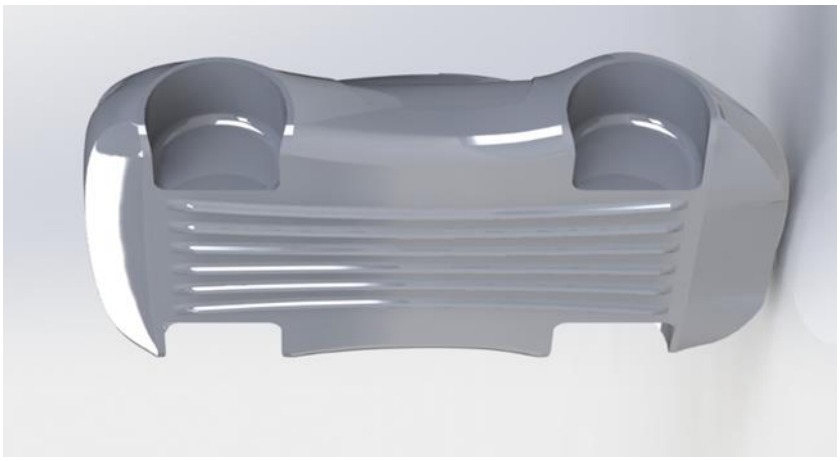

Figure 2: Monocoque chassis render image

Figure 3: Monocoque chassis render image

MONOCOQUE CHASSIS ADVANTAGES
Compared to the normal chassis, the design of the monocoque chassis can be made easier to edit and innovate.
The monocoque chassis has a greater ground clearance.
Provides flexibility in design.
They are light and therefore have low fuel consumption.
It costs less.
Their impact resistance is high.
Tire deformations are less.
It prevents the accumulation of stresses in one area, spreads them to the general.
Since it is not a rigid structure like a normal chassis, it provides flexibility and ensures that warnings from the road are not transmitted to the passenger area.
Due to the even distribution of stress, the torsional stiffness of the chassis is high and proves to be advantageous for the suspension as it can improve the performance of the car.
The area of use is wider.

[1]Chassis Analysis After the design stages are completed, static analyzes of the chassis are performed. The main issue considered in chassis analysis is torsional rigidity. Torsional rigidity is defined as the resistance of the chassis to incoming moments (Bhande et al., 2018). The most

important feature of the Formula Student racing car is its torsional rigidity. In this way, the race car resists torsion along its transverse axis in corners. If the chassis is not rigid enough, the suspension will not be able to fully perform its job. This has a serious impact on the performance of the vehicle. The comparison of the chassis of the race car with other chassis is made by proportioning its rigidity to its weight. But in this case, some problems arise.

[1] For example, if a chassis is too rigid and too heavy, the ratio will be too small. But in reality, there will be a decrease in the performance of the vehicle because the vehicle will be too heavy. Therefore, it is more important to ensure weight-rigidity balance rather than high rigidity (Krzikalla et al., 2019). When performing smash analyses, first of all, mesh (meshing) is performed on the chassis body. The process of networking can be expressed as the process of putting the chassis body together by dividing it into small pieces and analyzing each divided part individually. After meshing, it is necessary to apply forces and fix the chassis in the appropriate places. In chassis analysis, the fixation points are suspension connection points. The force points are again the suspension connection points in the analyzes made to measure the torsional rigidity. After all these procedures, analysis was applied.

REFERANCE

[1] Yigit Alp Oymak, Erol Feyzullahoglu. Mechanical Engineering, Kocaeli, Turkey "Formula Student Race Car Chassis Design and Analysis" https://web.archive.org/web/20210630024504id_/https://dergipark.org.tr/tr/download/article-file/1841790

[2] Neşeli, S., Yalçın, G., Terzioğlu H., Ağaçayak A.C. (2019). Nano Yüzey Kalitesi Oluşturmak İçin Lepleme Makinesi Tasarımı. V Scıence Technology and Innovatıon Congress, 374-380. (Tam Metin Bildiri/Sözlü Sunum)(Yayın No:5601104)

[3] Jingsi Wu, Owusu Agyeman Badu, Yonchen Tai, Albert R. George, Cornell Univ. New York, ABD, "Bir Otomotiv Karbon Fiber Monokok Şasinin Tasarımı, Analizi ve Simülasyonu" https://www.sae.org/publications/technical-papers/content/2014-01-1052/

[4] Erkan Karaca, https://bilgihanem.com/sasi-nedir/

[5] Mustafa Ersöz Volvo Cars-Group Design Leader-Battery Containment Systems/Traction Battery https://tr.linkedin.com/pulse/ara%C3%A7larda-bulunan-%C5%9Fasi-nedir-onu-etkileyen-temel-kuvvetler-ers%C3%B6z

[6] https://erlas.com.tr/fiberglass-endustriyel-urun-imalati/fiberglass-nedir

[7] https://tr.wikipedia.org/wiki/%C5%9Easi

[8] Aytaç Gören, Özgün BA ER, Res.Assist. DEU Mechanical Engineering,

[9] Cuma Polat, Micenaean Engineering, METU Aerospace Engineering Department https://www.mmo.org.tr/sites/default/files/4c4c17332cace21_ek.pdf

[10] Yalçin G.,Neşeli S.,Terzioğlu H.,Ağaçayak A.C. (2019). Design and Construction of Compact CNC Router. International Conference on Engineering Technologies (ICENTE'19), 1(3), 474-478. (Tam Metin Bildiri/Sözlü Sunum)(Yayın No:5642081)

[11] Yalçin G.,Neşeli S.,Terzioğlu H.,Ağaçayak A.C. (2018). Fatigue Tester Design and Frame Analysis for Estimation of Fatigue Life of Helical Compression Springs. International Conference on Engineering Technologies (ICENTE'1 8), 563-566. (Tam Metin Bildiri/Sözlü Sunum)(Yayın No:4509752)

CHAPTER 4

GULL-WING DOOR HINGE DESIGN AND MANUFACTURING

Emine ALAN[1]
[1] Selcuk University, Konya/Turkey
ORCID: 0000-0002-7970-5155

Namik Kemal YALÇIN[2]
[2] Selcuk University, Konya/Turkey
ORCID: 0000-0002-8715-2087

Süleyman NEŞELİ[3]
[3]Selçuk Üniversitesi, Konya/Turkey
ORCID: 0000-0003-1553-581X

INTRODUCTION

The door hinge system, which is one of the most important designs of today's vehicles, has undergone changes for years. The types of doors are traditional doors, butterfly doors, suicide doors, Gull-Wing wing doors, lambo doors, sliding doors and canopy doors. Car doors have been modified and developed by new designers since 1886. During the development, the models were devoted to the purposes of construction, and they were criticized by their negative effects and disappeared into history. The purpose of the Gull-Wing door; is the opening of the door upwards by holding on to the roof of the vehicle part. The door is supported by hinges and pistons so that the driver and passenger can exit.

Hadi et al. (2022) Door hinges and latches are door retention mechanism elements that play an important role in automobiles by holding the door open in the event of a side impact or rollover collision. Hinges are a group of components that are attached to the vehicle's door and frame, are related to one another, and can rotate along the same axis. Latches are mechanical devices that are used to position the door in a closed position relative to the vehicle body while allowing for controlled release. The standard specific conditions for side door latches and hinges installed on cars to reduce the risk of passengers being thrown out of the vehicle as a result of any impact. The objective of this paper is to identify the weakest point and to perform a structural analysis of automotive door hinge. Computer Aided Design (CAD) software is used to build a CAD model of the hinge and lock. The models of such components is meshed, and boundary conditions is defined, using the commercial meshing program. ANSYS is used to analyses the structural behaviour. Based on the results, the component will be further optimized for the future work. [1]

Yılmaz et al. (2017) Recently, lightweight design concepts have come into prominence for vehicle industry, especially for economic and environmental sustainability. Vehicle manufacturers have investigated new material usage to reduce fuel consumption and air pollution as increasing concerns. On the other hand, new legal obligations and global competition have accelerated this research and development process. Designing components with low-density materials is one the most common methods for reducing CO2 emissions. Among these materials, aluminum alloys stand out due to their adequate mechanical properties and specific strength. In this work, the study of lightening door hinges of a commercial vehicle is presented. To reduce the weight of vehicle door hinge, three different aluminum alloys are tried out and compared with steel. Finite element analysis (FEA) and experiments are conducted to determine if the safety requirements are fulfilled or not. According to results with an Al7075-T73 alloy, the weight of door hinge can be reduced by approximately 65%. Stress and strain values are suitable for FMVSS0206 standards. Additionally, it passed the corrosion test. [2]

Yang et al. (2010 The Door hinge is a very important part for door sagging performance of a vehicle. It is divided into two classes as a forge- and press-type according to a manufacturing technique. The press-type door hinge is cheap, but shows low strength. To apply the press-type door hinge to a fullsized car with satisfactory door sagging performance, we optimized the design parameters of the door hinge using the DFSS method. As a result, the effective design parameters of the press-type door hinge with good door sagging performance were obtained. [3]

Kusztelan et al. (2010) In comparison with vertical hinge doors which they are attached at the front-facing edge of the door to the vehicle's pillars, gull-wing doors are hinged at the roof enabling the passenger to egress and ingress into the vehicle far easier. This is due to the increased area created by the upward motion of the door. By using the gull-wing doors, the need for extra space between parallel-parked cars also decreases. The use of gull-wing doors for vehicles is born out of its necessity rather than an innate desire to use this type of door feature.

This could be for a variety of reasons. The most common reason being that the cooling ducts and radiators are found in the sills left and right of the vehicles doors, which is why gull-wing doors are used primarily in racing cars. The location of the ducts and radiators eliminate the use of conventional opening mechanisms and create the need for gull-wing doors. The door hinges act as a means of pivoting a door from an open and closed position, but must also withstand sufficient loads to protect passenger against injury during collision. In this paper, a review of various design possibilities for gull-wing door hinges specifically for automotive applications from available patents has been discussed and the advantage and disadvantage of each design highlighted. [4]

In this study, the Gull-Wing door design was made using SolidWorks program. The Gull-Wing is designed taking into account all the movements that the door is expected to make. In order to minimize the deformation and corrosion of the gull door hinge during the continuous opening and closing of the vehicle door selection of the material, galvanized sheet with high resistance and easy to shape was preferred. The designed gull door hinge consists of a total of 6 galvanized sheet parts, 2 of which are twisted, with a thickness of 2 millimeters in order to make the expected movements and to be used.

MATERIAL METHOD

In this study, the Gull-Wing door hinge was made by using galvanized sheet material that can be easily bent and resistant to deformation, corrosion in order to design and manufacture. The car is secured by means of 5 metric screws. It is fixed to the vehicle by means of 6 screws, 3 to the shell of the vehicle, 3 doors. The position of the Gull-Wing Door Hinge in Figure 1, the Explosion Technical Picture of the Gull-Wing Door Hinge in Figure 2, and the Gull-Wing Door Hinge Installation in Figure 3 are seen.

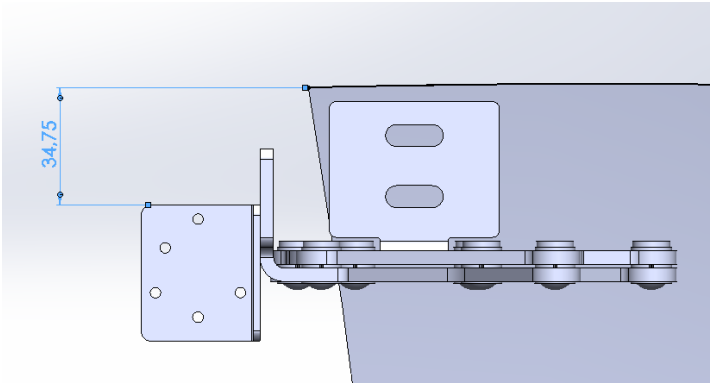

Figure 1. Position of Gull-Wing Door Hinge1

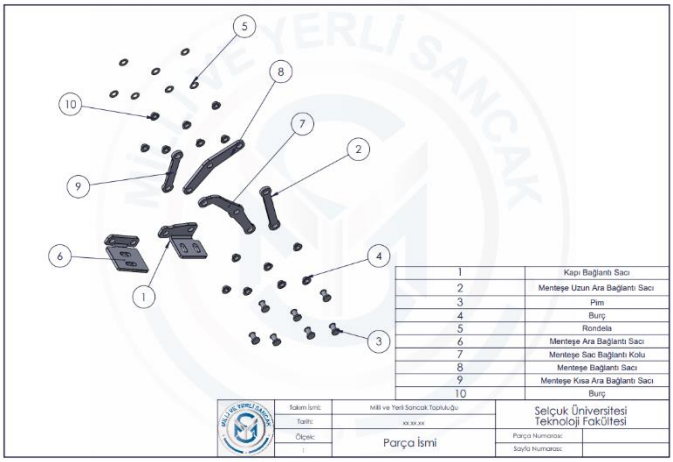

Figure 2. Gull-Wing Door Hinge Explosion Drawing2

Figure 3. Gull-wing Door Hinge Installation3

Door hinges allow tools to be rotated around a specific axis for their purpose. The angles of the door opening movements vary from supply to demand and are divided into 90°, 180° and 270°. The angle of movement of the gull-wing door hinge is determined as 180° for opening upwards and for a person to come out easily. In Figure 4, the Full Open State of the Gull-Wing Door Hinge, in Figure 5 the Fully Closed State of the Gull-Wing Door Hinge, in Figure 6 the Solid View of the Gull-Wing Door Hinge 1, in Figure 7 the Gull-Wing Door Hinge Solid View 2 is seen.

Figure 4. Gull-Wing Door Hinge Full Open4

Figure 5. Gull-Wing Door Hinge Fully Closed5

Figure 6. Gull-Wing Door Hinge Solid View 16

Figure 7. Gull-Wing Door Hinge Solid View 27

After the design of the designed gull door hinge was completed, it was put into maximum yield stress and total deformation analyzes. The results of these analyzes are given below.

The designed gull door hinge is designed according to the maximum force values that can be exited during operation. In Figure 7, Martı Door Hinge Total Deformation Analysis Picture is seen, and in Figure 8, Martı Door Hinge Maximum Yield Stress Analysis Picture is seen.

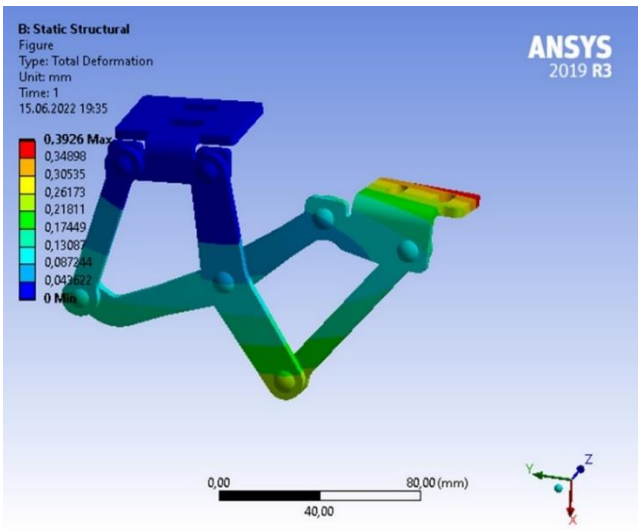

Figure 8. Gull-Wing Door Hinge Total Deformation Analysis Picture8

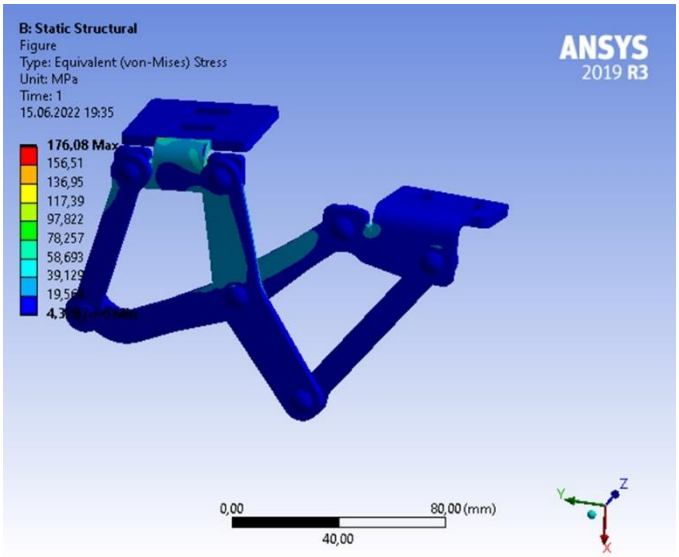

Figure 9. Gull-Wing Door Hinge Maximum Yield Stress Analysis Picture 9

GULL-WİNG DOOR HINGE WORKING PRINCIPLE

Gull-Wing door hinge design is designed and manufactured so that the range of motion is 180°. Gull-Wing door hinge can make movements on the X and Y axis synchronously. Before the manufacture of the Gull-Wing door hinge, simulations were made and monitored to check that it could make the desired movements correctly in the SolidWorks program, and also the maximum yield stress and total deformation analyzes that will affect the gull door hinge were made through the ANSYS program.

DISCUSSION AND CONCLUSION

The Gull-Wing Door Hinge, which has been designed and turned into a product, is the type of door that works in the best synchronous way with NFC card systems as well as adding a very

nice image to the vehicle design. The cost of the Gull-Wing Door Hinge, which is designed and produced, is approximately 300 Turkish Liras.,

As a result of this work, a gull door hinge made of easily bendable material resistant to deformation, corrosion was made. The designed Gull-Wing door hinge design will be revised according to the desired vehicle and can be used in all vehicles.

In the study to be carried out later, the dimensions can be revised according to the desired vehicle. It can be produced from a more durable material according to the dimensions and weights of the vehicle to be revised. Its design can be revised so that it can be applied more comfortably to different vehicles.

REFERENCES

[1] Hadi, M.I., Akramin, M.R.M., Shaari, M.S. (2022). Finite Element Analysis of Automotive Door Hinge. In: Ismail, M.Y., Mohd Sani, M.S., Kumarasamy, S., Hamidi, M.A., Shaari, M.S. (eds) Technological Advancement in Mechanical and Automotive Engineering. ICMER 2021. Lecture Notes in Mechanical Engineering. Springer, Singapore. https://doi.org/10.1007/978-981-19-1457-7_1, Print ISBN978-981-19-1456-0

[2] Yılmaz, T. G., Tüfekçi, M., & Karpat, F. (2017). A study of lightweight door hinges of commercial vehicles using aluminum instead of steel for sustainable transportation. Sustainability, 9(10), 1661.

[3] Yang, J. H. (2010). The Optimization of the Press-type Door Hinge of the Full-sized Car. Journal of the Korean Society for Precision Engineering, 27(5), 48-55.

[4] Kusztelan, A., Hadavinia, H., & Marchant, D. R. (2010). Recent Patents in Automotive Gull-Wing Door Hinge Mechanisms. Recent Patents on Mechanical Engineering, 3(1), 51-64

[5] https://books.google.com.tr/books?hl=tr&lr=&id=__o5AQAAMAAJ&oi=fnd&pg=PR1&dq=car+Gull-Wing+door+hinge+design&ots=BaiL3pjgOh&sig=GOcA4sVsD0BibD8WWLgIz-F-g8Q&redir_esc=y#v=onepage&q=car%20Gull-Wing%20door%20hinge%20design&f=false

[6] https://acikerisim.uludag.edu.tr/bitstream/11452/1403/1/455507.pdf

[7] Yalçın G.,Ağaçayak A.C., Bozkır M., (2020). Bölüm 1: Modern İmalat Yöntemlerine Genel Bakış. Elektriktrikli Araçlara Genel Bakış 1, İksad Yayınevi, Basım sayısı:1, ISBN:978-625-8423-15-0. pp. 3- 33..

.

CHAPTER 5

ENHANCING PERFORMANCE OF DATA PRIVACY ONTHE CLOUD USING CRYPTOGRAPHY WITH STEGANOGRAPHY IN PYTHON

Md Al Amin HOSSAIN
Selcuk University, Konya/Turkey
0000-0003-3382-5300

INTRODUCTION

Due to how efficient it is to deliver services through thecloud,cloud computing asrecently experienced significant growth in popularity. Users are working online todevelop applications and store data in a cloud environment. Cloud computing has three primary applications. Software as aService (SaaS) refers to internet-deployed software programsthat can serve as service providers to end users [1]. Othertypes of cloud services include Infrastructure as a Service(IaaS) and Platform as a Service (PaaS). Data security is nowa key concern because data is being stored online. In cloudtechnology, numerous users collectively keep a sizable amount of data in the cloud. Information security, secrecy, authenticity, fairness, and validation pose a wide range ofchallenges. Most cloud service providers keep data in an unencrypted format; therefore, if data security is necessary, users must use their encryption algorithm [1]. Every time thedata is transmitted, it must first be decrypted [1].

Cryptography in the cloud can be used to secure sensitive information in a business IT environment that is no longer under our control. By implementing encryption techniques, cryptography as a methodology ensures confidentiality and prevents illegal access to data. The Data Encryption Standard (DES), Advanced Encryption Standard (AES), ElGamal ECC, and RSA are among the algorithms designed for public key encryption to maintain network security [2]. All cryptosystems were built on arduous arithmetic computations in the beginning. Asymmetric encryption involves either factoring huge prime numbers (RSA) or focusing on discrete log problems (DLP). Symmetric encryption is dependent on a secret single key and simple mathematical implementations such as substitutions and permutations. A holomorphic cryptosystem is another name for the public cipher cryptography technique [1].

When using a shared cipher cryptosystem, the key size is crucial. Public key encryption demands a lot of computational resources because of the large key length. The difficulty of excessive key sizes has been resolved by elliptic curve encryption[1]. Elliptic curve cryptosystems can use fewer computing resources by using smaller keys, and they can be used in cloud environments [3, 4]. Additionally, elliptic curve cryptosystems can provide faster implementation, narrower bandwidth requirements, and reduced storage requirements. It is assumed that a 256-bit ECC is similar to a 3072-bit RSA [1,5]. It is well known that using ECC to encrypt data offers the same security as using RSA but is deployed considerably more quickly[6].

The ElGamal cryptosystem is analogous to ElGamal encryption utilizing Elliptic Curve mathematical functions over a finite field[5]. ElGamal and RSA factors are identical in size in the worst-case scenario [7]. ElGamal can be formed over elliptic curve groups, which minimizes factor size (1024bit RSA vs 160-bit elliptic curves at the same security level) [1]. The ElGamal algorithm is employed in encryption and decryption and is principally valued for its capacity to make key predictions incredibly difficult. The only goal of the ElGamal block cipher method is to make it nearly impossible for an adversary to figure out the encryption strategy even if they (unauthorized persons) are aware of some crucial facts. Its major focus is the difficulty of using the cyclic group to find the discrete logarithm [7].This technique is also perceived to be highly optimized for handling data transfer over a private or public network, especially for application-level security.

Steganography is a technique for concealing sensitive information by incorporating it into another piece of code, such as a text, image, audio, or video file [8]. Steganography differs from cryptography in that it hides the message's existence, whereas cryptography hides the message's content. Occasionally, encryption is used in combination with steganography. Even if the encrypted file is cracked, the hidden information cannot be displayed because steganography may still be employed to obscure data in an encrypted file [9]. The least significant bits (LSB), masking and filtering, and redundant pattern encoding are widely known ways to disguise a message. LSB is the easiest and most used method for all kinds of steganography [10]. But masking is more durable than LSB and allows images to pass cropping, compression, and some image segmentation [11].

Grayscale and 24-bit images are more suited to masking and filtering procedures [12]. They are sometimes employed as digital watermarks, concealing information in a manner like watermarks on actual paper. Instead of simply burying the secret message in the noise, masking techniques integrate information in key locations to make it a more integrated part of the cover image. This makes it better suited than LSB, for example, a lossy JPEG image [13].

Steganography and cryptography will be used in the model to increase security [14]. Several encryption techniques have different challenges. To improve the efficiency of the encryption method by utilizing less computational resources for the Cloud environment, this study suggests ElGamal using ECC to reap the benefits of tiny key sizes. Additionally, this model has been designed to combine masking and filtering as a steganographic technique to improve security. An effective and secure encryption system is essential to protect and store data in a cloud environment. In this work, a paradigm for storing data across many servers has been suggested, with the goal of ensuring both authentication and encryption. For the conclusion, we will use simulations and mathematical modeling to create a comparative analysis.

RELATED WORK

It is necessary to combine upgraded steganography with cryptography in order to strengthen a data privacy approach in an internet-based environment. Numerous researchers have recognized security concerns related to the deployment of cloud computing. They also propose potential methods and models that can be utilized to address these concerns. For this reason, a few relevant categories of literature on these strategies are summarized as follows, along with their corresponding features and challenges.

Kumar et al [15] mainly focused on the hybrid method of AES and the Full Homomorphic Encryption (FHE) method. Instead of adopting a single cryptosystem, the authors of this study secure cloud storage by using hybrid cryptographic techniques. They think that if AES can encrypt data via a 256- bit square with 14 cycles, then the technology may also be applied to cloud computing. The second phase's encryption process is based on a fully homomorphic encryption technique. Multiplication by holomorphs achieves two things: more substance and multiple holomorphs. Only computations for substances that have been added will be accessible to the user. The user is now using the shared secret and the ciphertext obtained from the initial scrambling. The cipher text and secret key will now be combined via homomorphic substance encryption. By using this technique, the user can protect data consistency, confidentiality, and secrecy from intruders.

Khan et al [1] suggested that encryption helps to reduce the danger of sensitive data loss or alteration by an unauthorized party when sending it via an insecure route.The authors claim that in today's enormous data centers and cloud computing, protection is a big concern. Since the key used in elliptic curve cryptography is quite small, ECC is utilized in this study to encrypt

data in the cloud. The elliptic curve needs the least amount of energy because of its small key size, which reduces the amount of computational power required. In this work, ECC is used for encryption, key generation, and decryption. Making a secure and reliable encryption technique requires careful consideration while choosing Point P (x, y). The report suggests a two-layered approach to cloud data protection. The data is divided into smaller pieces, and then it is encrypted with a random safe curve.

According to Denis et al [16], data transmission has been discovered to benefit from an improved security paradigm that combines cryptosystems with steganography. It must be upgraded in both phases in order to meet cloud-specific communication efficiency requirements. A successful Visually Imperceptible Hybrid Crypto Steganography (VIHCS) model is presented in this paper, which draws inspiration from Hybrid Cryptosystems and an Adaptive Genetic Algorithm with the help of the Least Significant Bit (LSB) embedding technique. To secure secret data that is later incorporated into a cover image, the authors meticulously combined the AES and RSA algorithms to produce a hybrid cryptosystem. Additionally, while keeping the best picture quality and ocular imperceptibility, AGA-OPAP (Adaptive Genetic Algorithm- based Optimal Pixel Adjustment) improved the LSB embedding.

To obscure the image, Hadisukmana et al [17], devised a unique RGB shuffling technique that shuffles every RGB component depending on the passcode the user enters, for each pixel in an image. The authors contend that as information technology improves, it is increasingly vital that we ensure digital data security. The use of both cryptography and steganography together is one of the more efficient methods of achieving this hiding. In this research, the message is encrypted using the Message Digest 5 (MD5) algorithm, and the picture is protected through RGB shuffling. The encrypted data was then included in an image and/or multimedia file (audio, video) using LSB techniques.

To secure cloud data, Adee et al [18] developed a dynamic four-step architecture using hybrid encryption, coupling the symmetric AES-256 algorithm with the asymmetric RSA algorithm. The authors have successfully combined steganography and cryptography security mechanisms to provide twice as much privacy and security for cloud data. The LSB steganography technique is then used to hide encrypted data within a picture. The results of the decryption procedure can be supported by the choice of tactics. The results of encryption and decryption can be distributed and reliably sent to authorized recipients using identity-based encryption (IBE). In comparison to other comparable attempts, the strategy additionally ensures the integrity and redundancy of cloud data.

Ali et al [19] proposed a hybrid encryption method employing the Blowfish and AES encryption algorithms for applications such as banks, the military, large websites that manage enormous databases, in-network enterprises, etc. Using hypothesis testing, the author also investigated other encryption methods, including AES, DES, the Blowfish encryption algorithm, and the RSA algorithm.

Panchal et al [20] used a steganographic cryptosystem for the secure transmission of information. First, the input image was converted into a cipher image by the authors using encryption combined with chirikov mapping. After that, during the series of stages, the authors applied steganography to obscure the encrypted image from the background image. The enforced situations of entropy and graph deformation, however, were not covered.

In contrast to computations using affine coordinates, Banerjee et al [21] demonstrated the energy efficiency of conventional projective coordinate-assisted elliptic curve computations. They have demonstrated that compared to affine coordinates, standard projective coordinates

are much more energy efficient. An analysis of the energy consumption of the Elliptic Curve-based Diffie-Hellman (ECDH) and Supersingular Isogenic-Based Diffie-Hellman (SIDH) implementations of Diffie-Hellman has also been conducted. Final findings show that SIDH uses around 40 times as much energy as ECDH.

Ahmed et al [22] suggested a user interface-based architecture where the sender may select the ideal mask and secret message, which would then be processed using ECC- based encryption followed by LSB embedding. Through several channels, the processed data was sent to the same destination. Nonetheless, it is possible to enhance their integration model to be attack-resistant and lightweight.

Alam et al [23] proposed a system that increases data safety over wireless networks by using McElice's cryptosystem, which differs from conventional cryptosystems. Their approach was ineffective for communicating with large datasets containing multimedia content in the cloud.

Christiansen et al [24] developed a new additive homomorphic technique called Secure Analytic with Vector- based Homomorphic Operation (SAVHO) based on the Paillier cryptosystem. This scheme is based on the vector randomization method. According to a thorough security investigation, the newly implemented system offers the necessary level of security. Additionally, they have demonstrated that the proposed strategy's performance assessment is very competitive with the well-known Paillier cryptosystem.

Siahaan [7] concentrated on comparing the performance of the RSA and ElGamal algorithms based on the speed of the encryption and decryption processes. They are also taken into account for the security level and key length of those algorithms. Testing revealed that RSA performs the encryption process faster than ElGamal, but on the other hand, the ElGamal decryption process proceeds more quickly than RSA. ElGamal uses sophisticated calculations to calculate discrete logarithms, making it more difficult to solve than the RSA algorithm in terms of security.

The authors [25] concentrated on an in-depth examination and comparison of the unpadded RSA, Paillier, and ElGamal algorithms, which are the three partial homomorphic asymmetric encryption techniques. Privacy, homomorphic properties, key generation time, main key size, encryption/decryption time, and cryptographic throughput are regarded as some of the standard requirements. The findings of this study demonstrate that each of the chosen algorithms has pros and cons and that each is advantageous in some situations but not in others. Paillier and ElGamal cryptosystems are typically preferred to unpadded RSA because of their semantic security. The authors also made the case that any one of the algorithms could be preferred over another, depending on the application and the necessary qualities.

METHODOLOGY

To increase data privacy, this work has used encryption and decryption techniques. The suggested model employed the ElGamal ECC encryption technique for message encoding on the sender end and message decoding on the receiver end. ElGamal and ECC are two different types of cryptographic methods. Even so, this study integrated these two techniques to achieve greater security and reduce the computational resources required for encryption. This technique utilizes public and private keys to encode and decode data, making it an asymmetric encryption scheme. The masking and filtering steganography technique is used to add an extra layer of protection after the initial cryptographic encryption of the data. Even when an image is compressed, the steganography method increases the privacy of information by hiding encrypted messages.

Proposed Model

The ElGamal ECC technique is used to apply encryption in the first phase of the suggested model. In order to meet the requirement of secure cloud data sharing, users receive their special private keys. The sender and the receiver are the first parties in the process, and the sender wants to securely communicate files with the recipient. Using the curve approach, a user (who could be the sender or receiver) creates an ElGamal key pair, consisting of a private and public key, and then distributes these keys to one another. The original message is then encrypted with these keys, and it is later decrypted. The ciphertext is subsequently encoded (encrypted) via the ElGamal public key.

The encrypted ciphertext is then covered up by an image using the Masking Filter steganography technique. The steganographic image method is the preferred authentication mechanism. The receiver then unpacks the ciphertext from the stego cipher image after receiving the stego cipher image. This model concludes with the receiver decrypting the ciphertext using the private key and receiving the plaintext(original data). Figure 1 provides an illustration of this strategy.

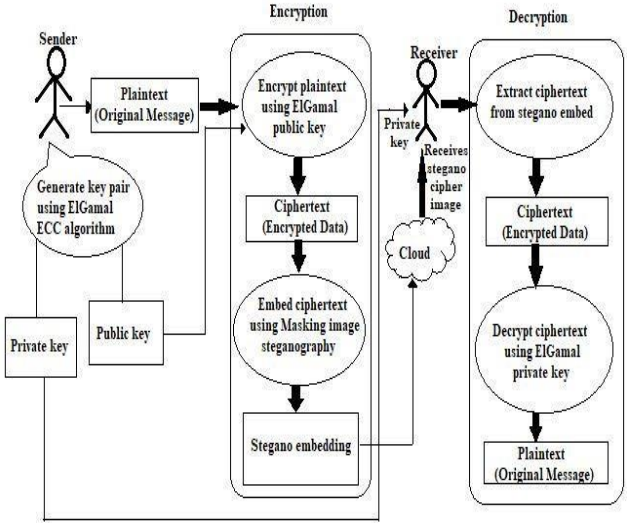

Figure 1: The proposed security model.

ElGamal ECC Approach

The ElGamal encryption scheme uses non-supersingular elliptic curve groups. Let E be the elliptic curve that is not supersingular [26].

1)Point generation

- Choose a base point P on the elliptic curve E. Where, $E=y^2=x^3+ax+b$ and P (bx, by) is a prime number of order n.

2)Key generations (User A end)

- User A (Alice) chooses a random integer d. where d is the private key of user A.
- Using private key (d) user A computes public key Q. Where Q= dP. So, Qx=dbx and

Qy=dby

3)Encryption (User B end)

- User B (Bob) wants to send Alice an encrypted message.
- Choose random integer k.
- Uses public key Q Bob creates cipher message pair C (C1, C2).
- Computes ciphertext C1 by using base point P (bx, by)
- and random value k. Where C1=kP. So, C1x=kbx and C1y=kby.
- Computes ciphertext C2 by using random value k and public key Q with original message M. Where C2=kQ+M. So, C2x=kQx+M and C2y=kQy+M.
- Then (user B)Bob sends the encrypted ciphertext to user A (Alice).

4)Decryption (User A end)

- Alice receives ciphertext C (C1, C2)
- Uses his/her private key d compute new decryption formula m=dC1.
- Then decrypt the encrypted ciphertext by the formula M=C2-m where Mx=C2x-dC1x and My=C2y-dC1y.
- Finally receives the original message by the calculation of: M=C2-m=kQ+M-dC1=kdP+M-dkP

ElGamal ECC approach is depicted in Figure 2.

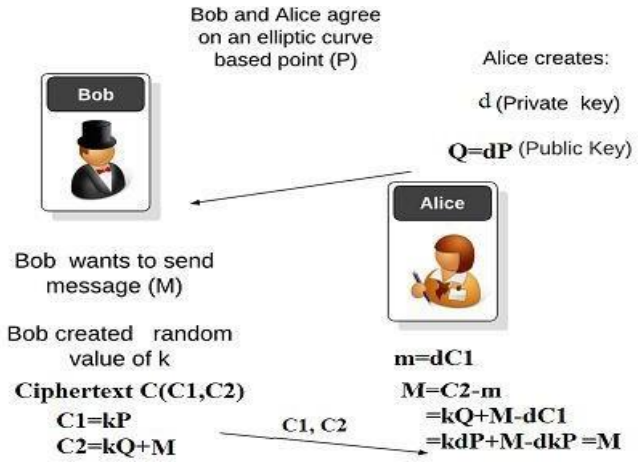

Figure 2 : Message Sharing with ElGamal ECC approach

Masking and filtering steganography method

The masking and filtering technique is often only applicable to 24-bit images. This technique picks out particular pixels from the cover image using precise masking algorithms or mathematical formulas. After appropriate pre-processing, the selected pixels can be utilized

to embed the hidden message. As a result, the cover image appears to be completely integrated with the hidden message [27]. The reliability of the steganographic image approach is boosted by using the right filter (an arithmetical expression) to choose the pixels, and the encoding capacity can be raised by picking further pixels.

1) Embedding process

- Using a mathematical function choose a set of pixels from the cover image. Where mathematical function is also known as secret/stego key.
- Processed the gray level values of these pixels.
- Convert secret text (encrypted message) information into bit stream (ASCII coding).
- The initial pixel value is not changed if the first bit in the text bit stream is zero but if the first bit is one then the first pixel is made odd by adding one.
- Continue this procedure until the text bitstream runs out.
- Then the changed pixels are inserted back into the original cover image and finally generate the Stego Image.

2) Debedding process

- Apply the same mathematical function as stego key to the stego image to identify the exact pixels.
- Inspect the values of the pixels. The embedded text bit was a one if the pixel value is odd. But if the pixel value is even then the embedded text was a zero.
- Retrieve the text bit stream using the above evaluation.
- Convert the bit stream first into ASCII and then to the relevant character. Finally, obtain the secret text (encrypted message).

Masking and filtering image steganography approach is illustrated in figure 3.

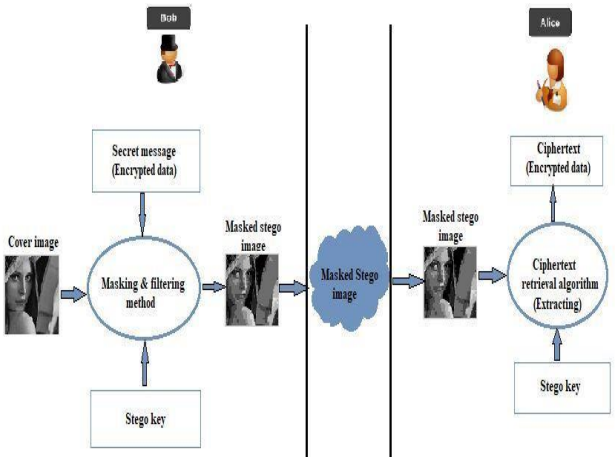

Figure 3: Masking and filtering image steganography approach

SECURITY ASSESSMENT

Elliptic curve functions are usually expressed over real numbers in mathematics. Round-off errors cause computations over real numbers to be unreliable and slow. For the ElGamal Elliptic Curve Cryptosystem, this paper designed an elliptic curve over a prime finite field.

For instance, an attacker can't steal the private key dx from Qx since Qx=dxP must be cracked. However, this is an elliptic curve discrete logarithm problem in a finite field. Once again, in the encryption phase, if a hacker obtains the ciphertext (C1, C2) and wishes to crack the random integer k from C1, he/she must compute C1=kP. Unfortunately, this is similar to a discrete logarithm issue over a prime finite field. If an attacker obtains the ciphertext (C1, C2) and intends to decrypt the message from (C1, C2), they must compute m = dC1, M = C2-m during the decryption phase. He should therefore first calculate (bx, by). However, since (bx, by) = kP, this query is identical to the encryption phase.

As a result, the security of the overall system is founded on discrete logarithm problems over a finite field and elliptic curves. Most crucially, an attacker must first obtain encrypted data from the masked image. The masking steganography method thus guarantees the dual security of messages sent through the cloud.

RESULT ASSESSMENT

The suggested method is put into practice utilizing various Python modules, including time, Crypto, and random, in the Jupyter Notebook (Anaconda3) environment. This paper first implements the ElGamal ECC method before comparing it to RSA and ElGamal in the same setting. ElGamal ECC uses the curve y2=x3+ax+b, which becomes y2 = x3 + b for a = 0 and b = 7.

For the identical plaintext (105116101), the times for key generation, encryption, and decryption are listed in table 1 of the above three algorithms.

Table 1 demonstrates that ElGamal ECC requires less time to generate keys because its key length is significantly shorter than that of other public key encryptions. Moreover, Table 1 shows that ElGamal ECC has a lower overall response timethan the RSA and ElGamal cryptosystems. In this way, ElGamal ECC provides strong security in a short time with fewer computational resources [26].

Table 1: Response time of ElGamal, RSA, and Elgamal ECC algorithm in seconds

Method	Key generation time	Encryption time	Decryption time	Total time
RSA	0.07615	0.00100	0.00200	0.07915
ElGamal	0.14061	0.01562	0.00100	0.15723
ElGamal ECC	0.00228	0.00201	0.00199	0.00628

After the encryption process, this study applied the masking filter image steganography technique to encrypt data. For implementation, this paper used a grayscale image and embedded the ciphertext in this image. It then utilized the cv2, NumPy, and Matplotlib libraries in Python to demonstrate the histogram of the original and embedded stego images to identify pixel distortion.

Figure 4: Original(cover) image

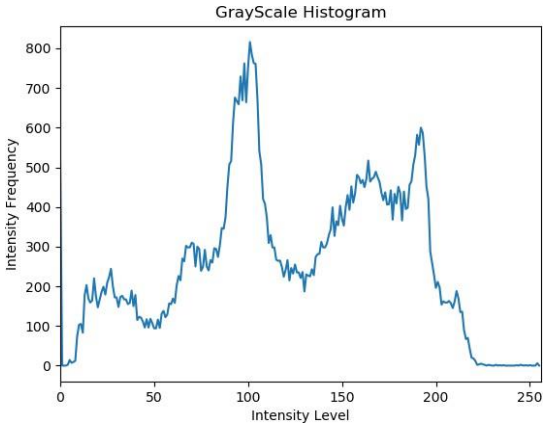

Figure 5: Histogram for cover image

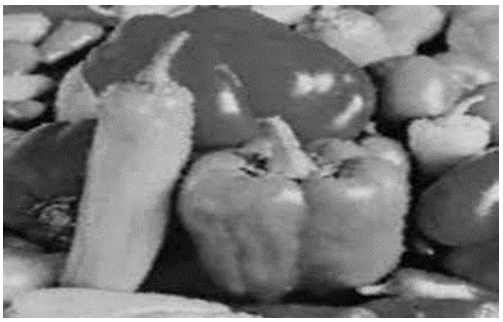

Figure 6: Mean filter(stego) image

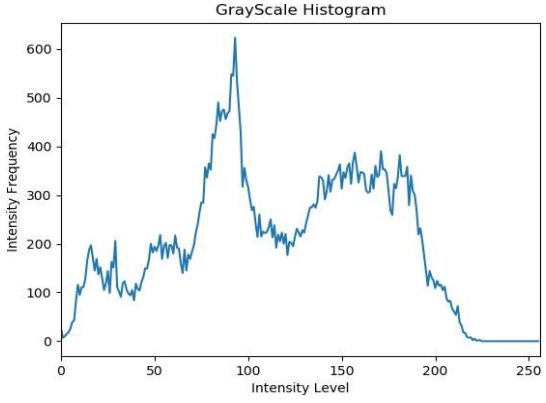

Figure 7: Histogram for stego image

CONCLUSION

A crucial aspect of the proposed system is providing security for user-sensitive information, particularly when data is shared over the cloud. To improve the performance of information privacy while gaining high levels of security, this study suggested a double information hiding approach based on ElGamal ECC and masking filter steganography. This research will take secure data storage and backup mechanisms into account in the future to beef up security.

REFERENCES

[1] I. A. K. and R. Qazi, "International Journal of Computing and Communication Networks," Data Secur. Cloud Comput. Using Elliptic Curve Cryptogr., vol. 1, no. 1, pp. 1–308, 2019, doi: 10.1049/PBSE007E.

[2] S. M. J. Islam, Z. H. Chaudhury, and S. Islam, "A Simple and Secured Cryptography System of Cloud Computing," 2019 IEEE Can. Conf. Electr. Comput. Eng. CCECE 2019, pp. 6–8, 2019, doi: 10.1109/CCECE.2019.8861845.

[3] A. Chhabra and S. Arora, "An Elliptic Curve Cryptography Based Encryption Scheme for Securing the Cloud against Eavesdropping Attacks," Proc. - 2017 IEEE 3rd Int. Conf. Collab. Internet Comput. CIC 2017, vol. 2017-Janua, pp. 243–246, 2017, doi: 10.1109/CIC.2017.00040.

[4] Khan Koffka, "The Security of Elliptic Curve Cryptosystems - A Survey," Glob. J. Comput. Sci. Technol., vol. 15, no. E5, pp. 25–35, Mar. 2015.

[5] R. Sunuwar and S. K. Samal, "Elgamal Encryption using Elliptic Curve Cryptography," 2015.

[6] C. Varma, "A Study of the ECC, RSA and the Diffie-Hellman Algorithms in Network Security," Proc. 2018 Int. Conf. Curr. Trends Towar. Converging Technol. ICCTCT 2018, pp. 1–4, 2018, doi: 10.1109/ICCTCT.2018.8551161.

[7] A. Putera Utama Siahaan, E. Elviwani, and B. Oktaviana, "Comparative Analysis of RSA and ElGamal Cryptographic Public- key Algorithms," 2018.

[8] M. Sajjad et al., "Mobile-cloud assisted framework for selective encryption of medical images with steganography for resource- constrained devices," Multimed. Tools Appl., vol. 76, no. 3, pp. 3519–3536, 2017, doi: 10.1007/s11042-016-3811-6.

[9] "Comparison of Digital Image Steganography Based on Techniques," Eng. Appl. Sci., vol. 13, no. 12, pp. 4442–4446, 2018.

[10] M. I. H. S. M. Masud Karim, Md. Saifur Rahman, "A New Approach for LSB Based Image Steganography using Secret Key," in 14th International Conference on Computer and Information Technology (ICCIT 2011), 2011, pp. 22–24.

[11] N. F. Johnson and G. Mason, "Exploring steganography: Seeing the unseen," pp. 26–34, 1998.

[12] S. Bhatt, A. Ray, A. Ghosh, and A. Ray, "Image steganography and

[13] "The Types and Techniques of Steganography," Jul. 21, 2021. https://www.ukessays.com/essays/computer-science/the-types-and- techniques-of-steganography-computer-science-essay.php (accessed Nov. 13, 2022).

[14] V. K. Pant, J. Prakash, and A. Asthana, "Three step data security model for cloud computing based on RSA and steganography," in Proceedings of the 2015 International Conference on Green Computing and Internet of Things, ICGCIoT 2015, 2016, pp. 490– 494. doi: 10.1109/ICGCIoT.2015.7380514.

[15] L. Kumar and N. Badal, "A Review on Hybrid Encryption in Cloud Computing," Proc. - 2019 4th Int. Conf. Internet Things Smart Innov. Usages, IoT-SIU 2019, 2019, doi: 10.1109/IoT- SIU.2019.8777503.

[16] R. Denis and P. Madhubala, "Evolutionary computing assisted visually-imperceptible hybrid cryptography

and steganography model for secure data communication over cloud environment," Int.

J. Comput. Networks Appl., vol. 7, no. 6, pp. 208–230, 2020, doi: 10.22247/ijcna/2020/205321.

[17] R. Nur Hadisukmana, "An Approach of Securing Data using Combined Cryptography and Steganography," Int. J. Math. Sci. Comput., vol. 6, no. 1, pp. 1–9, 2020, doi: 10.5815/ijmsc.2020.01.01.

[18] R. Adee and H. Mouratidis, "A Dynamic Four-Step Data Security Model for Data in Cloud Computing Based on Cryptography and Steganography," Sensors, vol. 22, no. 3, pp. 1–23, 2022, doi: 10.3390/s22031109.

[19] A. E. Taki and E. Deen, "Design and Implementation of Hybrid Encryption Algorithm," Int. J. Sci. Eng. Res., vol. 4, no. 12, pp. 669–673, 2013.

[20] P. H. Panchal D, Jani C, "An approach providing two phase security of images using encryption and steganography in image processing," Int. J. Eng. Dev. Res., vol. 3, no. 4, 2015.

[21] T. Banerjee and M. A. Hasan, "Energy Efficiency Analysis of Elliptic Curve Based Cryptosystems," in Proceedings - 17th IEEE International Conference on Trust, Security and Privacy in Computing and Communications and 12th IEEE International Conference on Big Data Science and Engineering, Trustcom/BigDataSE 2018, 2018, pp. 1579–1583. doi: 10.1109/TrustCom/BigDataSE.2018.00228.

[22] D. E. M. Ahmed and O. O. Khalifa, "Robust and Secure Image Steganography Based on Elliptic Curve Cryptography," in International Conference on Computer and Communication Engineering(ICCCE), 2014, pp. 288–291. doi: 10.1109/ICCCE.2014.88.

[23] M. S. Alam, "Secure M-commerce data using post quantum cryptography," in IEEE International Conference on Power, Control, Signals and Instrumentation Engineering (ICPCSI), 2017, pp. 649–654. doi: 10.1109/ICPCSI.2017.8391793.

[24] C. Zaraket, K. Hariss, M. Chamoun, and T. Nicolas, "Cloud based private data analytic using secure computation over encrypted data,"

J. King Saud Univ. - Comput. Inf. Sci., vol. 34, no. 8, pp. 4931– 4942, 2022, doi: 10.1016/j.jksuci.2021.06.014.

[25] S. J. Mohammed and D. B. Taha, "Performance Evaluation of RSA, ElGamal, and Paillier Partial Homomorphic Encryption Algorithms," in Proceedings of the 2nd 2022 International Conference on Computer Science and Software Engineering, CSASE 2022, 2022, pp. 89–94. doi: 10.1109/CSASE51777.2022.9759825.

[26] M. Fu and W. Chen, "Elliptic curve cryptosystem ElGamal encryption and transmission scheme," in ICCASM 2010 - 2010 International Conference on Computer Application and System Modeling, Proceedings, 2010, vol. 6, no. Iccasm, pp. 7–9. doi: 10.1109/ICCASM.2010.5620105.

[27] G. Sahoo and R. K. Tiwari, "Designing an Embedded Algorithm for Data Hiding using Steganographic Technique by File Hybridization," J. Comput. Sci., vol. 8, no. 1, pp. 228–233, 2008.

CHAPTER 6

A PERFORMANCE COMPARISON OF PYTHON, C++ AND JAVA PROGRAMMING LANGUAGES

Erkan ÜNSAL[1]
[1]Selcuk University, Konya/Turkey
ORCID: 0000-0002-0774-2934

Ahmet Cevahir ÇINAR[2]
[2]Selcuk University, Konya/Turkey
ORCID: 0000-0001-5596-6767

Şakir TAŞDEMİR[3]
[3]Selcuk University, Konya/Turkey
ORCID: 0000-0002-2433-246X

INTRODUCTION

In software studies, which language is more performant is one of the most important criteria when choosing a programming language because the performance criterion depends on many variables. The length of the code written by the developers, the running time of the application, and the memory consumption are the most important variables that constitute the performance criteria. In order to show how effective the performance criterion is in software studies and to guide the programming language selection, the performances of the object-oriented programming languages Python, C++, and Java, which have been increasing in popularity in recent years are aimed to be compared under the same conditions. [1,2]

In some of the similar studies in this field, the performance of a single programming language has been analyzed. [3] In others, when comparing many programming languages with each other, they are compared for a particular application, or the structures of the programming languages being compared are not taken into account. [4-6] 40% of the 400 research articles that need to be supported by experiments on software studies do not include any experiments. [7] In this study, taking into account the structures of the selected programming languages, experimental test algorithms are prepared to compare the performance of these programming languages.

In Chapter 2, the programming languages compared are introduced. In Chapter 3, the features of the specially prepared computer for the tests are mentioned. In Chapter 4, the experimental test algorithms prepared are described. In Chapter 5 performance comparisons made using tests are presented. The results are described in the last section.

COMPARED PROGRAMMING LANGUAGES

Python is an interpreted, interactive, object-oriented programming language. It incorporates modules, exceptions, dynamic typing, very high-level dynamic data types, and classes. [8] It supports multiple programming paradigms: procedural (imperative), functional, structured, reflective, and also usable as an extension language. It runs on many Unix variants and on Windows. Python 3.11.0 and accompanying IDLE (Python 3.11 64-bit) were used to prepare experimental test algorithms in Python.

C++ is a general-purpose programming language with a bias towards systems programming that is a better C, supports object-oriented, generic, functional programming and data abstraction. [9] Dev-Cpp 5.11 TDM-GCC 4.9.2 was used to prepare experimental test algorithms in C++.

Java is a programming language and computing platform first released by Sun Microsystems in 1995. [10] It supports multiple programming paradigms: generic, object-oriented (class-based) functional, imperative, reflective, and concurrent. Java SE Development Kit 19.0.1 and Apache NetBeans IDE 15 were used to prepare experimental test algorithms in Java.

When these programming languages are examined, the fact that they have similar structures and programming paradigms, and their popularity have been the most significant factors in choosing the languages for performance comparison.

PLATFORM

The properties of the computer, which is prepared by formatting for the preparation of experimental test algorithms created for use in performance comparisons and for running the prepared test applications, are as follows:

(1) Monster Abra A5 V13.2.2 Laptop (2) Operating System: Windows 10 Pro 22H2 (3) Processor: Intel Coffee Lake Core i7-8750H (4) Graphics card: 4GB GDDR5 Nvidia GTX1050 128 Bit (5) Ram: 16GB (2x8GB) DDR4 2666MHz (6) Solid-State Drive: XPG 256GB M.2 SSD

TESTS

While choosing the tests, similar studies in this field were examined, and the structures and common features of programming languages were taken into account. [11,12] Experimental test algorithms prepared for use in performance comparisons are shown in Table 1.

Table 1: Test Application

Test Code	Test Application
T1	Printing the integer variable whose value is 0 on the screen for 500,000 times
T2	Printing the string variable whose value is 'hello' on the screen for 500,000 times
T3	Finding the sum of prime numbers from 2 to 200,000
T4	Running empty loop, which runs 20,000 times, for 200,000 times
T5	Recursive calculation of 40th order Fibonacci number
T6	Multiplication of two 400X400 matrices whose elements are filled with random digits
T7	Creating object from class 500,000,000 times and changing integer and string value
T8	Writing '1234567890abcdefghijklmnopqrstuvwxyz' to file 5,000,000 times
T9	Sorting of the array with 25,000 elements, the element values of which are in the worst situation with the Bubble Sorting
T10	Sorting of the array with 50,000 elements whose elements are filled with random numbers between 0-100 with Quick Sorting

While preparing the experimental test algorithms shown in Table 1, some rules have been taken into consideration to ensure that the comparisons are made under the same conditions. These are:

(1) Using single letters such as “x”, “y”, “z” in variable naming, (2) Using single letters such as “i”, “j”, “k” for naming loop variables, (3) Using single letters such as “a”, “b”, “c” for array naming, (4) Using a letter and a number combination such as “a1”, “a2”, “b1”, “b2” for naming variables that specify the element numbers of arrays, (5) Using the combination of the letter “f” such as “f”, “ff”, “fff” for function naming, (6) Using single letters such as “a”, “b”, “c” to name integer variables in the function and a combination of letter “s” such as “s”, “ss”, “sss” to name string variables, (7) Using the combination of the letter “c” such as “c”, “cc”, “ccc” for class naming, (8) Using letter and number combinations such as “o”, “o1”, “o2” for object naming,

(9) Using the letter “r” for random object naming.

While paying attention to these rules, no spaces were used and no line starts were made unless a syntax error was made.

The tests were prepared as executable code (.exe) in Python and C++ and as Java archive (.jar) in Java.

PERFORMANCE COMPARISONS

In similar studies, older versions of programming languages were used in performance comparisons of programming languages, or the three languages selected in this study were not compared together. [11] Today, both the current versions of programming languages have been studied and the test platforms have changed with the rapid progress of technology.

Performance comparisons were made by running the prepared test applications 3 times under the same conditions.

Code Length

Code length affects the time developers spend writing code and time consumption. The code lengths of the prepared tests were measured. The code length of tests in Python in Table 2, the code length of tests in C++ in Table 3, the code length of tests in Java in Table 4 are shown.

Table 2: The Code Length of Tests in Python

Test Code	Line	Space	Length
T1	3	3	54
T2	3	3	60
T3	12	6	222
T4	3	6	73
T5	5	2	96
T6	4	3	109
T7	7	4	117
T8	4	3	112
T9	7	10	169
T10	20	12	420

Table 3: The Code Length of Tests in C++

Test Code	Line	Space	Length
T1	2	7	105
T2	2	7	114

T3	1	9	156
T4	1	4	74
T5	1	5	92
T6	3	15	376
T7	3	11	177
T8	2	7	173
T9	1	6	167
T10	3	13	407

Table 4: The Code Length of Tests in Java

Test Code	Line	Space	Length
T1	1	8	127
T2	1	8	136
T3	1	15	224
T4	1	8	125
T5	1	11	157
T6	1	24	460
T7	2	16	201
T8	1	14	314
T9	1	12	237
T10	1	31	480

The comparison of the code lengths of the tests created in languages compared is shown in Figure 1.

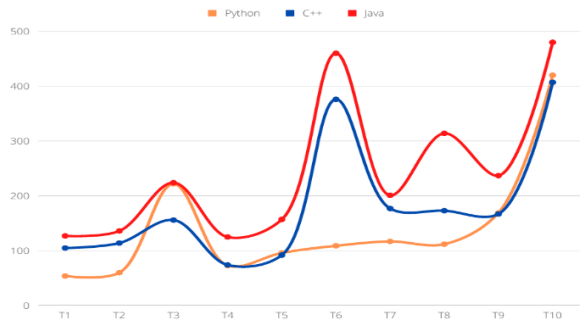

Figure 1: The Code Lengths of Tests

Run Time

Run time affects the optimality of the application. The run times of the tests were obtained with a Python application. The run times of tests in Python in Table 5, the run times of tests in C++ in Table 6, the run times of tests in Java in Table 7 are shown in sec (seconds).

Table 5: The Run Times of Tests in Python

Test Code	Run1	Run2	Run3
T1	1.031007	1.031042	1.062247
T2	1.015407	1.046663	1.046684
T3	78.184737	78.653342	74.226575
T4	110.752162	105.881337	107.751529
T5	23.744439	22.604084	22.447841
T6	1.077905	1.062259	1.062245
T7	73.904468	74.254532	72.199423
T8	2.077644	3.093022	3.077409
T9	67.749695	69.983544	67.812177
T10	1.046632	1.015385	1.062280

Table 6: The Run Times of Tests in C++

Test Code	Run1	Run2	Run3
T1	22.726994	22.494713	22.713404
T2	43.817814	43.708487	43.732469
T3	2.046416	2.030879	2.093177
T4	6.107928	6.154832	5.155038
T5	1.026564	1.046592	1.062276
T6	1.062262	1.077903	1.046679
T7	42.161950	41.956666	43.317921
T8	3.124300	3.108606	3.093079
T9	1.062274	1.031003	1.046594
T10	1.062281	1.013139	1.038235

Table 7: The Run Times of Tests in Java

Test Code	Run1	Run2	Run3
T1	12.372087	11.372320	12.244462
T2	13.278227	11.169241	11.188542
T3	2.030806	2.077665	2.066135
T4	1.046696	1.046625	1.046663
T5	1.062222	1.046617	1.015664
T6	1.062288	1.077872	1.031313
T7	1.077872	1.015901	1.046666
T8	2.077636	2.062051	2.030798
T9	1.062285	1.046635	1.062283
T10	1.031008	1.062287	1.046674

The comparison of the run times of the tests created in languages compared is shown in Figure 2.

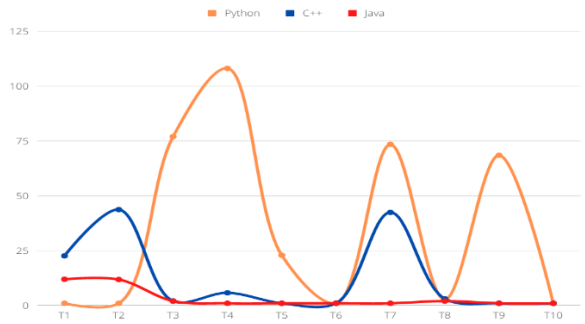

Figure 2: The Run Times of Tests

Memory Consumption

The memory consumption affects the hardware requirement and costs for the application to run. The memory consumption data of the tests were obtained from Windows Resource Monitor. The memory consumption of tests in Python in Table 8, the memory consumption of tests in C++ in Table 9, the memory consumption of tests in Java in Table 10 are shown in kB (kilobyte).

Table 8: The Memory Consumptions of Tests in Python

Test Code		Commit	Working Set	Shareable	Private	Total
	1	10640	18072	9204	8868	28712

T1	2	11092	18520	9204	9316	29612
	3	11748	19124	9204	9920	30872
	1	11472	18140	9204	8936	29612
T2	2	10684	17460	9204	8256	28144
	3	11472	18136	9204	8932	29608
	1	10868	17704	9216	8488	28572
T3	2	9836	16908	9200	7708	26744
	3	10824	17612	9200	8412	28436
	1	10508	17428	9212	8216	27936
T4	2	10708	17520	9196	8324	28228
	3	10600	17496	9196	8300	28396
	1	10852	18596	10096	8500	29448
T5	2	10000	16840	9196	7644	26840
	3	10808	17572	9196	8376	28380
	1	378956	27784	12760	15024	406740
T6	2	376512	23752	11412	12340	400264
	3	378208	25372	11512	13860	403580
	1	10148	17844	10096	7748	27992
T7	2	10236	16984	9196	7788	27220
	3	10320	17236	9196	8040	27556
	1	10944	17692	9212	8480	28636
T8	2	10632	17432	9196	8236	28064
	3	10712	17568	9196	8372	28280
	1	11772	19476	10100	9376	31248
T9	2	11844	18492	9200	9292	30336
	3	11120	17876	9200	8676	28996
	1	11580	19500	10148	9370	31080
T10	2	11648	18600	9248	9352	30248
	3	11440	18444	9248	9196	29884

Table 9: The Memory Consumptions of Tests in C++

Test Code		Commit	Working Set	Shareable	Private	Total
	1	588	2656	2344	312	3244
T1	2	588	2656	2344	312	3244
	3	584	2656	2344	312	3240
	1	564	2704	2404	300	3268
T2	2	560	2648	2348	300	3208
	3	560	2648	2348	300	3208
	1	472	2346	2168	268	2818
T3	2	468	2396	2128	268	2864
	3	468	2396	2128	268	2864
	1	472	2436	2168	268	2908
T4	2	472	2396	2128	268	2868
	3	472	2396	2128	268	2868
	1	472	2436	2168	268	2908
T5	2	472	2396	2128	268	2868
	3	468	2396	2128	268	2864
	1	2336	4292	2156	2136	6628
T6	2	2336	4292	2156	2136	6628
	3	2340	4292	2156	2136	6632
	1	648	3080	2700	380	3728
T7	2	560	2648	2344	304	3208
	3	568	2648	2344	304	3216
	1	660	3116	2736	380	3776
T8	2	580	2888	2584	304	3468
	3	576	2888	2584	304	3464
	1	644	3136	2696	440	3780
T9	2	556	2708	2352	356	3264
	3	556	2708	2352	356	3264
	1	556	1960	1772	188	2516
T10	2	540	1864	1688	176	2404

	3	556	1964	1776	188	2520

Table 10: The Memory Consumptions of Tests in Java

Test Code		Commit	Working Set	Shareable	Private	Total
	1	354856	43928	18600	25328	398784
T1	2	356600	43480	18600	24880	400080
	3	353936	52752	18708	34044	406688
	1	354992	30608	18592	12016	385600
T2	2	354820	30680	18584	12096	385500
	3	355148	30768	18592	12176	385916
	1	353992	29532	18108	11424	383524
T3	2	354360	29868	18108	11760	384228
	3	353948	29520	18108	11412	383468
	1	353176	25824	15936	9888	379000
T4	2	352604	23844	15152	8692	376448
	3	353192	26068	15984	10084	379260
	1	353988	29388	17984	11404	383376
T5	2	354228	29604	17984	11620	383832
	3	353788	29212	17984	11228	383000
	1	354652	32320	18308	14012	386972
T6	2	354408	32836	18940	13896	387244
	3	353364	26592	16236	10356	379956
	1	353464	27496	16720	10776	380960
T7	2	352976	25248	15760	9488	378224
	3	353548	27572	16712	10860	381120
	1	361052	192952	18712	174240	554004
T8	2	361368	193244	18712	174532	554612
	3	361032	192992	18712	174280	554024
	1	354212	30516	18696	11820	384728
T9	2	353920	29564	18068	11496	383484

	3	354056	29652	18068	11584	383708
	1	354796	31572	18908	12664	386368
T10	2	354952	30952	18280	12672	385904
	3	354788	31548	18908	12640	386336

The comparison of the memory consumptions of the tests created in languages compared is shown in Figure 3.

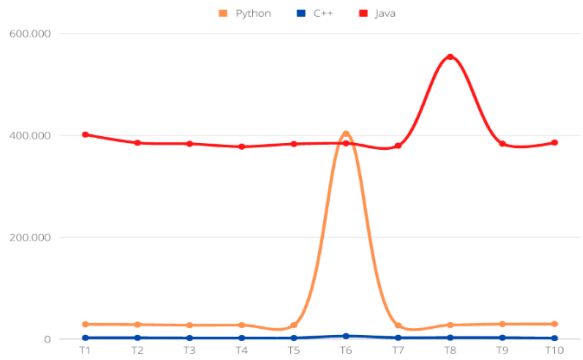

Figure 3: The Memory Consumptions of Tests

Comparison of total code lengths, total run times, and total memory consumption of the tests prepared in the languages compared are shown in Figure 4.

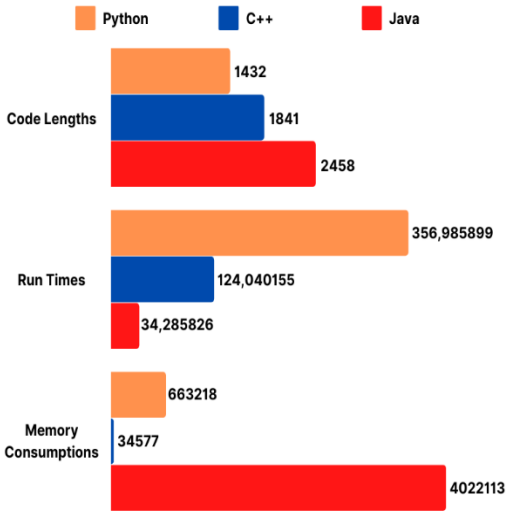

Figure 4: Performance Comparison

CONCLUSION

According to the performance comparisons, the total code length of the tests prepared with Python is 22.21% shorter than the total code length of the tests prepared with C++, and 41.74%

shorter than the total code length of the tests prepared with Java. The total run time of the tests prepared with Java is 65.25% faster than the total run time of the tests prepared with C++, and 90.39% faster than the total run time of the tests prepared with Python. The total memory consumption of the tests prepared with C++ is 94.78% less than the total memory consumption of tests prepared with Python, and 99.78% less than the total memory consumption of tests prepared with Java.

Considering all performance comparisons, it provides the benefit to choose Python for applications where code length is more significant, Java for applications where run time is more significant, and C++ for applications where memory consumption is more significant.

REFERENCES

[1] Cass, S. (2015). The 2015 top ten programming languages. *IEEE Spectrum, July, 20*.

[2] Kumar, K., & Dahiya, S. (2017). Programming languages: A survey. *International Journal on Recent and Innovation Trends in Computing and Communication, 5*(5), 307-313.

[3] Sestoft, P. (2005). Java performance: Reducing time and space consumption. *Royal Veterinary and Agricultural University of Copenhagen and IT University of Copenhagen, version, 2*.

[4] Hu, Y. F., Allan, R. J., & Maguire, K. C. F. (2000). Comparing the performance of JAVA with Fortran and C for numerical computing.

[5] Fourment, M., & Gillings, M. R. (2008). A comparison of common programming languages used in bioinformatics. *BMC bioinformatics, 9*(1), 1-9.

[6] Prechelt, L. (2000). An empirical comparison of seven programming languages. *Computer, 33*(10), 23-29.

[7] Juristo, N., & Moreno, A. M. (2013). *Basics of software engineering experimentation*. Springer Science & Business Media.

[8] Python. (2022). *General Python FAQ*. https://docs.python.org/3/faq/general.html#what-is-python.

[9] Isocpp. (2022). *Big Picture Issues*. https://isocpp.org/wiki/faq/big-picture#what-is-cpp

[10] Java. (2022). *What is Java technology and why do i need it?* https://www.java.com/en/download/help/whatis_java.html

[11] Şahin, M. (2007). Java, python ve ruby dillerinin performans karşılaştırması. *Akademik Bilişim*, 529-532.

[12] Karacı, A. (2015). A performance comparison of c# 2013, delphi xe6, and python 3.4 languages. *Int J Progr Lang Appl, 5*(3), 1-11.

CHAPTER 7

PHOTOVOLTAIC SYSTEM INTEGRATED ELECTRIC VEHICLE CHARGING STATION

Ali Atakan TURGUT[1]
[1] Selcuk University, Konya/Turkey
ORCID: 0000-0001-8900-7804

Hakan TERZİOĞLU[2]
[2] Selcuk University, Konya/Turkey
ORCID: 0000-0001-5928-8457

Abdullah Cem AĞAÇAYAK[3]
[3] Konya Technical University, Konya/Turkey
ORCID: 0000-0002-9285-5764

INTRODUCTION

Electric vehicles require intensive energy for their engines that provide movement. Electric vehicles are divided into more than one type [1]. Hybrid electric vehicles (HEV) have an electric motor that supports the internal combustion engine and does not need an external battery refill by self-charging the battery thanks to the regenerative braking system [2]. Plug-in hybrid electric vehicle (PHEV) has a larger battery than HEV and provides an increase in range by charging from the outside. If the battery occupancy rate decreases, it can continue to work with gasoline [3]. Fuel cell vehicles (FCEV) do not use an internal combustion engine, but fuel cell technology performs the charging process by transferring the energy obtained from hydrogen to the battery using the electrolysis method [4]. A battery-powered electric vehicle (BEV), which does not have an internal combustion engine in its body, provides energy to the electric motor by charging the battery from the outside. The electric motor directly rotates the wheels to ensure the movement of the vehicle [3].

The charging station system is a formation that starts with the electrical energy infrastructure and installation and extends to the units that carry out the energy flow and control to the vehicles and their communication infrastructure. Within itself, the energy infrastructure has a low voltage installation with a capacity that can meet the charging capacity. This installation includes the cable or busbar systems that supply the electrical panel and charging units. In addition, the necessary compensation and harmonic filtration units for energy quality elements are also available in this installation. Charging units realize the energy flow to electric vehicles within the system. These units are designed in accordance with international charging station standards such as IEC, SAE and are used to perform tasks such as ensuring user safety and charging consumption costs. They must be connected to and in contact with a communication network for both charging and remote monitoring and fault notifications [5].

The charging needs of EAS can be met with units in residential buildings or thanks to charging stations. Electric vehicle charging units are intermediary units that enable the safe, efficient and effective transfer of electrical energy to electric vehicle batteries and the practical completion of the charging process. Since the source of charging is electrical energy, charging of vehicles can be carried out wherever the electrical energy infrastructure is sufficient and appropriate. The length of the charging time inversely proportional to the power of the charging system differs from household simple charging systems to charging stations. Electrical energy infrastructure is important for charging stations. For EA technology to expand and the advantages of use to increase, it is necessary to provide easy and fast charging. With the increase in the number of EA and the development of technology, countries are gaining momentum in strengthening and improving the necessary electrical energy infrastructures, smart grid systems to protect the grid in case of grid overload, increasing the number of charging stations [6]. Charging services consist of three parts: vehicle-to-grid (V2G), vehicle-to-building (V2B) [7] and vehicle-to-vehicle (V2V) [8].

Renewable energy sources that are widely integrated into EA charging stations are photovoltaic (PV), biogas and wind (RES) systems [9,10]. Renewable energy sources can help reduce the amount of energy consumed from the electricity grid. PV energy systems have advantages such as ease of application and variety. Compared to wind energy systems, it is more preferred because it is more efficient, and its usage areas are spread over wider areas. For this reason, EA is also considered a good option for charging stations [11].

PHOTOVOLTAIC SYSTEMS

Photovoltaic panels are also known as solar panels or solar cell modules. Photovoltaic panels (PV) are used to obtain electrical energy from solar energy. The electrical energy obtained from a single PV cell operating as a semiconductor diode is quite low. For this reason, cells are connected in series or parallel to form modules, and modules are combined to form panels. In order to obtain large amounts of electrical energy and a level of power that can be used, the panels are connected to each other in parallel or in series to form a PV array [12]. PV panels work on the principle that photons hitting the semiconductor layers in the structure generate electrical energy by initiating atomic movement inside the panel by absorbing the sunlight (photon) coming to its surface [13]. Figure 1 shows the photovoltaic structure and working principle.

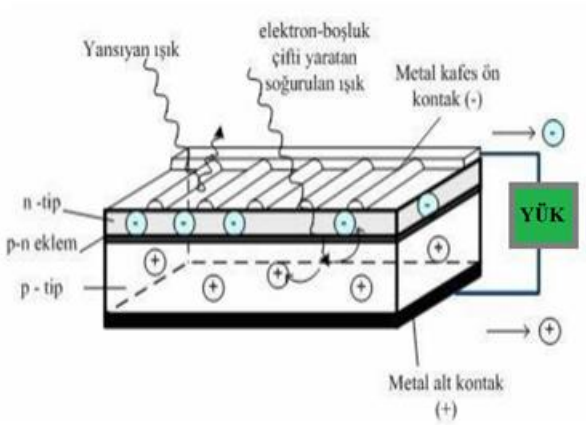

Figure 1. Photovoltaic structure and principle of operation [14].

The general model of solar cells consists of a current source (IFV) connected to a diode (D), a resistor (RP) parallel to the diode and current source, and a resistor (Rs) connected in series to the circuit. The PV panel equivalent electronic circuit model is shown in figure 2 [15].

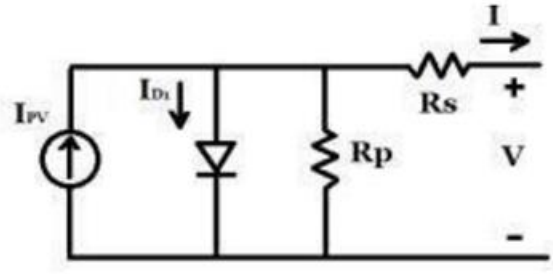

Figure 2. Photovoltaic panel equivalent electronic circuit [15].

The electrical energy production systems created by connecting solar panels to each other in series or parallel are called solar power plant. There are more than one type of solar panels and their structures and usage areas have differences [16]. Photovoltaic cells are basically divided into two parts. These are crystalline silicon cells and thin-film cells. Single and multiple silicones are used in crystal-silicon technology. This difference arises according to the degree of purity of silicon used in the production of solar cells. Monocrystalline solar cells are more efficient but more costly than polycrystalline solar cells because they have purer silicon. Due to the solar cell structures in monocrystalline and polycrystalline panels, the preference status may vary according to the usage areas [17].

CHARGING STATION

Working Principle

The electric vehicle charging station offers two different charging possibilities, AC and DC. The PV system and battery energy storage systems are integrated into the system. In this way, charging stations provide charging services to electric vehicles and at the same time perform energy production and storage. At the same time, the system is made ready for continuous energy problems and user grievances are prevented. The main components of the station include the grid, PV system, battery storage system, end users (EA) and energy management system. The energy management system provides control of all equipment used to collect, control and share production, energy storage and loading data [25].

Although the energy produced from the PV system is not constant, it differs according to the level of insolation and other environmental conditions. The output terminals of the PV are connected to a converter. Its function is to match the PV voltage level with that of the DC busbar and support the use of the maximum power point monitoring (MPPT) condition of the PV panel. Two charging converters are connected to the DC bus, namely the HOME charger and the energy storage converter. These converters are DC/DC converters. Thanks to a bidirectional DC/DC converter for the energy storage converter, the charging/discharging process is controlled. In addition, it participates in the regulation of the DC bus voltage against changes in the EV load and insolation level. An AC/DC dual converter connection is also provided for DC charging from the mains [11]. Figure 3 shows the charging station block diagram.

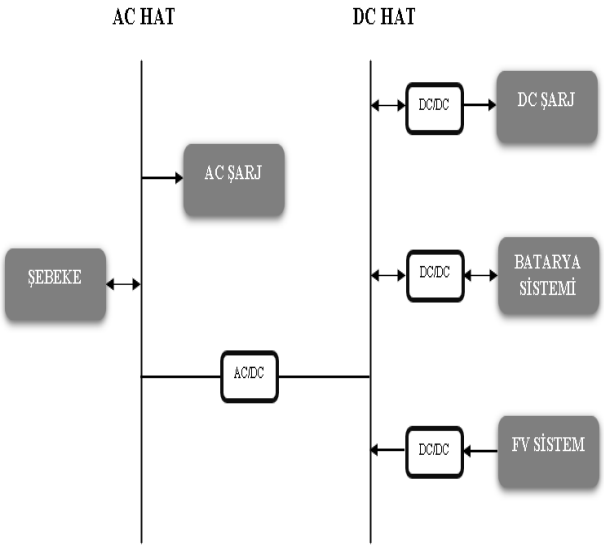

Figure 3. Charging station block diagram.

There are different working situations according to the station condition change. In cases where the PV system's energy production exceeds the requested energy, the energy flow directions of the system are stated below.

Charging With PV System Only

Charging When the solar radiation is provided in sufficient quantity, the energy of the EV charging station is completely provided by the PV system. In this case, if an electric vehicle is not charged, the energy provided is transmitted to the battery system and stored [18].

Charging Only From The Power Grid

In the absence of sunlight, this situation will be in effect. If the solar array cannot provide the necessary power for the EV charging station at night or due to extremely low radiation (rainy day, cloudy day), the necessary energy for the EA charging station will be provided by the grid [18].

Charging Both From The Solar Panel System And From The Power Grid

If the PV system is able to meet a certain amount of the energy required for the charging station and cannot provide all of it, the station is charged both from the solar energy system and from the electrical network. The amount of electricity supplied from the grid varies depending on the electricity produced from the solar energy system. In the absence of a certain volatility of solar radiation, it will allow the bidirectional converter to continuously monitor the maximum power point monitoring controller of the solar array and, accordingly, ensure the exchange of input power from the power grid to verify that the power required for EA charging is provided [18].

Transfer Of Energy Obtained From Solar Energy To The Grid

When there is no EA to charge at the station and the solar array provides energy, the transfer of all electrical energy to the grid will be carried out. EA energy transfer to the grid can also be achieved if the power capacity is less than the power generated from the solar panel system [18].

Charging From The Battery System

If for any reason the PV system cannot produce electricity and at the same time there is a fault in the power grid, the power of the charging station can be supplied directly from the battery system if the EA cannot be supplied with energy. Backup batteries can be recharged from the solar power system or from the power grid, but the backup battery capacity is designed to meet the minimum number of EA requirements in order to minimize the cost of investment [18].

CHARGING STATION DESIGN

Ease of access can be provided by positioning the station on the vehicle route. It is designed with a width of 26 m, a length of 9.08m and a height of 3 m in order to eliminate situations such as parking jams. The PV array was placed on a flat roof so that there is no shadow falling on it, which can structurally support it with low wind exposure. The dimensions of the roof on which the PV system will be installed are specified in the next section. The system should be positioned on the south facade according to the radiation angle. The average daily EA demand and the average daily solar radiation intensity are the main determinants of the PV array size. It covers a total area of approximately 236 m^2, with a roof area of 111 m^2.

Figure 13. 3D view of the charging station.

Solar Panel Selection

Since the life of the PV power system is determined by the life of the PV panels, solar panels with as long life as possible should be preferred [19]. In general, most manufacturers guarantee 80% panel strength in the twenty-fifth year. For PV system design, system power should be determined first. The total amount of solar radiation coming to the panel surface determines the electricity production. 55 panels were used for a 22kW system. After the system power is determined, the PV panel type selection should be made. Basically, the solar panels, which are structurally divided into monocrystalline and polycrystalline, can provide the desired power in a smaller area, since the monocrystalline type is more efficient than the polycrystalline type. In this way, the cost is minimized thanks to the use of fewer panels. Therefore, the monocrystalline type was chosen. Thanks to the panels with an output power of 400 W, the system takes up less space. The selected panel has a number of 72 cells. The panels create the voltage at the output thanks to the series connections between them, and the current at the output thanks to the parallel connections [16]. The panel to be used is indicated in figure 4, and its main characteristics are indicated in table 1 [20].

Table 1: Features of PV Panel

Power (W)	Vmp (V)	Voc (V)	Imp (A)	Isc (A)	Effi cienc y (%)	Sizes (mm)
400	41,4	49,45	9,68	10,18	20,13	1983 x 1002 x 40

Figure 4. Monocrystalline solar panel [20].

On the horizontal axis, the panels will be positioned in such a way that there will be 5 rows in the vertical plane, including 11 pieces. The installation should be carried out so that the horizontal and vertical gap distance between the panels is 2 cm. In this way, wind passage between the panels is provided, cooling the panels and increasing their durability. The length of the system is 21.98m from the first panel to the last panel in the horizontal plane and 5.08m in the vertical plane. The width of the cable tray is determined as 400mm, thickness 1.5mm, and height 40mm. Figure 5 shows the layout of the panels.

Construction

Some parameters should be taken into account for the selection of the location and characteristics of the installation of PV systems. It should be ensured that the health and durability of the system is at the highest level in case of exposure to effects such as snow load, earthquake, wind, and that the system is not damaged in the event of negative effects such as mold growth caused by rain and moisture. At this point, the installation should be carried out in accordance with the values such as earthquake degree of the region, soil class, safety stress, and building behavior coefficient [21].

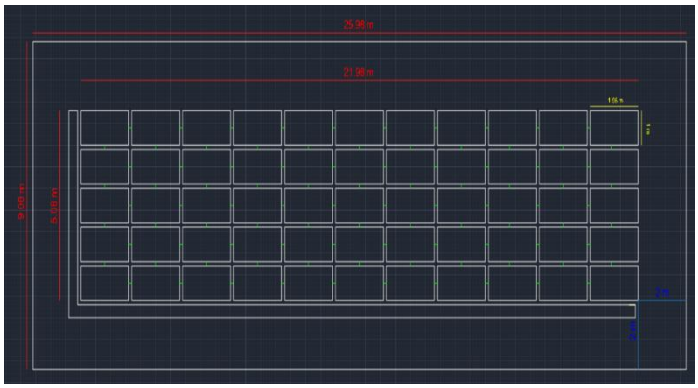

Figure 5. Layout of the panels.

Storage System

For such complex energy systems, an energy storage system is necessary in order to be able to offer an alternative to any possible problem. The PV system cannot produce energy and provides energy to the circuit in case of a fault in the network. It can be fed from the excess energy produced by the PV system or from the grid system. Gel batteries or special batteries are used for the storage system [22].

Power Converters

Amplifier type converters are circuits used to increase the input voltage value to the voltage at the desired output value. Figure 6 shows the basic circuit model of an amplifier type DC/DC converter. The principle of operation of this circuit is; charging of the inductance L is provided by entering the S switch into the transmission. It charges the C element by ensuring the discharge of the L inductance by entering the S switch into the cut-off. The transmission-cutoff frequency of the S switch controls the circuit [26].

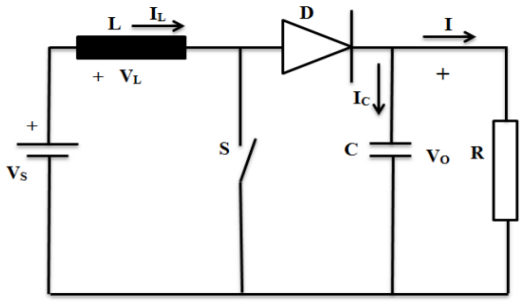

Figure 6. DC/DC Amplifier type converter circuit model [26].

Step-down type converters are circuits used to reduce the input voltage value to the voltage at the desired output value. Figure 7 shows the basic circuit model of a step-down type DC/DC converter. The principle of operation of this circuit is; charging of the inductance L is provided by entering the S switch into the transmission. By switching the S switch to the cut-off state, it charges the C element by ensuring the discharge of the L inductance. The transmission-cutoff frequency of the S switch controls the circuit [26].

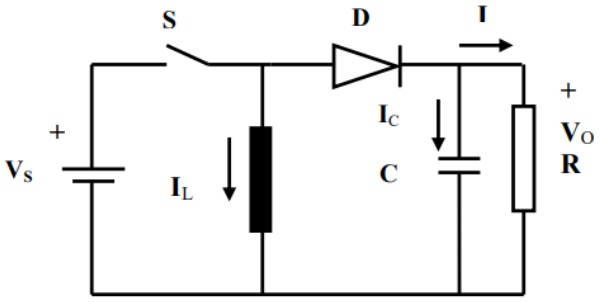

Figure 7. DC/DC Step-down type converter circuit model [26].

Step-up-step type converters are also called reverse output converters because they can create negative voltage by reversing the input voltage. They perform the operation of lowering or raising the output voltage according to the input voltage [26].

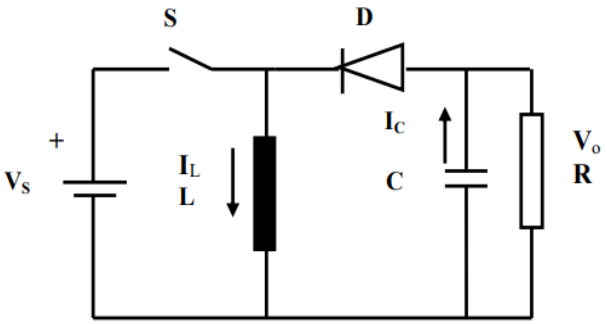

Figure 8. Lowering - raising type converter [26].

The switching sequence of all power electronics converters is controlled according to different parameters measured from the DC bus and the vehicle connected to the charging station. The MPPT DC-DC converter of the PV system side is controlled according to the voltage and current measured from the PV devices. The converter of the EV side to be controlled depends on the state of charge and the current drawn by the battery [23].

A bidirectional DC-DC converter controls the charging and discharging process of the battery system. The charge-discharge efficiency and bidirectional converter efficiency can be determined as 90% [24].

CONCLUSION

With the development of EVs and the increase in their number, their ability to be charged has become a critical situation. For this reason, the development of the charging infrastructure and network is of great importance. In this study, the structure, operation and use of EV charging stations are mentioned and the charging station model, which includes the PV system and the battery system, is introduced. A three-dimensional model of the station has been developed and its visualization has been provided. The station has a length of 26 m and a width of 9.08 m and covers an area of 236 m2. In this way, the ease of use of the station is aimed at the users. For the improvement and development of the charging station network, the use of PV systems and battery storage systems should be preferred. Thanks to the charging stations with a PV system, a more environmentally friendly and cost-effective charging process can be performed. The block diagram and three-dimensional design of the charging station model have been realized. PV panel selection criteria are important in the area and efficiency points to be used. With the use of panels with high power, the area to be occupied by the system is reduced. Due to its high efficiency, the desired power is provided with a smaller amount of panels. With the PV system, it is aimed to reduce the charging costs of the users when the PV system produces energy by saving the electrical energy to be used from the grid. The generated DC energy can be transferred without conversion to AC as long as there is no need. Due to the fact that the model is connected to the network, the network has two separate sources, as well as the PV system supports the network at the same time. In addition, energy continuity is ensured in case of possible failures with the battery storage system. Energy to the storage system will be supplied primarily from solar panels, otherwise from the grid. The necessary drawing for the installation of the solar panel system has been made. The length of the roof is 22 m, width is 5.08 m, and the area it covers is 111 m2. This drawing will be mounted between each panel with a space of two centimeters horizontally and vertically. In this way, the effects of wind will be reduced and the panels will work at lower temperatures. The panels are designed to be located in 5 rows on 11

verticals horizontally, but later, when the system power is requested to be increased, development can be achieved by adding. This model can be used in any desired area.

ACKNOWLEDGMENT

if any, should be placed here before the references section without numbering.

REFERENCES

[1] Kaymaz H. (2018). Hibrit ve Elektrikli Metrobüs Araçları İçin Sürüş Çevrimi Oluşturulması. Doktora Tezi, Marmara Üniversitesi FBE.

[2] Liao, F., Molin, E., & van Wee, B. (2017). Consumer preferences for electric vehicles: a literature review. Transport Reviews, 37(3), 252–275. https://doi.org/10.1080/01441647.2016.1230794

[3] Egbue, O., & Long, S. (2012). Barriers to widespread adoption of electric vehicles: An analysis of consumer attitudes and perceptions. Energy Policy, 48(2012), 717– 729. https://doi.org/10.1016/j.enpol.2012.06.009

[4] Kerem, A. (2014). Elektrikli Araç Teknolojisnin Gelişimi ve Gelecek Beklentileri. Mehmet Akif Ersoy Üniversitesi Fen Bilimleri Enstitüsü Dergisi, 5(1), 1–13.

[5] Birleştirici, A., Şalcı, S., Dikkulak A. Güler F. Ve Turhan E., "Elektrikli Araç Şarj İstasyonları", Elektrik Mühendisleri Odası Dergisi

[6] Nas, M., Cihangir, S., 2019. Dünya'da ve Türkiye'de Elektrikli Araçlar ve Şarj İstasyonları Üzerine Son Gelişmeler. GRÜ, Fen Bilimleri Enstitüsü, Gümüşhane.

[7] Contreras-Ocana, J.E.; Sarker, M.R.; Ortega-Vazquez, M.A. Decentralized Coordination of a Building Manager and an Electric Vehicle Aggregator. IEEE Trans. Smart Grid. 2016, 9, 2625–2637.

[8] You, P.; Yang, Z. Efficient optimal scheduling of charging station with multiple electric vehicles via v2v. In Proceedings of the 2014 IEEE International Conference on Smart Grid Communications (SmartGridComm), Venice, Italy, 3–6 November 2014; pp. 716–721

[9] Gao, Z.; Liu, X. An Overview on Fault Diagnosis, Prognosis and Resilient Control for Wind Turbine Systems. Processes 2021, 9, 300.

[10] Polimeni, S.; Nespoli, A.; Leva, S.; Valenti, G.; Manzolini, G. Implementation of Different PV Forecast Approaches in a MultiGood MicroGrid: Modeling and Experimental Results. Processes 2021, 9, 323

[11] Atawi I.E., H.E., Zaid S.A., Analysis and Design of a standalone electric vehicle charging station supplied by photovoltaic energy. Processes, 2021. 9(7).

[12] The Ohio State University." Photovoltaic Systems for Solar Electricity Production". https://ohioline.osu.edu/factsheet/AEX-652-11, (Erişim Tarihi: 12.10.2022).

[13] Ceylan, İ., Gürel, A.E., Güneş Enerjisi Sistemleri ve Tasarımı 2. Basım. Bursa, 2018.

[14] Kılıç, M.I., Fotovoltaik Sistemi Eğitimi İçin Bir Simulink Araç Kutusu Tasarım ve Uygulaması. MSKÜ, Fen Bilimleri Enstitüsü, Muğla, 2007.

[15] Karaca, M., 2020. Değişken Frekanslı Evirgeç Tasarımı ve Uygulaması (Yüksek Lisans Tezi, basılmamış). YYU, Fen Bilimleri Enstitüsü, Van.

[16] Karamanav, M., 2007. Güneş Enerjisi ve Güneş Pilleri (Yüksek Lisans Tezi, basılmamış). SAÜ, Fen Bilimleri Enstitüsü, Sakarya, 2007.

[17] Ceylan, M., 2018. "Kampüs Binalarında Şebekeden Bağımsız Bir Çatı Üstü Fotovoltaik Sistem Tasarımı Ve Benzetimi", Yüksek Lisans Tezi, İstanbul Teknik Üniversitesi Fen Bilimleri Enstitüsü, İstanbul,

[18] Minh P.V., Q.S.L., Pham M.H., Technical Economic Analysis of Photovoltaic Powered Electric Vehicle Charging Stations under different solar irradiation conditions in vietnam. Sustainability, 2021. 13(6).

[19] Boztepe, M. (2017). Fotovoltaik Güç Sistemlerinde Verimliliği Etkileyen Parametreler. EMO İzmir Şubesi Aylık Bülteni, 321, 13-17.

[20] https://arerenerji.com/2h-enerji-winasol-72-m3-400-w-watt-monokristal-gunes-paneli/ [Erişim Tarihi: 09.10.2022]

[21] Boyekin T., Kıyak İ., "Çatı Tip Güneş Enerjisi Santrali İle Beslenen Elektrikli Araç Şarj İstasyonu", Yüksek Lisans Tezi, Marmara Üniversitesi Fen Bilimleri Enstitüsü, İstanbul, 2020.

[22] Öter A., Baltacı F., "Elektrikli Araçlar İçin Akıllı Hibrit Şarj İstasyonu Örneği", BŞEÜ Fen Bilimleri Dergisi 9(1), 160-175, 2022.

[23] Savio D.A., J.V.A., Chokkalingam B., Padmanaban S., Holm Nielsen J.B., Blaabjerg F., Photovoltaic Integrated Hybrid Microgrid Structured Electric Vehicle Charging Station And Its Energy Management Approach. Energies, 2019. 12(1).

[24] Biya T.S., S.M.R., 2019. Design and Power management of solar powered electric vehicle charging station with energy storage system. IEEE.

[25] Dai Q., L.J., Wei Q., 2019. Optimal photovoltaic/battery energy storage/electric vehicle charging station design based on multi-agent particle swarm optimization algorithm. Sustainability.

[26] Özçelik, M.A., 2015. Fotovoltaik Sistemlerde Verim ve Performansın Artırılmasına Yönelik Maksimum Güç Noktası İzleyicisi Tasarımı (Doktora Tezi, basılmamış). KSÜ, Fen Bilimleri Enstitüsü, Kahramanmaraş.
[27] Ağaçayak A.C., Terzioğlu H., Neşeli S., Yalçın G., "Small Power Wind Turbine Design," Acad. Studies in Eng., Gece Publishing, pp. 121-130, 2018.

CHAPTER 8

ANALYSIS OF PYTHON USE ON DEEP LEARNING METHODS AND ALGORITHMS IN APPLICATIONS

Susilowati, Qoriah INDAH
Selcuk University, Konya/Turkey
ORCID: 0000-0003-4328-785X

INTRODUCTION

The industrial revolution 4.0 plays a full role in the development of human life today because human life cannot be separated from technology. One of the rapidly developing technologies is Artificial Intelligence (AI). AI is a broad term that is used very often in every field of automation devices[1]. One of the most popular approaches is through Machine Learning. ML enables the processing of large amounts of data by learning patterns in the data so that predictions can be made in the future. One of the most used parts of Machine learning is deep learning. Deep Learning is a technique based on artificial neural networks that has been widely used in recent years in processing information. Deep Learning will process it with machines that are modelled on the structure and actions of biological neural networks in the brain. Based on data from research for the last 10 years, deep learning has been widely used by researchers [2]. This is because deep learning can achieve an extraordinary level of success. The deep learning approach consists of multiple abstraction structures and multiple processing layers combined to learn representative data[3]. In deep learning, there is a structure based on learning more than one featured level or representation of data. Top level properties derive from lower-level properties, creating a hierarchical representation [4]. In deep learning applications, many languages can be used, such as C, Java, C++ and JavaScript. Python programming language is often used by data scientists in processing big data analysis [5]. This is also directly proportional to the 2019 IEEE Spectrum report which states that the Python programming language is a popular programming language [6]. Python is a general-purpose interpreted, interactive, object-oriented, and high level programming language [7]. This programming language is easy to learn and is open source. Especially for deep learning there are many open source libraries that allow the creation of deep neural nets in Python, without having to write the code from scratch [8]. This study aims to identify the use of the Python language in Deep Learning and then describe packages that are popular in deep learning and machine learning such as NumPy, SciPy, Keras, etc.

MACHİNE LEARİNG

In the past couple of decades machine learning has become a common tool in almost any task that requires information from large data sets. Nowadays, machine learning is demonstrating the promise of producing consistently from a training set of completed projects[9]. Machine learning is a machine designed or programmed to learn on its own without human direction. We often encounter the use of machine learning in our daily lives, such as the use of security using fingerprints, product recommendations in marketplaces, detecting spam in email, etc. There are many types of machine learning models that defined the presence or absence of human influence on raw data whether a reward is offered, specific feedback is given, or labels are used. • Supervised learning: The dataset being used has been pre-labelled and classified by users to allow the algorithm to see how accurate its performance is. • Unsupervised learning: The raw dataset being used is unlabelled and an algorithm identifies patterns and relationships within the data without help from users.

• Semi-supervised learning: The dataset contains structured and unstructured data, which guides the algorithm on its way to making independent conclusions. The combination of the two data types in one training dataset allows machine learning algorithms to learn to label unlabelled data. • Reinforcement learning: The dataset uses a “rewards/punishments” system, offering feedback to the algorithm to learn from its own experiences by trial and error.

DEEP LEARİNG

Basically, deep learning is branch of machine learning is based on a set of algorithms. This algorithm follows the working structure of the human brain. This algorithm can process complex data such as images, text and sound. Deep learning has enabled many practical applications of machine learning and by extension the overall field of Artificial Intelligence. This algorithm follows the working structure of the human brain. It can process complex data such as images, text and sound. Deep learning has enabled many practical applications of machine learning and by extension the overall field of Artificial Intelligence [10]. The most important property of deep learning methods is that it can automatically learn feature representations thus avoiding a lot of timeconsuming engineering [11]. Traditional machine learning relies on shallow networks which are composed of one input and one output layer, and no more than one hidden layer between input and output layers. Deep learning is qualified when more than three layers exist in a network including input and output layers. Therefore, the more the number of hidden layers is increased the more the network gets deeper.

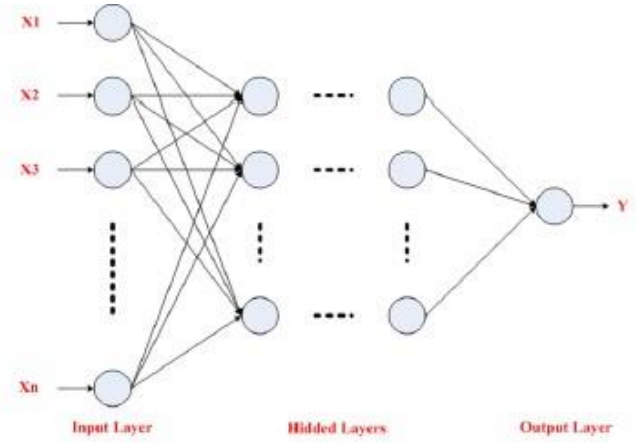

Figure 1. *An example of deep neural network*

Based on the picture, the basis for deep learning models, each layer may be assigned a specific portion of a transformation task, and data might travers the layers multiple times to refine and optimise the ultimate output.

These “Hidden Layers” serve to perform the mathematical translation tasks that turn raw input into meaningful output.

Based on picture we learned deep learning architectures consist of multiple processing layers. Each layer is able to produce non-linear responses based on the data from its input layer. Unlike other types of machine learning, deep learning has the added benefit of being able to decisions with significantly less involvement from human trainers.

While basic machine learning requires a programmer to identify whether a conclusion is correct or not, deep learning can gauge the accuracy of its answers on its own due to the nature of its multi-layered structure. Deep learning classified into three types:

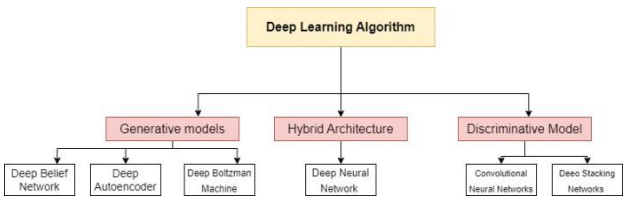

***Figure 2**. Deep Learning Classification Types*

Based on the picture above 3 model, such as:

Generative Models: Generative models used for unsupervised learning.

- Discriminative models: Discriminative models usually provide supervised learning approaches.
- Hybrid Models: Hybrid models incorporate the benefits of both discriminative and generative models.

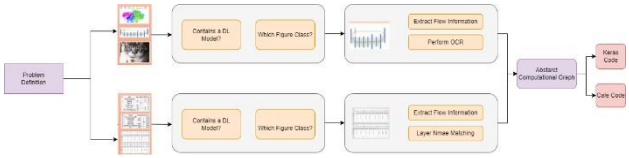

***Figure 3**. Workflow of Deep Learning*

Based on the picture the workflow of Deep Learning

1) Extract all the images and tables in the problem definition
2) Train a binary classifier to detect which image and tables describe a deep learning model flow
3) Parse the image to extract the nodes, edges, and flow to construct the computational graph
4) The table could be described either in a row-major or a column-major format. Based on the table alignment in the PDF research paper, the table is independently parsed to extract the deep learning model flow.
5) If a table and image describe the same design flow, we combine them to extract designs to improve the accuracy of the model designs.
6) From the extracted design, represented in a JSON format, we support source code generation in Keras (v2.1.2), Caffe (v1), Tensorflow (v1.4), and PyTorch (v0.3) using a manually curated template based code generation method.

PYTHON

Python is an interpreted, object -oriented, high level programming language with dynamic semantics. It’s highlevel built in data structures, combining with dynamic typing and dynamic binding [12]. Python was created by Guido van Rossum during 1985-1990 [7].

Python has not compilation step, the edit-test-debug cycle is incredibly fast. Debugging Python programs is easy: a bug or bad input will never cause a segmentation fault. Instead, when the interpreter discovers an error, it raises an exception. When the program doesn't catch the exception, the interpreter prints a stack trace. A source level debugger allows inspection of local and global variables, evaluation of arbitrary expressions, setting breakpoints, stepping through the code a line at a time, and so on. The debugger is written in Python itself, testifying to Python's

introspective power. On the other hand, often the quickest way to debug a program is to add a few print statements to the source: the fast edit-test-debug cycle makes this simple approach very effective

Python is often compared to other interpreted languages such as Java, JavaScripts, Perl, Tcl, or Smaltalks. Regarding widely used of Python, here are five main reason why developers love python [13]:

1) Simplicity because it is effortless to write and read.
2) Open-Source means that the developers don't have to pay for anything. They can share, copy, and change it
3) Compatibility with numerous platforms
4) Object oriented because python support procedure oriented as well as object-oriented programming
5) Libraries the python community has created a massive pile of various libraries.

Implementing of Python is easy enough so that whenever a programmer needs a prototype of software, Python will come with its rich library. Advantages of Python are significant, so using it as the primary language to learn programming can highly affect the speed of learning computer science in general [14]. These are example for demonstrate the code of "Hello World" program written in 3 different languages: Java, C++ and Python as shown in picture 1,2 and 3 respectively:

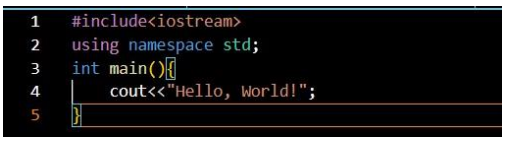

***Figure 2**. C++ code of 'hello world' program*

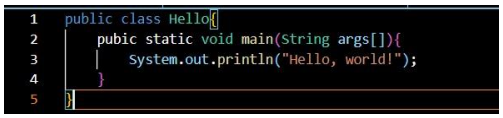

***Figure 5**. JAVA code of 'hello world' program*

So, from the 3 pictures above to explain the first

***Figure 6**. Python code of 'hello world' program*

program user will need to explain many other useful, but unnecessary terms like public static void main or using namespace std, but in case of Python there is only a single line of code and nothing else.

PYTHON LİBRARİES AND PACKAGES FOR DEEP LEARİNG

Since python creation in February of 1991, Python has slowly but steadily become the first used programming language in 2022s. One of Python's most beneficial yet most-overlooked features is its plethora of open source libraries and can be used in everything from data science and visualisations to image and data manipulation [15]. Here are Python libraries for machine learning and deep learning.

NumPy

NumPy (Numerical Python) is the most commonly used for scientific computing especially for data analysis [16]. NumPy can create N-dimensional array objects like Python lists. This library has an advantage over Python, which is that it only consumes a small amount of memory so that when the code is executed it will be faster. NumPy will help user to manage multi-dimensional arrays very difficult [7]. There has been a lot of improvement of the NumPy library over the years.

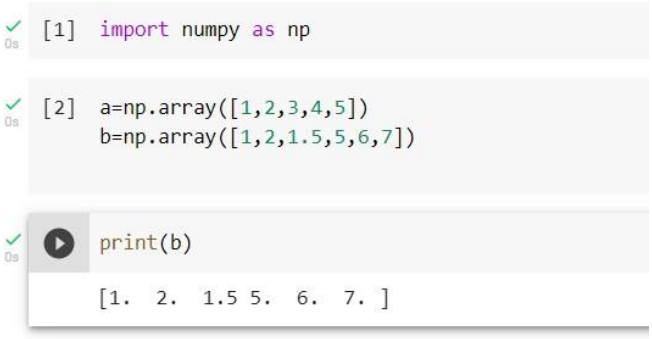

Figure 7. *Example use of the numpy library*

Scikit-Learn

Scikit-learn is a Python module integrating a wide range of state-of-the-art machine learning algorithms for medium-scale supervised and unsupervised problems [17]. This library is usually used for complex data. This library supports various supervised and unsupervised algorithms such as linear regression, classification, clustering and so on. One of the greatest aspects of Scikit-Learn is that it is easily interoperable with other SciPy stacks. Scikit-Learn includes DBSCAN, gradient boosting, support vector machines, and random forests within the classification, regression, and clustering methods [18].

Figure 8. *Example use of the Scikit-Learn library*

Matplotlib

Matplotlib is python library that used to visualise the data. Data visualisation is very important [7]. This library provides many functions like bar chart, scatterplot, pie chart, histogram which are useful for project.

```
import keras
from keras.models import Sequential
from keras.layers import Dense, Dropout, Activation
from keras.optimizers import SGD
# Generate dummy data
import numpy as np
x_train = data.data
y_train =  keras.utils.to_categorical(data.target, num_classes=3)
x_test = data.data
y_test = keras.utils.to_categorical(data.target, num_classes=3)
```

Figure 9. *Example of Matplotlib Library*

TensorFlow

Tensor flow is a Python library for fast numerical creation and released by Google. TensorFlow is an opensource library for fast numerical computing. It was created and is maintained by Google and released under the Apache 2.0 open-source lisense. The API is nominally for the Python programming language, although there is access to the underlying C++ API. TensorFlow was designed for use both in research and development and in production systems, not least Rank Brain in Google search It can run on single CPU systems, GPUs as well as mobile devices and large scale distributed systems of hundreds of machines [19].

```
# Example of TensorFlow library
import tensorflow as tf
# declare two symbolic floating-point scalars
a = tf.placeholder(tf.float32)
b = tf.placeholder(tf.float32)
# create a simple symbolic expression using the add function
add = tf.add(a, b)
# bind 1.5 to a , 2.5 to b , and evaluate c
sess = tf.Session()
binding = {a: 1.5, b: 2.5}
c = sess.run(add, feed_dict=binding)
print(c)
```

Figure 10. *Example of TensorFlow Library*

Scipy

SciPy is a scientific compotation library that uses NumPy, it provides more utility functions for optimizations, stats and signal processing. SciPy is predominantly written in Python, but a few segments are written in C.

Keras

Keras is best known for being one of the easiest machine learning libraries out there because it is coded entirely in Python. can run on top of Theano and TensorFlow, making it possible

to start training neural networks with a little code. The Keras library is modular, flexible, and extensible, making it beginner- and userfriendly. It also offers a fully functioning model for creating neural networks as it integrates with objectives, layers, optimizers, and activation functions. Here are advantages of Keras over deep learning models

a. Allow the user to use the model or extract feature-fit

b. Can make the model by yourself

c. API made simple so user can be easy to learn

Keras provides implementation options according to user requirements

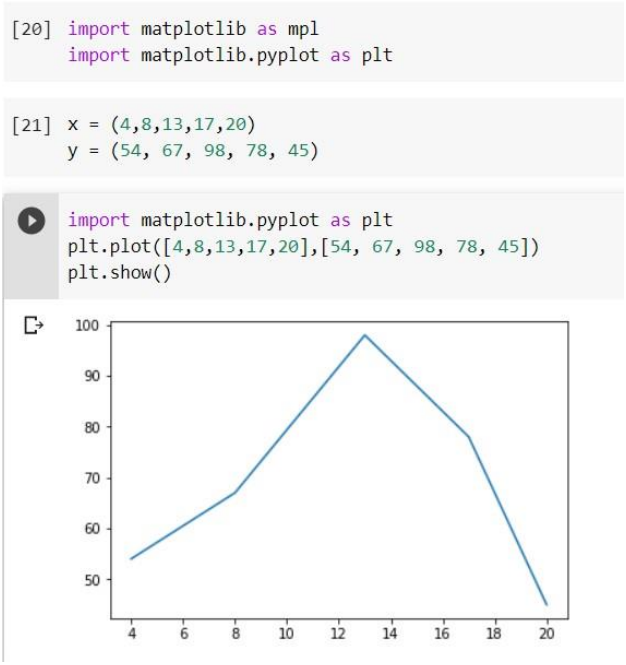

Figure 11. *Example for Keras Using*

RELATED RESEARCH WORKS

Modern Face Recognition with Deep Learning Jothi Thilaga.P et.al[19] has proposed that most predictable way to measure a face is by using deep learning techniques. The python applications is used for identifying the faces of the persons that pass by the admin. Histogram of Oriented Gradients (HOGs) is applied for face recognition. The result obtained was the original image turned into a very simple representation that features the basic structure of a face. A deep convolutional neural network is used to train the images and store the measurements using OpenFace. OpenFace is the python and torch implementation for facial recognition. Python language is used to code the software since python is scalable and portable. It uses network mapper package as a plugin. Hence, the result of person identification using HOG techniques performs promising results.

Implementation of Deep-Learning based Image Classification on Single Board Computer Hasbi Ash Shiddieqy et al.,[20] , represented an algorithm based on convolutional neural-network which is performed using raspberry pi 3 platform in deep learning. TfL earn is a highlevel API and a transparent deep learning library built on top of TensorFlow. The raspberry pi 3 is efficient to run the CNN in 2D. The images of cats and dogs were used in the classification. The train folder consists of 25,000 images of dogs and cats. The output from these images will be a

NumPy array 50x50 for every image. Thus, the result shows as the technique implemented in system has the ability to classify two category cat and dog which have man y similarity. By increasing the size of network, the accuracy can be improved.

Data Classification with Deep Learning using Tensor flow Fatih Ertam et al. [9] , illustrates the TensorFlow, one of the most popular deep learning libraries to classify MNIST dataset, which is frequently used in data analysis studies. The functions used for implementations are Rectified Linear Unit (ReLu), Hyperbolic Tangent (tanH), Exponential Linear Unit (eLu), sigmoid, softplus and softsign In this approach, Convolutional Neural Network(CNN) and SoftMax classifier are used as deep learning artificial neural network. The "Modified National Institute of Standards and Technology"(MNIST) is a huge dataset which has handwritten numbers used for training of image processing. This dataset was used to measure the performance of the TensorFlow library. Hence, in this study, a classification task was carried out on the MNIST data set which is widely using TensorFlow in deep learning applications. The accuracy values acquired according to the iteration numbers of the ReLu activation function obtained as the best result.

CONCLUSION

In this paper we have presented usage of python in various research like machine learning and especially deep learning. Beside Python language there are many languages are used for data science, machine learning and deep learning. But right now, most the developers use python scripting language than C++ and JavaScript. Because of simplicity because it is effortless to write and read, Open Source it means that the developers don't have to pay for anything. They can share, copy, and change it, compatibility with numerous platforms, object oriented because python support procedure oriented as well as object-oriented programming and also libraries the python community has created a massive pile of various libraries.

Python can interact with most of the other languages and platforms which are used to solve complex data like image, sound, text etc. This paper provides the comparative study of various papers implemented using python libraries and shows the benefit of python in solving the complex algorithms in deep learning.

REFERENCES

[1] M. Chandel *et al.*, "A Study on Machine Learning and Python ' s Framework," vol. 10, no. 5, 2022.

[2] K. M. Azhar, I. Santoso, and A. Adi, "Implementasi Deep Learning Menggunakan Metode Convolutional Neural Network Dan Algoritma Yolo Dalam Low Vision," vol. 10, no. 3, pp. 502–509, 2021.

[3] Y. Lecun and Y. Bengio, "Deep Learning," *Nature*, vol. 521, pp. 436–44, 2015.

[4] A. Şeker, B. Diri, and H. H. Balık, "Derin Öğrenme Yöntemleri ve Uygulamaları Hakkında Bir İnceleme," *Gazi*, vol. 3, pp. 47–64, 2017.

[5] "4 Alasan Mengapa Memilih Machine Learning Python." https://www.dqlab.id/4-alasan-mengapa-memilih-machinelearning-python (accessed Nov. 21, 2022). [6] Stiki-indonesia.ac.id, "Perkembangan Python dan Alasan Penting Untuk Data Analitik." 2021. [Online]. Available: https://stiki-indonesia.ac.id/2021/03/23/perkembanganpython-dan-alasan-sangat-penting-untuk-data-analitik/

[7] P. N. Siva and R. Yamaganti, "A Review on Python for Data Science, Machine Learning and IOT," *Int. J. Sci. Eng. Res.*, vol. 10, no. 12, pp. 851–858, 2019.

[8] "Deep Learning." http://www.deeplearningbook.org/ (accessed Nov. 11, 2019).

[9] F. Ertam and G. Aydin, "Data classification with deep learning using Tensorflow," 2017 International Conference on Computer Science and Engineering (UBMK)," *IEEE*, pp. 755–758, 2017, [Online]. Available: https://ieeexplore.ieee.org/document/8093521

[10] M. COŞKUN, Ö. YILDIRIM, A. UÇAR, and Y. DEMIR, "an Overview of Popular Deep Learning Methods," *Eur. J. Tech.*, vol. 7, no. 2, pp. 165–176, 2017, doi: 10.23884/ejt.2017.7.2.11.

[11] D. Sarkar, R. Bali, and T. Sharma, *Practical Machine Learning With Python*. California: Apress, 2018. [12]"What is Python? Executive Summary | Python.org." https://www.python.org/doc/essays/blurb/ (accessed Jun. 14, 2019).

[13] D. R, "Python vs Other Programming Languages," Nov. 14, 2022. https://www.cleveroad.com/blog/python-vs-otherprogramming-languages/ (accessed Nov. 21, 2022).

[14] A. Bogdanchikov, M. Zhaparov, and R. Suliyev, "Python to learn programming," *J. Phys. Conf. Ser.*, vol. 423, no. 1, 2013, doi: 10.1088/1742-6596/423/1/012027. [15]S. Gupta, "15 Best Python Libraries for Machine and Deep Learning," *Springboard*, 2022. https://www.springboard.com/blog/data-science/pythonlibraries-for-machine-learning/ (accessed Nov. 21, 2022).

[16] A. Sapre and S. Vartak, "Scientific Computing and Data Analysis using NumPy and Pandas," pp. 1334–1346, 2020.

[17] D. K. Barupal and O. Fiehn, "Generating the blood exposome database using a comprehensive text mining and database fusion approach," *Environ. Health Perspect.*, vol. 127, no. 9, pp. 2825–2830, 2019, doi: 10.1289/EHP4713.

[18] ''10 Best Python Libraries for Deep Learning (2022) – Unite.Al''https://www.unite.ai/10-best-python-librariesfor/ (accessed Nov. 21, 2022). Classification on single board computer IEEE, pp.133-137, doi: 10.1109/ISESD.2017.8253319.

[19] J. Brownlee, *Develop Deep Learning Models on Theano and TensorFlow Using Keras*. Melbourne, 2016.

[20] H. A. Shiddieqy, F. I. Hariadi, and T. Adiono, "Implementation of deep-learning based image

CHAPTER 9

SOME APPLICATION METHODS OF KITOSAN COATING IN FOOD AND A COMPARISON OF THESE METHODS: A REVIEW

Betül FİLİZ[1]
[1] Selcuk University, Konya/Turkey
ORCID: 000000023850113X

C SARIÇOBAN[2]
[2] Selcuk University, Konya/Turkey
ORCID: 0000-0001-9898-0884

INTRODUCTION

Chitin forms a structure with N-acetyl-D-glucosamine units. It has little industrial use because it is insoluble in aqueous and organic solvents. It is a renewable and easy to obtain biopolymer that is very common in nature after cellulose [5]. Found in some fungi, aquatic crustaceans, and insects. Chitosan, one of the most important derivatives of chitin, is obtained by converting N-acetyl-D-glucosamine units in the molecular chain into D-glucosamine units, that is, by deacetylation. Chitin with a deacetylation degree of at least 60% is called chitosan, and the main parameter that distinguishes chitosan from chitin is the degree of deacetylation [1].

Chitosan is a polyaminosaccharide obtained by the deacetylation of chitin in an alcaline environment and is soluble in weak organic acids [14]. Chitosan, a white, odorless and tasteless, translucent particle or powder, is resistant to digestive enzymes.

However, it is decomposed by some bacteria [31]. Chitosan is insoluble in water, alcali and organic solvents, but soluble in most organic acid solutions for pH 7 and above. Likewise, prolonged storage at room temperature adversely affects the stability of chitosan solutions [31]. Chitosan; It is applied in many fields such as medicine, bioengineering, environment, agriculture, food and textile due to its antimicrobial activity, toxicity, biocompatibility, biodegradability, and chelating ability [50]. The functional properties of chitosan films can be improved by combining them with other hydrocolloids. In this sense, by using chitosan together with methylcellulose, a decrease in water vapor transmission rates was achieved. Moreover, the addition of lipid materials such as fatty acids to hydrophilic coatings can sometimes improve their moisture barrier properties [47]. Chitosan is also attracting attention as a potential food preservative of natural origin due to its antimicrobial activity against a wide variety of foodborne molds, yeasts and bacteria [48]. Chitosan has a better antimicrobial activity against molds. Recent studies on the antibacterial activity of chitosan and chitosan oligomers have shown that chitosan is more effective in inhibiting the growth of microorganisms than chitosan oligomers [29].

APPLICATION METHODS OF CHITOSAN IN FOOD COATING

The choice of coating method depends on several factors, including the surface properties of the food and the purpose of the coating layer. In the coating method, firstly, the components are dispersed on the food surface, and then adhesion occurs between the coating material and the food surface [10]. Five different methods are used in the application of edible films and coatings to foods.These; dipping, dyeing, pouring, spraying, and extrusion methods [12].

Dipping Method

The simplest of these methods is the dipping method. In this application, the food is made by dipping directly into the coating solution for 5-30 seconds [36, 12]. The food is completely dipped in the coating solution and coating material accumulates on the food surface. In the final step, the solvent evaporates from the coating, forming a solution and leaving a thin coating on the surface of the product [24]. Thus, in this method, the food absorbs the solution and forms a film layer of the desired thickness on the surface [36]. Although this method has advantages such as homogeneous coating of uneven surfaces, removal of excess coating material and providing drying opportunity, it is not suitable for coating large volumes of foods. It is also recommended to apply acetyl glycerides to foods such as meat, fish and chicken [37, 13]. The dipping method is mostly used in fruits and vegetables.

Spraying Method

Another method most commonly used is the spraying method. This technique offers uniform coating, thickness control and sequential application that does not contaminate the coating solution [2]. It has been reported that beef gelatin has been successfully applied to the surfaces of beef tenderloin, pork loin, salmon fillet and chicken breast to improve their storage quality [3]. Spraying method preferred because it creates a thinner, smoother and homogeneous film compared to the dipping method [45]. This method is suitable for foods that only want to be coated on one surface and can also be used to form a second film on the coated food surface. For example, it is a suitable method for materials that will only be protected on one surface, such as pizza bases to be covered with sauce [23].

Electrostatic Spraying Method

Starting in the paint industry, electrostatic spraying has a number of advantages over conventional spraying technique. This method can control droplet size, increase droplet coverage and deposition, achieve homogeneous distribution, and reduce waste. It has been reported that the application efficiency can be increased up to 80% with 50% less spraying dose by using electrostatic spraying [26]. Namvd. (2011) stated that electrostatic spraying of 500 mg/kg ascorbic acid can effectively prevent both lipid oxidation and color change in minced meat.

Pouring Method

Pouring Method; It is the method of forming a film by pouring the film-forming solution on a smooth surface in the desired thickness, spreading and drying [23]. This method is used as an aid to spraying and dipping methods. Its direct application is not seen in the sector. This is because the gas permeability of the product will be very low when the surface of the coatings is covered with a large amount of coating material. Therefore, if the product to be coated is fruit, it will cause deterioration in the product [22].

Painting Method

The painting method is generally used to obtain a homogeneous and thin layer or to cover a certain area of the food. In this method, the food is painted and coated with a coating solution in liquid form with the help of a brush [37,13]. After this application, the food surface should be dried at ambient temperature or with the help of heating. Short drying time provides a more homogeneous structure on the product surface [45].

Extrusion Method

The extrusion method is used in the coating of starch-based edible films. The basis of the method is based on the thermoplastic properties of polymers. In this method, plasticizers such as 10-60% polyethylene, glycol and sorbitol are added to the polymers. It is more suitable for industrial applications than the pouring method, as it does not need drying and the addition of solvent is not required [12].

COMPARISON OF COATING METHODS

In the food industry, in coating fruit and vegetable surfaces; Spraying and dipping are traditional techniques [18, 52]. The conditions of the application process have a significant influence on the physical properties of the resulting coating. [43]. The choice of a suitable coating method not only affects the protective effect of coatings on foodstuffs, but also determines the production cost and process efficiency [49]. Dipping method; It is the most common method used on a laboratory scale because of its simplicity, low cost, and good coverage on an uneven

food surface. However, the dipping method has obvious disadvantages, eg. It causes a high amount of coating material residue in coating-solution dilution and generally causes microorganism growth in the dipping tank. In addition, process control and automation of continuous production are the biggest challenges [2, 18]. The spraying method, on the other hand, offers uniform coating, thickness control and sequential application that does not contaminate the coating solution [2].

Ganesh et al. (2012) noted that electrostatic spraying of foodgrade acids and plant extracts was more effective in decontaminating Escherichia coli O157:H7 on spinach and lettuce compared to conventional spraying method Baby carrots are covered with chitosan film using dipping and spraying method and packed in modified atmosphere packaging. Carrots stored at 4°C for 15 days were compared. It was stated that the mass loss rate of the carrots covered with the immersion method was slightly higher than the carrots coated with the spray method, the carrots coated with the spray method preserved the product hardness for a longer period of time, and similar hardness values showed a close relationship between weight loss and hardness [16]. In addition, it has been reported that the microbial load value of the samples applied by immersion is slightly lower than the samples coated with the spraying method [27] . Mozzarella cheese was coated with chitosan film by electrostatic spraying method, spraying method and dipping method and monitored for 14 days at 4 °C. As a result of the study, the weight loss was mostly seen in the two spraying methods, and although the spraying methods resulted in thinner films which should mean less water loss, it was stated that the films were heterogeneous and some parts of the cheese surface were not coated, so the weight loss was particularly stronger.

Since the two spraying methods produce thinner films with nearly equal shielding abilities compared to dipping method, and have advantages in terms of raw material savings and better process control, their application in the food industry will reduce production cost and help implement fully automated production. However, it is also stated that the progressive parameters of the spraying methods, especially for electrostatic spraying, need to be optimized in the future to control the deposition uniformity of the coating and to achieve the best shielding effect [49].

METHODS APPLIED WITH CHITOSAN COATING

Heat Treatment Application

Gala apples were heat treated at 38°C for 4 days before being coated with 1% chitosan, and then the apples were stored at 0°C for 8 weeks and at 20°C for 7 days. Heat-treated and chitosan-treated fruit showed the lowest respiration rate, ethylene evolution, malondialdehyde and membrane leakage, and the highest hardness and consumer acceptance among treatments. It has also been reported that this combined application can prevent loss of green color, titratable acidity and wastage compared to heat treatment alone [42].

The synergistic application of immersion in hot water at 42 °C for 30 minutes and 1% chitosan coating on differentiation in postharvest quality properties, microstructure as well as microbiological evolution of goji berry fruits was investigated. Fresh goji berry berries were stored at 2 ± 0.5 °C and 90% relative humidity (RH) for 28 days. The results showed that the combination of pre-storage heat treatment and chitosan coating resulted in higher ascorbic acid, total phenolic content and antioxidant capacity as well as lower rot compared to untreated goji berry berries. The possible mechanism is stated to be that the heat treatment closes the nearly open stomata to independently limit the sites of pathogen penetration into the fruits, followed by the biofilm formed by chitosan, which controls secondary infections and also slows down the changes in fruit respiration and metabolic activity in goji berry. Synergistically treated fruit

has been reported to exhibit a higher acceptability obtained by sensory analysis after cold storage. In this sense, the integrated application of heat treatment and chitosan coating can be considered as an effective strategy to extend the storage life and preserve the postharvest quality of goji berry fruits [4].

Application Of Hypobarcic Procedure

Among the physical tools to control postharvest rot of fruits and vegetables, the use of subatmospheric pressure applications has been largely unused to date. It has been reported that hypobaric treatments applied during the entire or almost all of the storage period delay the ripening of some climate fruits [20].

The efficacy of chitosan and short hypobaric treatments to control storage rot of cherries has been investigated for 2 years. The results show that the combination of hypobaric and chitosan treatments is a valid strategy to increase the effectiveness of treatments in controlling postharvest rot of sweet cherries [39,40].

Modified Packaging Application

Modified atmosphere packaging (MAP) is an important technique for changing the in-pack atmosphere using polymeric films with or without holes to reduce quality deterioration and increase shelf life of packaged fruits and vegetables through water loss, reduction of metabolic and microbial activity. Reuck et al (2009) found that the combination of chitosan (1.0 g/L) + MAP (control) was effective in preserving rot, browning and pericarp color in McLean's Red compared to single MAP.

Freshly cut cucumbers were stored at 5 °C and analyzed at 3- day intervals during a total storage period of 12 days. Freshly cut cucumbers are covered with chitosan film and packed with MAP. The results showed that the chitosan coating somewhat preserves the quality of the fresh-cut cucumber, but its efficacy alone may not be sufficient during the long storage period. In general, the combination of chitosan coating and argon-based MA packaging has been shown to preserve the best quality and extend shelf life of freshly cut cucumbers during 12 days of storage. Therefore, it has been reported that the combination of chitosan treatment and argon-based MA packaging has potential application in the food industry to preserve the overall quality and extend shelf life of fresh-cut cucumber [31].

Vacuum Tumbling Application

It has been reported that vacuum tumbling can be an effective method in meat products. It is a process designed to increase brine uptake and protein extraction in meat products [25]. It has been stated that it can improve the distribution and activity of antibacterial agent in a food product [6]. Physically, the main purpose of tumbling is to increase the penetration of the marinade solution by repeatedly squeezing meat from impact with other muscle parts and drum [21].

Chitosan was applied to the catfish fillets by dipping and spraying method, and another sample was vacuum tumbling with chitosan solution and the fillets were stored at 4 °C for 16 days. Catfish fillets vacuum tumbling with chitosan reported greater solution uptake and lower pH compared to those treated with other application techniques. According to the results of aerobic bacteria count and total volatile basic nitrogen in catfish fillets vacuum tumbling with chitosan, the solution was found to be more effective in extending the microbiological shelf life compared to direct application techniques (spraying and dipping). This could be explained by greater retention and potentially greater penetration of the chitosan solution. Thus, it was stated that the

antimicrobial activity of chitosan increased its effectiveness during storage. Sprayed and dipped fillets have been reported to have less physical change over time in terms of color and shear strength. Sprayed and dipped fillets have been reported to have less physical change over time in terms of color and shear strength. This study showed that chitosan applied to catfish fillets by vacuum tumbling can provide the most effective extension in microbiological shelf life[7].

CONCLUSION

Chitosan is used in food products to extend the shelf life. When chitosan is used in product coating, it is commonly used; dipping method, spraying method, painting method, dipping methods [12]. Each method has advantages and disadvantages.

The physical properties of the food as well as the production cost of the coating method and the process efficiency are effective in determining the method to be applied. Today, combined methods are used to increase the effect of chitosan coating. These methods are heat treatment application, hypobaric application, modified atmosphere packaging and vacuum tumbling applications. Studies have shown that combined methods are more effective than methods using chitosan coating alone.

REFERENCES

[1] Aiba, S. (1992). Studies on chitosan: 4. Lysozymic hydrolysis of partially n-acetylated chitosans, International Journal of Biological Macromolecules, 14, 225-228.

[2] Andrade, R. D., Skurtys, O., & Osorio, F. A. (2012). Atomizing spray systems forapplication of edible coatings. Comprehensive Reviews in Food Science and FoodSafety, 11(3), 323e337

[3] Antoniewski, M. N., Barringer, S., Knipe, C., & Zerby, H. (2007). Effect of a gelatincoating on the shelf life of fresh meat. Journal of Food Science, 72(6), E382eE387.

[4] Ban Z,Wei W, Yang X, Feng J,Guan J,Li L (2015). Combination of heat treatment and chitosan coating to improve postharvest quality of wolfberry (Lycium barbarum). International Journal of Food Science and Technology, 50, 1019–1025.

[5] Bartnicki-Garcia, S. (1968). Cell wall chemistry morphogenesis and taxonomy of fungi.Annual Review of Microbiology, 22, 87-108.

[6] Bharti, S. K., Anita, B., Das, S. K., & Biswas, S. (2011). Effect of vacuum tumbling time on physico-chemical, microbiological and sensory properties of chicken tikka. Journal of Stored Products and Postharvest Research, 2, 139–147.

[7] Bonilla F, Chouljenko A, Reyes V, BechtelP J, KingJ M, SathivelS. (2018). Impact of chitosan application technique on refrigerated catfish filet quality. LWT - Food Science and Technology, 90 (2018) 277–282.

[8] Caner, C. ve Küçük, M.(2004). Yenilebilir Film ve Kaplamalar: Gıdalara Uygulanabilirliği. Gıda Mühendisliği ve Gıda Sanayi Dergisi, 2, 8.

[9] Castro, S.P.M., Paulín, E.V.G. (2012). Is Chitosan a New Panacea? Areas of Application. http://dx.doi.org/10.5772/51200. 2012.

[10] Cerqueira, M. A. P. R., Pereira, R. N. C., da Silva Ramos, O. L., Teixeira, J. A. C., Vicente, A. A. (2017). Materials and processing technologies. Edible Food Packaging, 469, 64.

[11] Dhall, R. K. (2015). Advances in Edible Coatings for Fresh Fruits and Vegetables : A Review Advances in Edible Coatings for Fresh Fruits and Vegetables :, 8398(November). http://doi.org/10.1080/10408398.2010.541568

[12] Dhanapal, A., Sasikala, P., Rajamani, L., Kavitha V., Yazhini. G., Banu, M.S.(2012). Edible films from polysaccharides. Food Science and Quality Management 3: 1-10

[13] Dursun Oğur, S.,(2012). Dumanlanmış Balıkların Kalite ve Raf Ömrü Üzerine Yenilebilir Protein Film Kaplamanın Etkisi. Doktora Tezi, İstanbul Üniversitesi, Fen Bilimleri Enstitüsü, Su Ürünleri Avlama ve İşleme Teknolojisi Anabilim Dalı, İstanbul

[14] Fernandez-Kim, S.O. (2004). Physicochemical and Functional Properties Of Crawfish Chitosan as Affected by Different Processing Protocols. A Master Thesis, Submitted to the Graduate Faculty of the Louisiana State University and Agricultural and Mechanical College, Seoul National University. 99 s.

[15] Ganesh, V., Hettiarachchy, N. S., Griffis, C. L., Martin, E. M., & Ricke, S. C. (2012).Electrostatic spraying of foodgrade organic and inorganic acids and plant ex-tracts to decontaminate Escherichia coli O157: H7 on spinach and iceberg let-tuce. Journal of Food Science, 77(7), M391eM396.

[16] Gonzalez-Aguilar, G.A., Ayala-Zavala, J.F., Ruiz-Cruz, S.,Acedo-Felix,E.,Díaz-Cinco, M.E., 2004. Effect of temperature and modified atmosphere packaging on overall quality of fresh-cut bell peppers. LWT – Food Sci. Technol.37,817–826.

[17] Goosen, F.A. 1997. Applications of chitin and chitosan, CRC Pres LLC, Florida,336p

[18] Hernandez-Munoz, P., Almenar, E., Ocio, M.J., Gavara, R..(2006). Effect of calcium dips ˜ and chitosan coatings on postharvest life of strawberries (Fragaria × ananassa). Postharvest Biol. Technol. 39, 247–253

[19] Hirano, S. (1996). Chitin Biotechnology Applications, Biotechnology Annual Review, (eds: El-Gewely, M.R.), Elsevier, 237-258.

[20] Jianglian D, Shaoying Z. (2013). Application of Chitosan Based Coating in Fruit and Vegetable Preservation. Journal of Food Processing & Technology 2013, 4:5, 1-4.

[21] Karales, S. (2001). Vacuum tumbling of meats and other foods. United States Patent, 1–5.

[22] Koyuncu M.A., Savran H.E. (2002). Süleyman Demirel Üniversitesi Fen Bilimleri Enstitüsü Dergisi (Yıl 6, Sayı 3), 73-83

[23] Krochta, J., Baldwin, E. ve Nisperos, M.(1994). Edible Coating and Film to Improve Food Quality. Technomic Publishing Co. Inc. Lancaster, Basal, 379 s.

[24] Kumar, L., Ramakanth, D., Akhila, K., Gaikwad, K. K. (2021). Edible films and coatings for food packaging applications: a review. Environmental Chemistry Letters, 1- 26.

[25] Lin, G. C., Mittal, G. S., & Barbut, S. (1990). Effects of tumbling speed and cumulative revolutions on restructured hams' quality. Journal of FoodProcessing and Preservation, 14, 467–479

[26] Maski, D.,& Durairaj, D. (2010). Effects of charging voltage, application speed, targetheight, and orientation upon charged spray deposition on leaf abaxial andadaxial surfaces. Crop Protection, 29(2), 134e141.

[27] MolinaroS., GuerreroP., KerryJ. P, LecetaI., KerryJ.P., de la Caba K. (2015).Quality attributes of map packaged ready-to-eat baby carrots by using chitosan-based coatings. Postharvest Biology and Technology 100, 142–150.

[28] Nam, K., Seo, K., Jo, C., & Ahn, D. (2011). Electrostatic spraying of antioxidants on theoxidative quality of ground beef. Journal of Animal Science, 89(3), 826e832.

[29] No HK, Meyers SP, Wand P, Xu Z (2007). Applications of chitosan for improvement of quality and shelf life of foods: A Review.Journal of Food Science, 72: 87-100.

[30] No, H.K., Kim., S.H., Lee, S.H., Park, N.Y. and Prinyawiwatkul, W. 2006. Stability and Antibacterial Activity of Chitosan Solutions Affected by Storage Temperature and Time. Carbohydrate Polymers, 65, 174-178.

[31] Olawuyi I F,Park J J, Lee J J,Lee W Y(2019). Combined effect of chitosan coating and modified atmosphere packaging on fresh-cut cucumber. Food Science & Nutrition, 7(3): 1043–1052.

[32] Özbay, T., Özden B., Mehmet A.S. (2002). Manta Karidesi (Squilla sp.), Sübye (Sepia sp.) ve Mavi Yengeç (Callinectessapidus, Rathbun, 1896) Atık Kabuklarının Kitin ve Kitosan Verimi. Yunus Araştırma Bülteni, 1, 13-19.

[36] Pavlath, A.E., Orts, W.(2009). Edible Films and Coatings: Why, What, and How? In Edible Films and Coatings for Food Applications, Edited by Milda E. Embuscado, Kerry C. Huber, Springer Dordrecht Heidelberg London New York, 403p.

[37] Polat, H.(2007). İşlenmiş Et Ürünlerinde Yenilebilir Filmlerin ve Kaplamaların Uygulamaları. Yüksek Lisans Tezi, Afyon Kocatepe Üniversitesi, Fen Bilimleri Enstitüsü, Gıda Mühendisliği Anabilim Dalı, Afyon.

[38] Reuck KD, Sivakumar D, Korsten L (2009). Effect of integrated application of chitosan coating and modified atmosphere packaging on overall quality retention in litchi cultivars. J Sci Food Agr 89: 915-920.

[39] Romanazzi G, Nigro F, Ippolito A (2003) Short hypobaric treatments potentiate the effect of chitosan in reducing storage decay of sweet cherries. Postharvest Biol Tec 29: 73-80.

[40] Romanazzi G, Nigro F, Ippolito A, Salerno M (2001) Effect of short hypobaric treatments on postharvest rots of sweet cherries, strawberries and table grapes. Postharvest Biol Tec 22: 1-6. 36.

[41] Sandford, P.A. (1989). Chitosan: commercial uses and potential applications, in: G. Skjak-Brack, T. Anthonsen, P.Sandford (Eds.), Chitin and Chitosan Sources, Chemistry, Biochemistry, Physical Properties and Applications, pp. 51- 69, Elsevier Science Publishers Ltd, England.

[42] Shao XF, Tu K, Tu S, Tu J (2012) A Combination of Heat Treatment and Chitosan Coating Delays Ripening and Reduces Decay in "Gala" Apple Fruit. J Food Quality 35: 83- 92.

[43] Skurtys, O., Acevedo, C., Pedreschi, F., Enrione, J., Osorio, F., Aguilera, J.M., 2010. Food hydrocolloid edible films and coatings. In: Food Science and Technology Series. Nova Science Publishers, New York.

[44] Üney S.(2016). A Thesis Submitted to the Graduate School of Engineering and Sciences of Izmır Institute of Technology In Partial Fulfillment of the Requirements for the Degree of Master of Science in Food Engineering, İzmir.

[45] Üstünol, Z., 2009. Edible Films and Coatings for Meat and Poultry. In Edible Films and Coatings for Food Applications, Edited by Milda E. Embuscado, Kerry C. Huber, Springer Dordrecht Heidelberg London New York, 403p.

[46] Valero D, Romero DM, Valverde JM, Guilléna F,Seranno M (2003) Quality improvement and extension of shelf life by 1-methylcyclopropene in plum as affected by ripening stage at harvest. Innov Food Sci Emerg 4: 339-348.

[47] Vargas M, Chiralt A, Albors A and González-Martínez C (2008). Characterization of Chitosan-Oleic Acid Composite Films. Food Hydrocolloids, 23: 536–554.

[48] Vargas M, Albors A, Chiralt A and Gonzalez-Martinez C (2006). Quality of Cold Stored Strawberries as Affected by Chitosan–Oleic Acid Edible Coatings., Postharvest Biology and Technology, 41: 164-171.

[49] Yu Zhong, George Cavender, Yanyun Zhao (2014). Investigation of different coating application methods on the performance of edible coatings on Mozzarella cheese. LWT - Food Science and Technology, 56 (1), 1-8.

[50] Wang H, Qian J and Ding F (2018). Emerging ChitosanBased Films for Food Packaging Applications, Journal of Agricultural and Food Chemistry, 66(2): 395-413.

[51] Zhao Y, Tu K, Su J, Tu S, Hou Y, et al. (2009). Heat treatment in combination with antagonistic yeast reduces diseases and elicits the active defense responses in harvested cherry tomato fruit. J Agric Food Chem 57: 7565-7570.

[52] Zhong, Y., Cavender, G., Zhao, Y., (2014). Investigation of different coating applicationmethods on the performance of edible coatings on Mozzarella cheese. LWT –Food Sci. Technol. 56, 1–8.

CHAPTER 10

CHASSIS DESIGN AND MANUFACTURING

Emine ALAN[1]
[1]Selcuk University, Konya/Turkey
ORCID: 0000-0002-7970-5155

Murat BOZKIR[2]
[2]Selcuk University, Konya/Turkey
ORCID: 0000-0003-4585-5347

Gökhan YALÇIN[3]
[3]Konya Technical Universty, Konya/ Turkey
ORCID: 0000-0003-4491-0228

INTRODUCTION

On theA-races, the chassis system acts as a skeleton, carrying all the apparatus in the body. Until the 1930s, a separate structural chassis was designed for each vehicle from the body. This structure is called frame-top body. In the 1960s, the monolithic structure became widespread.

Parts such as vehicle body, wheels, engine and transmission are mounted on the chassis and the vehicle is made whole.

Types of chassis according to its structure:

- Ladder type chassis
- Type X chassis
- Offset frame
- Cross-element framed offset
- Perimeter framework
- Monocoque chassis

Usually carbon steel is used for chassis construction in vehicles or aluminum alloy materials are used to create lighter structure. In the case of a separate chassis, the frame consists of structural elements called "profiles" or "beams".

The International Journal of Science, Technology and Design (2020) has said that automobiles are one of the most important inventions that make the life of mankind easier. Cars have been widely used for over a century. Although cars make our lives easier, fossil fuel-powered cars play an important role in air pollution and ozone depletion because they release CO2 gas during operation. For these reasons, fossil fuel-powered cars have now begun to be replaced by fully electric or hybrid cars. Since the automobile-moving parts of electric vehicles are different from those of conventional vehicles, it has led to design differences in certain parts of vehicles. In this study, the design differences of electric vehicles in terms of chassis, body and interior trim compared to conventional vehicles were discussed. [1]

MATERIALS AND FEATURES

The measurements we take as the basis for the chassis design in the vehicle are made by taking into account the shell dimensions. Since it is our main goal in this design to obtain the most effective and lightest chassis remaining in the dimensions, the material we have chosen for our chassis is Aluminum 6061-T6. 6061 Aluminum alloy, aluminum is one of the most versatile heat-treatable alloys. Originally called "Alloy 615", this grade of aluminum was developed in 1935. This alloy is one of the most widely used aluminum grades. This is due to the fact that it exhibits a wide range of mechanical properties as well as corrosion resistance.

6061 aluminum alloy consists of 95.8% to 98.6% aluminum, 0.8% to 1.2% magnesium and 0.4% to 0.8% silicone. Figure 1 shows the table of 6061 aluminum alloy and Figure 2 shows the table of 6061 quality characteristics.

Elementler	6061 Alüminyum Alaşımı
Alüminyum	95.85 – 97.90 %
Silis	0.40 – 0.80 %
Çinko	0.00 – 0.25 %
Magnezyum	0.80 – 1.20 %
Mangan	0.00 – 0.15 %
Krom	0.04 – 0.35 %
Bakır	0.15 – 0.40 %
Demir	0.00 – 0.70 %
Titanyum	0.00 – 0.15 %
Zirkonyum	–
Bakiye	0.00 – 0.15 %

Figure 1. 6061 Aluminum Alloy Table10

The material has a maximum total deformation of 0.86 and a safety coefficient of 3.2. For this reason, weld seams are environmentally and gapless. The dimensions of the profiles used for the chassis are determined as "40x40x2". The maximum length of the chassis is 2773.62 millimeters and the maximum width is 1587.88 millimeters.

Özellikler	6061 Kalite
Akma Mukavemeti	276 MPa
Erime noktası	582 ila 652˚C
Isıl iletkenlik	167 W/mK
Elastisite Modülü	68.9GPa
Elektriksel Direnç	3.99×10^{-6} ohm-cm
İşlenebilirlik	İyi
Sertlik (Brinell)	95

Figure 2. 6061 Quality Characteristics Table11

MANUFACTURING

The welded aluminum material may crack due to internal stresses after welding. In order to minimize this possibility of cracking, the undergas welding, which is the most suitable source for aluminum, is used in the chassis. 5% Magnesium (Mg) alloy aluminum inert gas (MIG) welding wire should be used. Welding current is 100 Ampere, wire speed is 2 123 mm/sec, welding speed is 4 mm/s, welding voltage is 30 Volt and gas flow rate is 9 atm. The gas to be used is pure argon gas. Since the gas is poisonous gas and explosive, care has been taken to keep a constant distance between the tors and the machine. While welding the chassis is done in Figure 3, the chassis welding end image is seen in Figure 4.

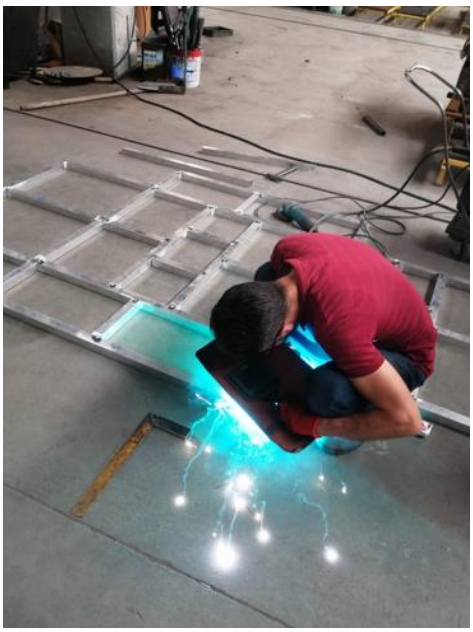

Figure 3. When Welding the Chassis12

Figure 4. Chassis Weld Finish Image13

The chassis consists of 66 parts in total. Each part is also cut to the correct size using a miter (cutter tolerance 1 mm). Each part was cut forward to form a template and the chassis was visually inspected before the spotting process to check the missing or incorrect parts. All parts were first spotted, corrected if there was deflection, and then welded. The welded parts were first stoned, the points that would form a notch were completely removed. Resources were sanded so that there were no sharp corners. While welding, deflection was minimized by making it counter-diagonal in cartazian shape. Figure 5 shows the chassis drawing, Figure 6 shows the chassis render image 1, Figure 7 shows the chassis render image 2, Figure 8 shows total deformation, Figure 9 shows maximum stress.

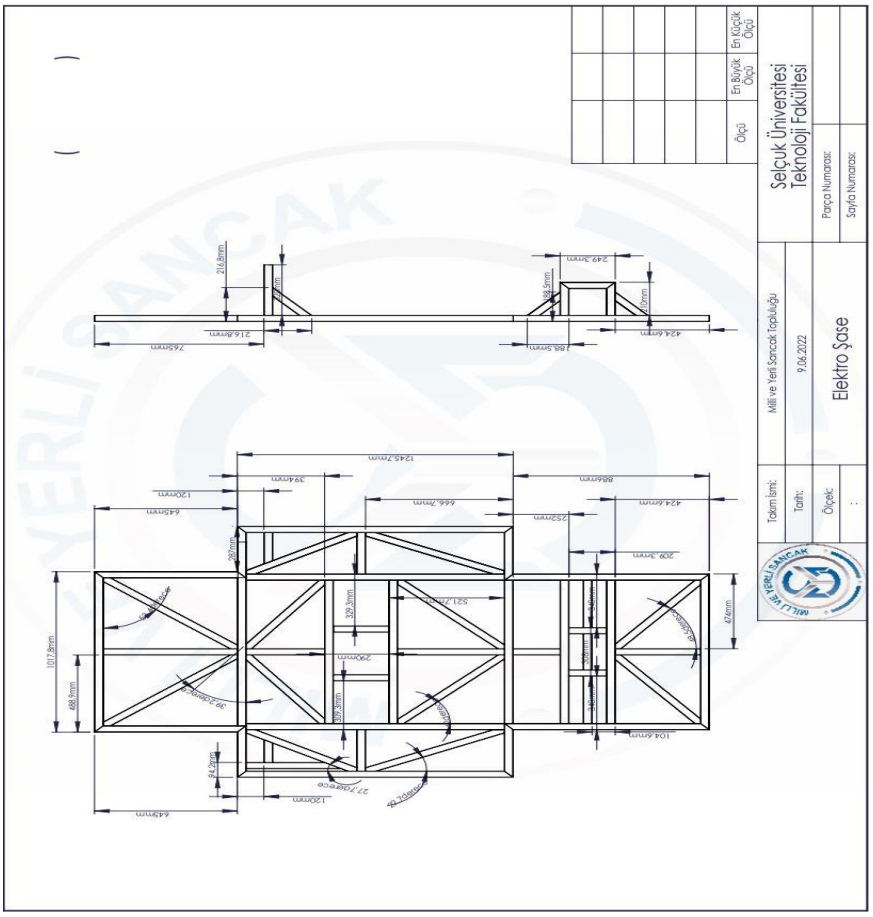

Figure 5. Chassis Drawing14

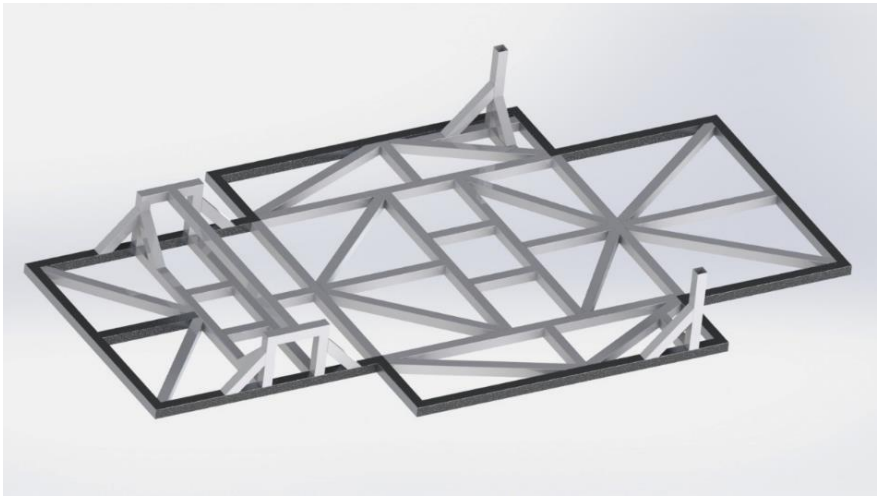

Figure 6. Chassis Render Image 115

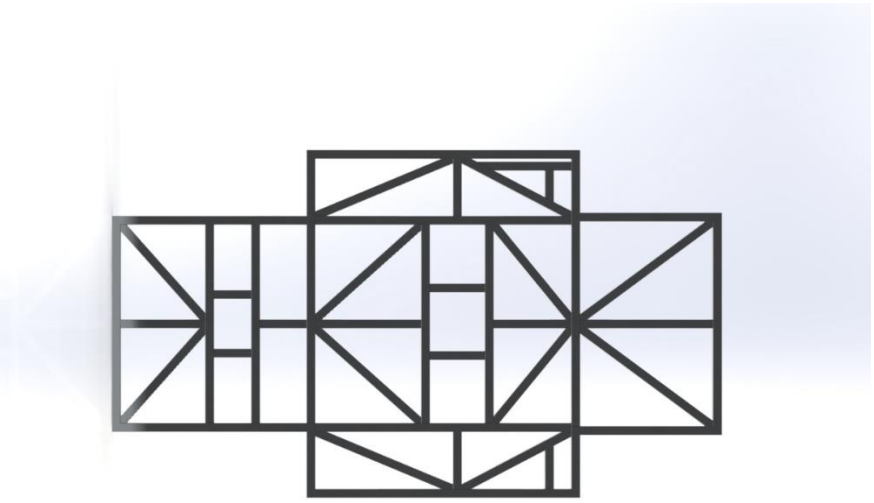

Figure 7. Chassis Render Image 216

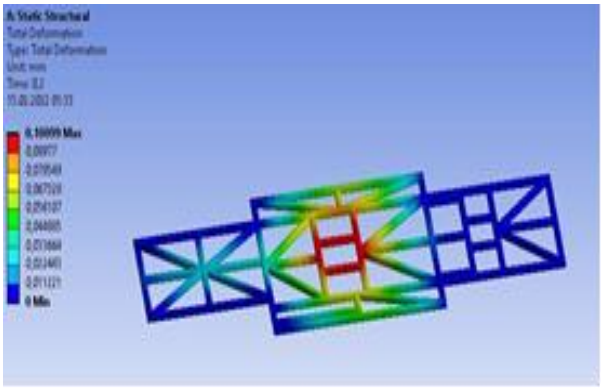

Figure 8. Total Deformation 17

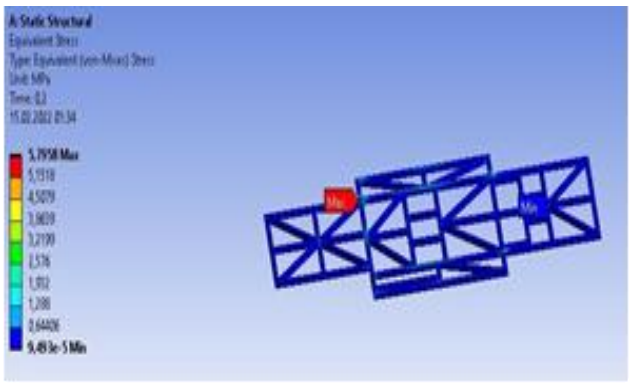

Figure 9. Maximum Stress18

Structural static analysis was performed using ANSYS 2019 R2 program to test the strength of our chassis design. The resulting values showed that the chassis had the desired durability criteria.

REFERENCES

[1] Isilak, C. (2020). "Design differences of electric vehicles in terms of body, chassis and interior trim compared to conventional vehicles". International Journal of Science, Technology and Design, 1(1), 46-58.

[2] https://aydinlarmakinametal.com.tr/6061-ve-7075-aluminyum-alasimi/

[3] https://tr.wikipedia.org/wiki/%C5%9Easi

[4] https://www.otoshops.com/araba-sasisi-nedir-numarasi-nerede-yazar-haber-489

CHAPTER 11

WASTE TO SUSTAINABLE: MARBLE DUST AS GREEN CONCRETE FİLLER

Agil Fitri HANDAYANI[1]
[1]Civil Engineering Department, Universitas Negeri Malang,
ORCID: 0000-0003-3754-4047

Dyah Hayu ROSYIDAH[2]
[2]Industrial Mechanical Engineering Department, Sepuluh Nopember Institute of Technology,

INTRODUCTION

The worldwide cement production estimated around 4500 million tons per year produces a large amount of CO2 emission which contributes to climate change. The calcination process in cement manufacture provides CO2 with an outsized [2,3]. The CO2 produced by the cement industry globally has quite tripled since 1992. Recently, carbon emissions caused by cement production reached 2.6 billion metric tons a year, more than 7% of the total global carbon emissions on 2021, and have increased by 9.3% from 2015 to 2020 [16]. The high production of cement is aligned with the construction industry development using concrete as its material. Therefore, alternative materials are needed to reduce the use of cement in concrete as an effort to maintain global climate change.

Green concrete is defined as a planning concept for environmentally friendly concrete constituents such as reducing cement volume and reducing the use of natural resources, using materials from waste as at least one of its components, or its production process does not cause environmental damage or its high performance and sustainability of its life cycle, e.g. saving energy, CO2 emissions, or waste. [9].

The mining and processing of marble in Indonesia are spread over several islands. Tulungagung is one of the oldest and largest marble-producing areas in Indonesia. The largest marble mining activity is carried out by PT. Industri Marmer Indonesia Tulungagung with a mining area of 5.93 hectares and a production of 9.9 million tons per year. Additionally, around 150 small and medium business units are engaged in processing marble with production reaching 2,250 tons/day [7].

Marble production activities generate waste in the form of marble fragments and water mixed with marble dust which features like slurry, with an amount of around 40% of the marble industry final product [18]. Marble production in large quantities continuously causes problems in the amount of waste produced. The waste disposal system on the open land around the production site is less effective and it pays less attention to land conservation. Consequently, a solution is needed to solve this waste problem.

The research has been done to investigate the possibility of using marble dust as a filler to reduce the use of cement in concrete. Its result shows that the compressive strength of concrete increases with the substance of marble dust by up to 50% and therefore the compressive strength of concrete decreases with the addition of marble dust with more composition [16].

The utilization of marble powder as a partial replacement for cement in concrete shows an increase in compressive strength of 17.7% at 28 days of concrete age achieved by replacing 10% by weight of cement with marble dust. The use of marble powder gradually increases the strength of concrete to a certain extent, but then gradually decreases [15].

The use of pozzolanic waste was motivated not only by cost savings but also by the desire to improve the durability of concrete assets. Concrete manufacturing advancements will reduce natural resources and energy consumption, lowering the environmental impact of contaminants even further [4]. The addition of minerals to concrete generally will affect the behavior of fresh concrete and the mechanical properties of concrete [1]. Due to that, observations were made on the concrete mixture with variations in the use of marble dust as filler and substitute amount of cement weight.

The observations of the physical and chemical properties of marble dust were carried out to determine the possibility of utilization of marble dust in concrete and to determine the effect of using marble dust as a filler in concrete on the behavior of fresh concrete and the mechanical properties of concrete.

The effect of the utilization of marble dust on the properties of fresh concrete was observed and the mechanical properties of the concrete were tested at 28 days of age.

This research is expected to provide benefits as solutions to deal with the waste problems in marble industrial area. Finding materials that will reduce the use of cement in concrete. An additional purpose for environment issue is to create the possibility of reducing CO2 emissions generated during cement production

Figure 1. Marble industrial waste

METHOD A.

Cement

The experiment used Portland Pozzolan cement type IP-U to meet the requirements of ASTM C 595-03 (2007). The specifications for Portland Pozzolan cement are shown in Table 1.

Table 1. Specifications for PPC type IP-U

Test Type	ASTM C 595 - 03	Result
Calcium Oxide (CaO), %	-	58,66
Silicon Dioxide (SiO_2), %	-	23,13
Aluminum Dioxide (Al_2O_3), %	-	8,76
Ferric Oxide (Fe_2O_3), %	-	4,62
Sulfur Trioxide (SO_3), %	≤ 3,50	2,18
Lost of Incandescent (LOI), %	≤ 3,00	1,69
Initial setting time, minute	≥ 45	153
Final Initial setting time, minute	≤ 375	249

Aggregate

In this experiment, fine aggregate in the form of river sand and coarse aggregate were used as crushed stone with the maximum grain size of 20 mm. The used aggregate is a natural aggregate forming. The aggregate specifications used in the study are shown in Table 2.

Table 2. Specifications of aggregate

Aggregate Properties	Fine Aggregate	Coarse Aggregate
Dry specific gravity	2,70	2,56
Specific gravity SSD	2,73	2,67
Absorption (%)	1,08	3,47
Water content (%)	3,79	1,08
Kadar lumpur (%)	0,57	2,38
Modulus of fineness	3,91	6,45

Marble Dust

This experiment used marble dust from Tulungagung Regency. Before being used on waste concrete in the form of sludge, it is dried in an oven at 110º±5ºC. The constant weight of marble dust was obtained after baking for 72 hours with a weight loss of 34.67%. The weight loss in marble dust is shown in Figure 2.

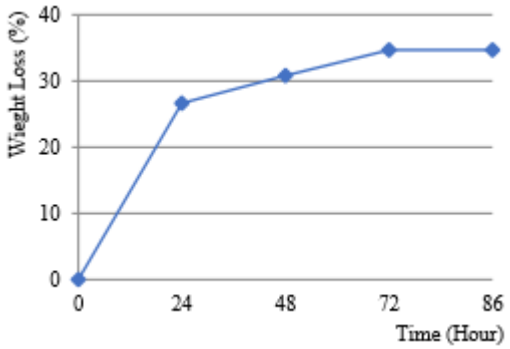

Figure 2. Weight loss of marble dust

Physically, marble dust is bright white and has a specific gravity of 2.79. Marble dust has a fine grain size with 100% of the granules passing through the No.200 sieve with a diameter of 0.075 mm [11,12]. The physics of marble dust can be seen in Figure 3.

Figure 3. Marble Dust

The chemical composition of marble dust is carried out by several methods. The Atomic Absorption Spectrophotometry (ASS) method was used to determine the composition of Calcium (Ca), Ferrum (Fe), and Magnesium (Mg). The Gravimetric method is used to determine the composition of Silicon (Si) and the Spectrophotometric method is used to determine the Aluminum (Al) composition.

The results of the chemical analysis showed that the composition of the marble dust was Silicon Dioxide (SiO2) at 17.63%, Calcium Carbonate (CaO3) at 2.73%, and several other elements. The chemical composition of marble dust is shown in Table 3.

Table 3. Chemical composition of marble dust

Chemical composition	Content (%)
Silicon Dioxide (SiO_2)	17,63
Calcium Carbonate ($CaCO_3$)	2,73
Calcium Oxide (CaO)	1,53
Magnesium Carbonate (MgO_3)	0,20
Magnesium Oxide (MgO)	0,09
Ferric Oxide (Fe_2O_3)	0,01
Aluminum Dioxide (AlO_3)	0,002

Mix Design

To produce high-quality concrete, a mixed design is important. The concrete is designed according to its proportion of materials [13]. Mix design based on Indonesia Standard the planned concrete compressive strength is 20MPa [6]. The specimen is cylindrical with a diameter of 150 mm and a height of 300 mm. The mixture was prepared in 4 groups of specimens with variations using marble dust 0%, 5%, 10%, and 15% by weight of cement with a cement water factor of 0.5 for all specimens.

Concrete Curing

Curing concrete is the process of maintaining the acceptable moisture content of the concrete at the right temperature to support the hydration of the cement in the initial period. Hydration reactions occur when cement is mixed with water, a chemical process will take place, and the chemicals in cement react with water and form new compounds. To obtain the planned compressive strength value, the concrete is soaked until the concrete test time is 28 days, then the specimen is removed from the treatment site and aired until the test time [6]

Testing Method

To determine the behavior of cement paste with the addition of marble powder filler, the initial setting time and final setting time were tested. Abraham’s cone was carried out to define the workability of fresh concrete. Testing the compressive strength of concrete is carried out by applying a load until the specimen is crushed [5]. Tests for the modulus of elasticity and Poisson's ratio are carried out by measuring the longitudinal and transverse strains of the specimen at a load of 40% of the maximum load. Method. The test setting up is shown in Figure 4.

Figure 4. Setting up

THE RESULT

Initial setting time

The initial setting time for testing normal concrete is 120 minutes. The use of marble dust generally causes the initial setting time of cement paste to be longer. The use of 5% marble dust gives an initial setting time of 135 minutes, the longest initial setting time occurs when using 15% marble dust as a filler to replace part of the cement in the concrete. The results of the initial setting time testing are shown in Figure 5.

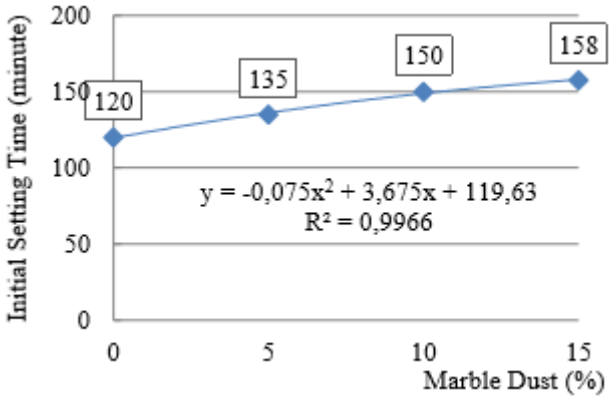

Figure 5. Initial setting time test results

Final Setting Time

The setting time becomes longer with the use of marble dust. The final setting time of a normal concrete mix without additives is 240 minutes. The mixture with the use of 15% marble dust showed the longest final setting time, namely 337.5 minutes. The final setting time test results are shown in Figure 6.

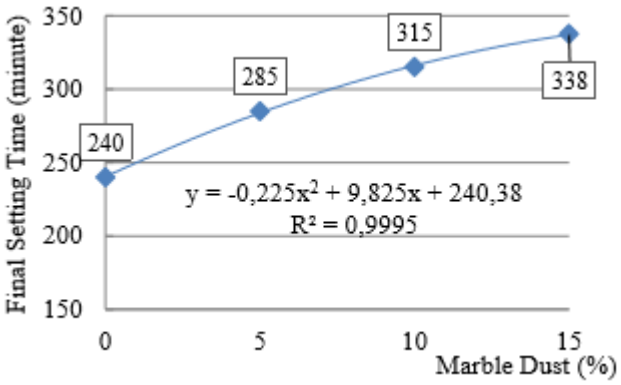

Figure 6. Final setting time test results

Slump Test

The workability of fresh concrete is indicated by the slump value. The slump for normal concrete without the use of marble dust is 120 mm. The use of marble dust in concrete shows an increase in the workability of fresh concrete. The slump test result is shown in Figure 7.

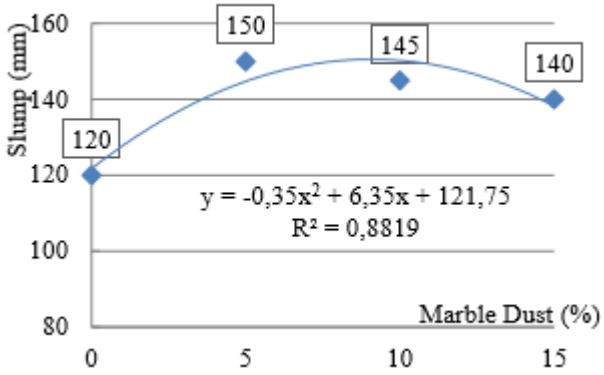

Figure 7. Slump test results

Compressive Strength

The compressive strength of concrete is determined by applying the load gradually to the concrete cylinder specimen. Normal concrete without the use of marble dust shows a compressive strength of concrete of 22.36 MPa. The use of 5% marble dust in concrete increases, showing a compressive strength of concrete of 25.31 MPa. The compressive strength decreases with the use of 15% marble dust as a filler by reducing the amount of cement. The compressive strength results for various variations of marble dust are shown in Figure 8.

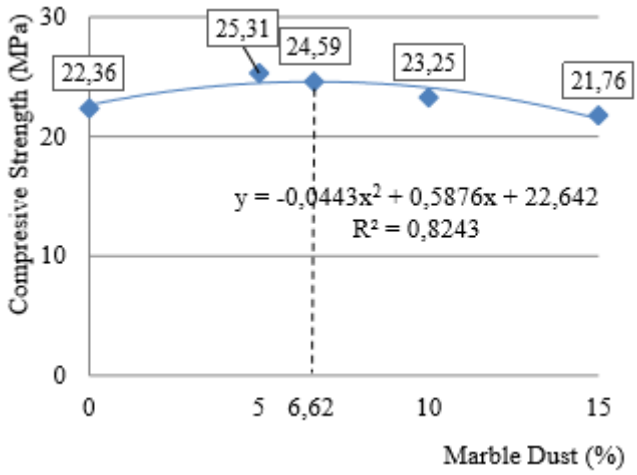

Figure 8. Compressive strength test results

Modulus of Elasticity

The modulus of elasticity of normal concrete without the use of marble dust is 21.331 MPa. The modulus of elasticity increases with the use of marble dust on concrete, the highest modulus of elasticity is shown by concrete with variations of 5% marble dust of 25821 MPa. The use of marble dust of 10% shows a concrete modulus of elasticity of 24.036. The use of marble dust generally gives a better value of the concrete's modulus of elasticity. The complete results of the concrete modulus of elasticity test can be seen in Figure 9.

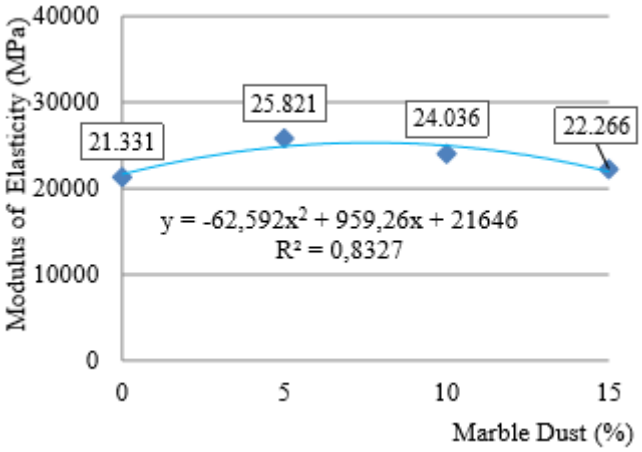

Figure 9. The modulus of elasticity

Poisson's Ratio

The Poisson's ratio for normal concrete without the use of marble dust is 0.20. A variation of 5% marble dust gives a Poisson's ratio of 0.18. The Poisson's ratio decreases with the addition of more marble dust. The results of the concrete Poisson's ratio (μ) test are shown in Figure 10.

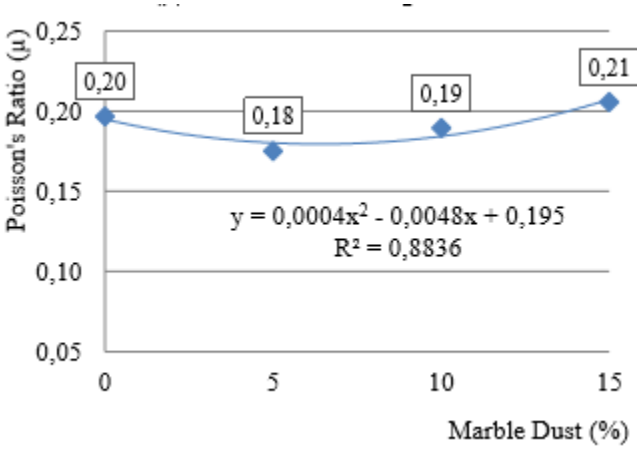

Figure 10. Poisson's ratio test results

DISCUSSION

Based on an analysis of the marble dust chemical composition, there is a significant difference when compared to the chemical composition of portland pozzolan cement (PPC). Where Calcium Oxide (CaO) and Silicon Dioxide (SiO2) in PPC cement are 58.66% and 23.13% respectively [17] whereas in marble dust the CaO content is 1.53% and SiO2 is 17.63%. Additionally, marble dust which comes from marble is classified as a natural rock that has a large rate enough Oxygen (O2) of ± 49.0% so that the loss of glow in marble dust is quite large [18].

Based on physical and chemical analysis, marble dust can be used as a filler in concrete and reduces the use of cement in concrete. The utilization of marble dust in concrete provides an advantage due to its fine grains can fill the spaces between the aggregates and makes the concrete more cohesive also increases concrete's density. Furthermore, besides reducing the impact of waste for environment, it also produces concrete with better mechanical properties.

The favorable mechanical properties of concrete are characterized by high compressive strength, large modulus of elasticity, and little Poisson's ratio. The test results showed that the optimum results were obtained in the mixture with the use of marble dust at 6.62, the use of 10% marble dust increased the mechanical properties of concrete but the increase was not significant. Using 15% marble dust showed a relatively small decrease in compressive strength.

The use of marble dust as a concrete filler with the amount of 6.62% gives a benefit in increasing the compressive strength of concrete until 9.97%. The reduction of cement in concrete has an impact on reducing carbon emissions produced by cement calcination process which affects global climate change. This also provides a solution to solve the waste problem happening in the marble industrial area.

CONCLUSION

Based on the physical and chemical analysis results, it is concluded that marble dust can be used as an eco-friendly concrete filler. The use of marble dust shows an optimum result with a percentage of 6.62% giving compressive strength at 24.69 MPa. It has a good effect on the mechanical properties of concrete, high compressive strength, large modulus of elasticity, and small Poisson's ratio. The use of 6.62% marble dust increases the concrete compressive strength until 9.97%. In addition, further research is recommended to analyze the chemical composition of marble dust with different methods to determine the overall chemical composition. The use of marble industrial waste as concrete aggregate needs to be

studied to optimize waste utilization and reduce the industrial impact on the environment. Besides it is also necessary to develop a machine-based waste system.

REFERENCES

[1] A. A. Aliabdo, M. A. Elmoaty, E.M. Auda, "Re-use of waste marble dust in the production of cement and concrete," Construction and Building Materials Volume 50 Pages 28-41, January 2014.

[2] A.K. Thakur, A. Pappu, V.K. Thakur, "Resource efficiency impact on marble waste recycling towards sustainable green construction materials," Current Opinion in Green and Sustainable Chemistry 13 91–101, October 2018.

[3] A. S. Gaharwar, N. Gaurav, AP Singh, H. S. Gariya, Bhoora "A Review Article on Manufacturing Process of Cement, Environmental Attributes, Topography and Climatological Data Station: IMD, Sidhi M.P," Journal of Medicinal Plants Studies 2016; 4(4): 47-53, June 2016. [4] A. Shukla, N. Gupta, A. Gupta," Development of green concrete using waste marble dust", Materials Today: Proceedings, April 2021.

[5] ASTM. "Annual Book of ASTM Standards Vol 04.02 Concrete and aggregates,"2007.

[6] Badan Standarisasi Nasional," SNI 03 – 2834 – 2000 Tata cara pembuatan rencana campuran beton normal"

Jakarta, 2000.

[7] BPS-Statistic of Tulungagung Regency, "Kabupaten Tulungagung dalam angka," ISSN: 0215-5885, 2022.

[8] G. Harbert "Assessing the environment impact of conventional and green cement production," Life Cycle Assessment (LCA), Eco-Labelling and Case Studies Pages 199-238, 2014.

[9] G. L. Golewski, "Green Concrete Based on Quaternary Binders with Significant Reduced of CO2 Emissions," Energies 2021, 14, 4558, July 2021.

[10] Omar M., Ghada D. Abd Elhameed, M. A. Sherif, Hassan

A. Mohamadien, "Influence of limestone waste as a partial replacement material for sand and marble dust in concrete properties," Housing and Building National Research Center, Pages 193-203, June 2012.

[11] N. Bheel, K.A.Kalhoro, T. A. Memon "Use of Marble dust and Tile Powder as Cementitious Materials in Concrete," Engineering Technology & Applied Science Research Vol 10. No. 2, April 2020.

[12] N. Intaboot and K.Chartboot, "Influence and Possibility of Using Limestone Dust Replacement of Sand for Sustainability in Concrete Production," Applied Science and Engineering Progress, Vol. 15, No. 3, November 2021.

[13] R.B. Oza, M. Z. Kangda, M. R. Agrawal, P. Ra. Vakharia, D. S. M. Solanki, "Marble dust as a binding material in concrete: A review," Materials Today: Proceedings 60 (2022) 421–430, February 2022.

[14] R. Kajaste, M. Hurme, "Cement industry greenhouse gas emissions e management options and abatement cost," Journal of Cleaner Production Volume 112, Part 5, Pages 4041-4052, January 2016.

[15] Shirule, P. A., Rahman, A & Gupta, D. R. Partial replacement of cement with marble dust powder. J. Advance Engineering Research and Studies. E – ISSN 2249 – 8974, pp: 175–177. June 2012.

[16] Sakalkale, G. D. Dhawale, R. S. Kedar, "Experimental Study on Use of Waste Marble Dust in Concrete". Journal of Engineering Research and Applications, Vol. 4, October 2014.

[17] Semen Gresik, "Komposisi kimia dan pengujian fisika PPC Tipe IP-U," November 2022.

[18] V.M.Shelke, Prof. P.Y.Pawde, R..Shirvastava "Effect of marble powder with and without silica fume on mechanical properties of concrete," Journal of Mechanical and Civil Engineering (IOSRJMCE) ISSN: 2278-1684 Volume 1, Issue. June 2012.

CHAPTER 12

INVESTIGATION OF THE EFFECT ON THE DRONE'S ENERGY CONSUMPTION THE FLYING AT DIFFERENT ALTITUDES

Salim AKSOY[1]
[1] Selcuk University, Konya/Turkey
ORCID: 0000-0001-5536-0204

Fatih Alpaslan KAZAN[2]
[2] Selcuk University, Konya/Turkey
ORCID: 0000-0002-5461-0117

Abdullah Cem AĞAÇAYAK[3]
[3] Konya Technical University, Konya/Turkey
ORCID: 0000-0002-9285-5764

INTRODUCTION

Unmanned aerial vehicles (UAVs) are devices that can fly owing to the propellers that take their mechanical energy from the engines, can be controlled from the ground, or fly according to a planned flight path. Today, they are widely used for military, civil, commercial, and hobby purposes.

UAVs that work with more than one rotor and propeller and whose motors are individually adjusted and whose linear and angular movement in 3 axes are controlled are called multi-copters. They are preferred more than other UAVs due to their flight capability, vertical take-off and landing capabilities, and ability to hover in the air. According to the number of rotors and propellers, they are called different names as bicopter (2 propellers), tricopter (3 propellers), quadcopter (4 propellers), hexacopter (6 propellers), and octocopter (8 propellers).

Quadrocopter; It is a rotary wing UAV that can take off and land vertically, can hover in the air, has high maneuverability, is structurally simple despite its complex control system, and creates a carrying force through its propellers by utilizing the propulsion power produced by four motors (Figure 1). It is more popular than other UAVs and is now referred to as a drone.

Figure 1: Quadcopter

Drones are used for different purposes and expectations may vary according to the intended use. Some carry relatively heavy loads, while some are only used for aerial image acquisition. However, for whatever purpose it is used, the biggest expectation is that the drone should have a longer flight time. In order to achieve this, simply increasing the battery capacity will increase the drone's weight, so the drone's flight performance will decrease. The easiest solution that can be produced here is for the drone operator to have knowledge of the parameters affecting the flight time and for the operator to manage the flight accordingly. This can only be done in light of the data obtained as a result of experimental studies.

In the literature review conducted to examine the studies on this, very different studies were found on the drone and its components. For example; the study of drones, their types, and components [1], control of brushless DC (BLDC) motors used in drones [2], flight control in quadrotor-type multicopters [3], creation of the PID control algorithm of the quadrotor UAV by using Arduino [4], height and position control in quadrotor UAVs [5], creating the mathematical model of the quadcopter by obtaining the equations of motion and rotation according to Newton's laws [6], quadcopter design that can carry a fire extinguisher ball [7], examination of lion batteries used in UAVs [8-10], estimation of the lifetime of the batteries [11], wireless battery management system for lion batteries [12], Investigation of aging in battery cells using strain gauge sensors [13], monitoring the swelling of the battery by using a micro strain gauge sensor and ensuring battery safety [14], development of software for reducing the use of batteries in drones [15], improving battery performance in drones [16], estimating flight time in drones

[17, 18], creating a model for the battery [19], detecting the location of the drone in the face of mechanical failure and cyber-attack with an external system added to the drone's battery [20], development of an algorithm to reduce energy consumption in drones used in the commercial package works and performing autonomous flights [21], determination of battery capacity in lion batteries using artificial intelligence [22], theoretical review of structural factors and models that will affect energy consumption in drones [23], and drone design that does not hit obstacles [24] are some of them.

As can be seen, a wide variety of studies have been conducted on the multicopter and its components. However, no experimental study has been found to see the effect of flight altitude on total energy consumption. Therefore, in this study, it was experimentally investigated how the total energy consumption would be affected if the same task (i.e., the same route) was performed by flights at different altitudes. In this context, first of all, a drone was designed, the details of which are given below. Then, the results obtained by performing flights at four different altitudes, 18, 45, 60 and 75m, were examined.

HARDWARE AND SOFTWARE COMPONENTS OF THE DRONE USED IN THE EXPERIMENTAL STUDY

The drones consist of different hardware components such as a frame, motor, propeller, electronic speed controller, flight control card, remote control, telemetry system, and battery. In addition, the relevant sensors and cameras are also used to obtain the altitude and location information required for autonomous flights.

BLDC motors are widely used in drones due to the lack of brush and collector arrangement and the high power/weight ratio. In this study, four BLDC motors were used to produce the mechanical energy required by the propellers. So, in this study, four BLDC motors were used to produce the mechanical energy required by the propellers. The motors used are X4110S 400kV model BLDC motors produced by Sunnysky. 15x5.5 inch carbon fiber propellers were used as propellers. The BLDC motor and propellers used are shown in Figure 2.

Figure 2: BLDC motor and propellers used in the drone.

However, as it is known, BLDC motors are not plug-and-play motors and need to be driven. The device that allows the speed and direction of the drone to be controlled by controlling the speeds of these motors is the electronic speed control (ESC) unit. In this study, the T-Motor Air 40A model ESC, which is shown in Figure 3, was used.

Figure 3: The ESC used in the drone.

It is necessary to control the drone's flight by evaluating both the commands from the user and the data from the sensors on the drone. Electronic devices used for this purpose are called flight control cards. For this purpose, the Pixhawk 2.4.8 flight control card, which is shown in Figure 4, was preferred and used in the study.

Figure 4: The flight control card used in the drone.

In order to meet all the electrical needs of the drone for flight, a Leopard Power Lipo battery with a capacity of 10.000 mAh was used as the battery shown in Figure 5.

Figure 5: The battery used in the drone.

Providing location information during the flight of the drone is very important, especially during autonomous flight. In this study, Radiolink Se100 M8n with 0.5m position sensitivity, which is shown in Figure 6, was used as a GPS sensor to obtain the location information of the drone during flight.

Figure 6: GPS used in the drone.

All the basic components mentioned above were mounted on the frame and the drone to be used in the experimental study was obtained. The related drone weighs 4.2 kg and is shown in Figure 7.

Figure 7: The drone used in the experimental study.

The FrSky Taranis X9D Plus remote control shown in Figure 7 was used to control the drone in Figure 8 from the ground. The controller in question is 24-channel and has an ISRM-S-X9 built-in RF module.

Figure 8: Remote control of the drone used in the experimental study.

Instant display of flight data such as instantaneous speed, altitude, battery parameters, and position on the remote control provides better management of the flight. In this study, the RFD 900X model telemetry system in Figure 8 was used in order to instantly monitor the data to be obtained on the control in Figure 9.

Figure 9: The RFD 900X telemetry system used in the drone.

The program called Mission Planner was used in order for the drone, of which all its components were introduced in terms of hardware, to both perform its task autonomously and to monitor the data during the flight instantly from the computer, apart from the remote control. This program, which is constantly evolving due to its open-source feature, also allows the recorded data to be examined after the flight, in addition to the aforementioned features. The interface of the program, which has support for many languages, is shown in Figure 10.

Figure 10: The interface of the program called Mission Planner.

In order to better study the effect of choosing different altitudes on energy consumption in the performance of the same task, the experimental study should be performed autonomously. To carry out this autonomous flight, a route of about 300m has been established. The route in question is given in Figure 11.

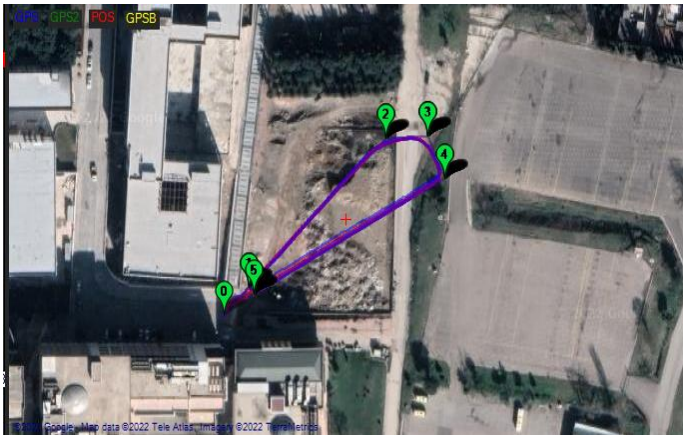

Figure 11: The route created using the Mission Planner for the experimental study.

EXPERİMENTAL STUDİES

A parameter or parameters belonging to the experiments performed can be graphed by selecting them from the red highlighted section on the right side of the interface, which can be seen in Figure 12. However, it is not possible to show the parameters of the experiments performed at different altitudes on the same graph. Therefore, in order to be able to draw the parameters of different altitude experiments on the same graph, the data obtained from experimental studies were transferred to Matlab and the graphs were drawn in Matlab.

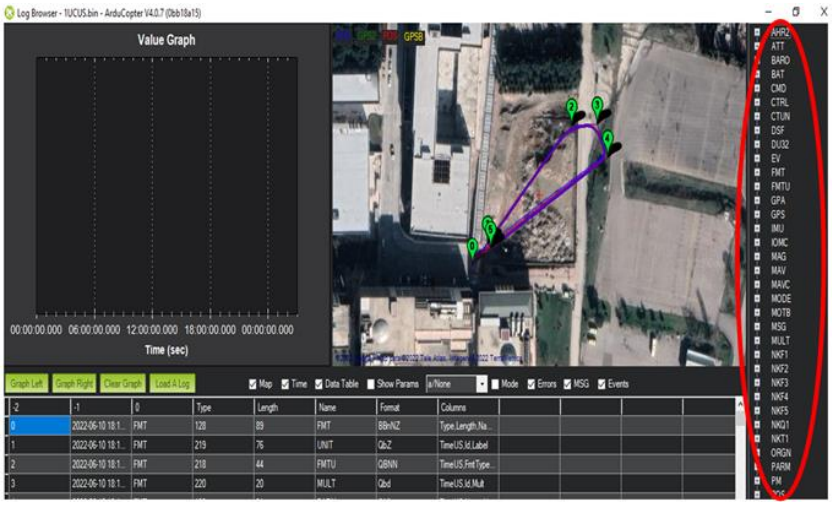

Figure 12: The section that allows any parameters of the flights performed to be selected in Mission Planner and displayed in graphical form.

The experiments were carried out at four different altitudes (18m, 45m, 60m, and 75m) and at a constant speed. No load was added to the drone during the experiments. When the drone reaches the relevant altitude, the altitude value is kept constant as seen in Figure 13. The reason for this is to ensure that the effect of altitude on energy consumption can be seen more clearly.

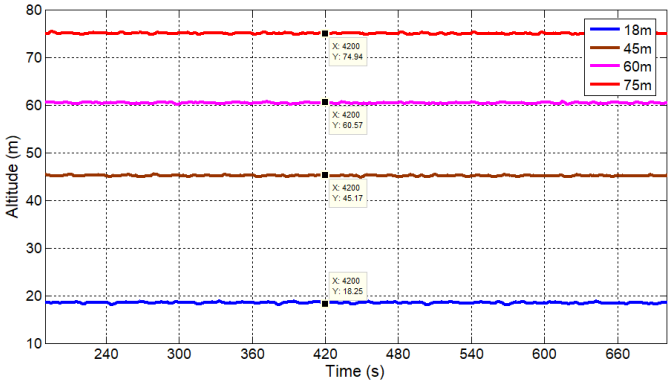

Figure 13: The altitudes at which the experiments were carried out.

The battery was fully charged before each flight. However, despite this, sometimes a very small decrease of 2% was observed in the occupancy rate of the cells. This cellular difference can be seen in Figure 14.

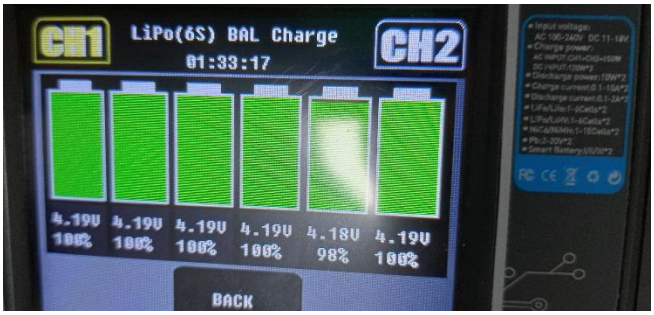

Figure 14: Charge rate of the battery cells before the flight.

Differences similar to those in Figure 12 can also be seen in Figure 15, where the battery terminal voltage changes for each altitude experiment are presented graphically. The largest difference in Figure 15 was measured as 0.3V. The sudden drops in the battery terminal voltages at the end of the first 30 seconds are the usual drops caused by the high current that the drone suffers due to the start of the flight.

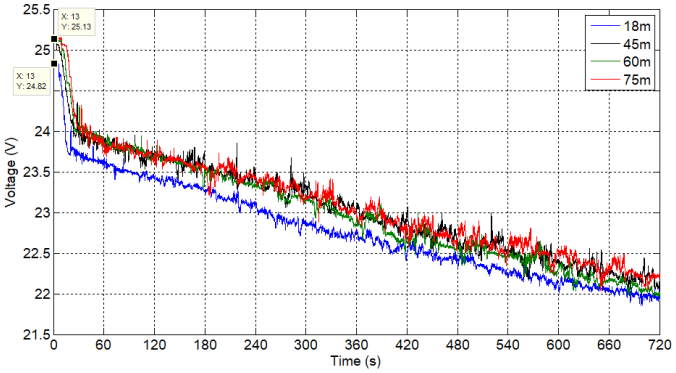

Figure 15: Variation of battery terminal voltage at different altitudes.

The changes in the currents were also examined in the experiments carried out at different altitudes. The obtained current curves are given in Figure 14 for a certain flight period. When the curves in Figure 16 are examined, it is seen that there is a change in currents depending on altitude. However, since there are sudden changes up to 8A in the measured currents, it has not been possible to interpret the graphs as they are and to reveal the change in proportion to the altitude.

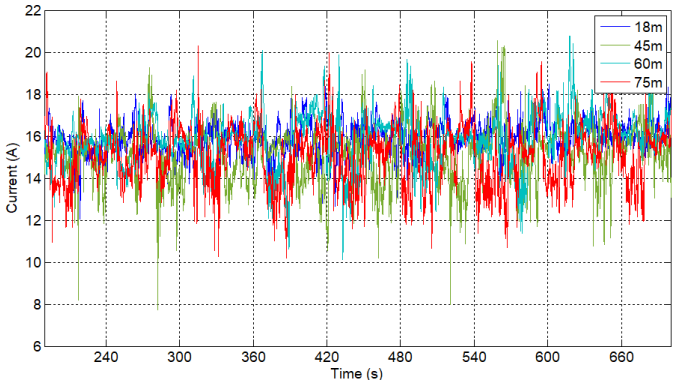

Figure 16: Variation of battery current at different altitudes.

Presenting the change in the instantaneous total energy amount consumed graphically will provide a clear understanding of the change depending on altitude. However, since this data is started to be collected from the moment the drone is activated, the consumption, when the drone is activated but not started to fly, is also included. In order to eliminate this undesirable situation and to find the total energy consumption for only after the drone takes off, the battery terminal voltage (V), current drawn from the battery (I), and time (t) values are used. Using these parameters, the value (W) of the energy in Wh was calculated as in equation (1).

$$W = \frac{V \cdot I \cdot t}{3600} \qquad (1)$$

These calculated instantaneous values were then added up and the total energy value consumed during the flight was obtained. It is seen in Figure 15 that the total energy consumption of 18, 45, 60 and 75m altitudes is 74.6Wh, 77.1Wh, 78.8Wh and 83Wh, respectively.

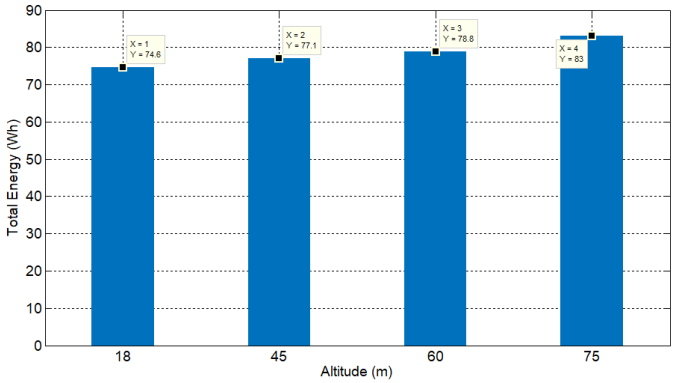

Figure 17: Total energy consumption values for flights at 18, 45, 60, and 75m altitudes.

CONCLUSION AND DISCUSSION

In this experimental study, the effect of flying at different altitudes on the total energy consumption was investigated. In order to examine this effect, a flight route of approximately 300m has been determined. Then, flights were carried out on this route at four different altitudes, 18, 45, 60, and 75m.

At the end of the flights performed, the following results were reached:

- The total energy consumptions for the altitudes of 18, 45, 60, and 75 m were 74.6Wh, 77.1Wh, 78.8Wh, and 83Wh, respectively.
- When the energy consumption at 18m altitude is taken as a reference, the energy consumption at 45m altitude is increased by 3.35%, the energy consumption at 60m is increased by 5.63%, and the energy consumption at 75m is increased by 11.26%.
- When the percentage increase values in energy consumption per meter were calculated, the results of 0.12%, 0.13%, and 0.20% were obtained, respectively. Therefore, the average increase was realized as 0.15%.

In experimental studies, it was tried to perform the flights in a windless weather as much as possible. However, unpredictable sudden weather changes and wind speed differences that may be experienced at different altitudes are the parameters that should be taken into account on these results. Therefore, researchers who will conduct such studies in the future should also take into account wind speed and record it as a parameter. In this way, it will be possible for them to reveal more clearly the altitude-related changes in energy consumption. In addition, the voltages of the battery cells should always be checked before the flight, and if they are not equal, the experiments should not be started before they are equalized.

REFERENCES

[1] R. Clarke, "Understanding the drone epidemic," Computer Law & Security Review, vol. 30, no. 3, pp. 230-246, 2014.

[2] B. Ulu, "Brushless direct current motor (BLDC) speed control," Yüksek Lisans, İnönü Üniversitesi Fen Bilimleri Enstitüsü, İstanbul, 2011.

[3] İ. Dikmen, A. Arisoy, and H. Temeltaş, "Dikey İniş-Kalkış Yapabilen Dört Rotorlu Hava Aracının (Quadrotor) Uçuş Kontrolü," Journal of Aeronautics & Space Technologies/Havacilik ve Uzay Teknolojileri Dergisi, vol. 4, no. 3, 2010.

[4] E. Kıyak and G. Göl, "Arduino Geliştirme Kartı ile Döner Kanatın Kontrolü ve Kontrol Yazılımlarının Geliştirilmesi," in Otomatik Kontrol Türk Milli Komitesi Ulusal Toplantısı, Denizli, Türkiye, September 10-12, 2015.

[5] C. Altın, " Multirotor Unmanned Aerial Vehicle Attitude And Altitude Control," Yüksek Lisans, Bozok Üniversitesi Fen Bilimleri Enstitüsü, Yozgat, 2013.

[6] E. Selim, E. Uyar, and M. Alcı, "Quadrocopterin Matematiksel Modeli Ve Kontrolü," TOK2013-Otomatik Kontrol Ulusal Toplantısı, pp. 548-553, 2013.

[7] S. Köz, "Yangın Topu Kullanılarak Yangın Söndüren Quadrocopter Tasarımı Ve Prototip İmalatı," Yüksek Lisans, Trakya Üniversitesi, Fen Bilimleri Enstitüsü, 2019.

[8] X. Chen, W. Shen, T. T. Vo, Z. Cao, and A. Kapoor, "An overview of lithium-ion batteries for electric vehicles," in 2012 10th International Power & Energy Conference (IPEC), 2012: IEEE, pp. 230-235.

[9] T. Horiba, "Lithium-Ion Battery Systems," Proceedings of the IEEE, vol. 102, no. 6, pp. 939-950, 2014.

[10] M. Berecibar, I. Gandiaga, I. Villarreal, N. Omar, J. Van Mierlo, and P. Van den Bossche, "Critical Review of State of Health Estimation Methods of Li-Ion Batteries for Real Applications," Renewable and Sustainable Energy Reviews, vol.

56, pp. 572-587, 2016.

[11] E. Cabrera-Castillo, F. Niedermeier, and A. Jossen, "Calculation of The State of Safety (SOS) for Lithium Ion Batteries," Journal of Power Sources, vol. 324, pp. 509-520, 2016.

[12] J. Farmer et al., "Wireless Battery Management System for Safe High-Capacity Energy Storage," Lawrence Livermore National Lab.(LLNL), Livermore, CA (United States), 2013.

[13] X. Cheng and M. Pecht, "In Situ Stress Measurement Techniques on Li-Ion Battery Electrodes: A Review," Energies, vol. 10, no. 5, p. 591, 2017.

[14] Ö. C. Kıvanç, "Fiziksel Değişimlerin Li-ion Batarya Üzerine Etkilerinin İncelenmesi," Avrupa Bilim ve Teknoloji Dergisi, no. 16, pp. 235-241, 2019.

[15] L. Corral, I. Fronza, N. E. Ioini, and A. Ibershimi, "A Measurement Tool to Track Drones Battery Consumption During Flights," in International Conference on Mobile Web and Information Systems, 2016: Springer, pp. 334-344.

[16] J. Kim, Y. Choi, S. Jeon, J. Kang, and H. Cha, "Optrone: Maximizing Performance and Energy Resources of Drone Batteries," IEEE Transactions on Computer-Aided Design of Integrated Circuits and Systems, vol. 39, no. 11, pp. 3931-3943, 2020.

[17] A. Abdilla, A. Richards, and S. Burrow, "Power and Endurance Modelling of Battery-Powered Rotorcraft," in 2015 IEEE/RSJ International Conference on Intelligent Robots and Systems (IROS), 2015: IEEE, pp. 675-680.

[18] K. Maekawa, S. Negoro, I. Taniguchi, and H. Tomiyama, "Power Measurement and Modeling of Quadcopters on Horizontal Flight," in 2017 Fifth International Symposium on Computing and Networking (CANDAR), 2017: IEEE, pp. 326-329.

[19] Y. Chen, D. Baek, A. Bocca, A. Macii, E. Macii, and M. Poncino, "A Case for A Battery-Aware Model of Drone Energy Consumption," in 2018 IEEE International Telecommunications Energy Conference (INTELEC), 2018: IEEE, pp. 1-8.

[20] L. He and J. Pace, "Estimating Altitude of Drones Using Batteries," in 2020 IEEE/ACM Fifth International Conference on Internet-of-Things Design and Implementation (IoTDI), 2020: IEEE, pp. 264-265.

[21] S. Park, L. Zhang, and S. Chakraborty, "Battery Assignment and Scheduling for Drone Delivery Businesses," in 2017 IEEE/ACM International Symposium on Low Power Electronics and Design (ISLPED), 2017: IEEE, pp. 1-6.

[22] S. M. Qaisar and A. E. E. AbdelGawad, "Prediction of the Li-Ion Battery Capacity by Using Event-Driven Acquisition and Machine Learning," in 2021 7th International Conference on Event-Based Control, Communication, and Signal Processing (EBCCSP), 2021: IEEE, pp. 1-6.

[23] P. Beigi, M. S. Rajabi, and S. Aghakhani, "An Overview of Drone Energy Consumption Factors and Models," arXiv preprint arXiv:2206.10775, 2022.

[24] H. Solak, "Drone'larda Engellere Çarpmayı Önleyecek Sistemin Geliştirilmesi," Yüksek Lisans, Selçuk Üniversitesi Fen Bilimleri Enstitüsü, Konya, 2022.

CHAPTER 13

VSC BASED HVDC TECHNOLOGY: A REVIEW AND COMPARISON OF CONVENTIONAL VECTOR CONTROL AND MODERN ADAPTIVE CONTROL TECHNIQUES

Fatih BURAK
Selcuk University, Konya/Turkey
ORCID: 0000-0001-5204-5639

INTRODUCTION

High voltage direct current (HVDC) transmission is a high power electronics technology utilized in electrical network systems based on its characteristics such as being efficient, economic and flexible to realise a large amount of power flow over long distances especially for overhead lines or underground/submarine cables which exists for transmission line [2, 3].

An experimental realisation of this technology was first carried out by Gotland and Sweden national operators as a transmission line between in 1954 with 20 MW and 100 kV. This first commercial HVDC transmission was employed with traditional thyristors which has nominal values of 50 kV and 100 A [4].

Over the past 40 years there has been a significant increase in HVDC transmission system settlement with first examples called line commutated converters (LCC-HVDC) using thyristors. The main advantage of this method is operation of large amount of power however some drawbacks such as high harmonic content, lack of the full system control availability and high investment costs. There were two basic approaches in the past being adopted in research into HVDC. One is LCC approach described before and the other is Voltage Source Converter (VSC) approach. Although, LCC had given a high power management, the LCC type converter had a main shortcoming of possessing Short Circuit Ratio (SCR) more than 2 that creates instability and poor efficiency [1, 5]. So, in 1997, VSC technology was easily established instead of LCC in high voltage applications by the help of improvement at power electronics and high switching technology (turn onoff concept). Therefore VSC based HVDC with selfcommutated switches became more common compared to the line commutated converters as VSC differs from LCC in a number of important ways slightly enhancing of disadvantages which are described above [4, 2].

This review study is having a role to describe VSCHVDC developments and its control mechanism from the conventional point of view to the more advanced concept in Section IV. Before employing these methodologies to examine VSC-HVDC deeply it is necessary to mention general concept of Classical HVDC, HVAC and VSC-HVDC with advantageous and disadvantages which is discussed in Section II and III. In the Section III that follows, it will be argued that possible average modelling of VSCHVDC based on voltage, current and power management. Finally, issues and challenges in the existing VSC based HVDC control systems will be explained in results and discussion title.

APPLICATIONS OF HVDC TECHNOLOGY

HVDC method can be employed in the following areas which are separated independently.

- Asynchronous operation between AC power systems

Sometimes, the connection between two AC networks might be difficult or even impossible because of stability reasons. As a solution to this problem, HVDC modelling can provide a useful and economical way to realize this connection which seems to be the only way to make a consistent process of power transmission between these two Alternative Current (AC) networks. This is exemplified in the system undertaken by applying different nominal frequencies (50 and 60 Hz) HVDC link established in Japan and South America [6-7].

- Submarine/underground cable transmissions

The HVDC lines can be settled across land as overhead or underground lines, or installed under water as submarine cables. This application supplies no physical restriction without concerning distance,

economical and safety power range of HVDC link about a few tens of Megawatts (MW). Furthermore it can be beneficial in order to take into account all system savings which is basically investment cost of cable [7-8].

- Long distance bulk power transmissions

As was pointed out in the introduction to this paper, HVDC is a powerful equipment which transmits electric power taken from one point in a three-phase AC network, converted to DC in a converter and transported to the ending point by an overhead line or cable. The energy is converted again to AC at inverter stage and delivering to the end-point AC network such as hydroelectric plants or large scale wind farms even if the possible excessive distances come across with. Thus, it is also possible that HVDC technology are easily adapted to the Power system topologies since it is assumed more economical and attractive option than conventional AC lines by assuring a higher power transfer capability for its designers and users over long distances [2,9].

- Stabilization process of power transmission in integrated power systems

DC network system has the capability of fast operation based on its nature. Therefore, DC systems tend to perform better than AC systems on controllable capability handling electrical circuit overloads and stabilisation problems. The IPP link in USA can be given as an example to represent this situation. [2].

- The offshore transmission use

Although AC technology has the advantage of less investment necessity and can also be used for applied system successfully, it can bring about some disadvantages which affect the offshore wind farm directly. The origins of these problems sourced from the charging current of the cables, limitation of the traditional AC cable, the demand of reactive power compensation and high power loss. Moreover, VSCbased HVDC transmissions have a capability of injecting more reactive power to the offshore wind farms. Overall these opportunities support the view that it can be considerate as a server for isolated loads on islands as a consequence of the some positive features such as self-commutation, black-start and dynamic voltage control [10, 11].

VSC-HVDC TECHNOLOGY AND SYSTEM CONFIGURATION

Until recently, there has been several type of HVDC technology apart from VSC and LCC especially for current source converter (CSC) based on siliconcontrolled rectifiers (SCRs), symmetrical gate commutated thyristors (SGCTs) or gate commutated thyristors (GCTs).On the other hand VSC based HVDC system consists of more innovative and controllable components such as insulated gate bipolar transistors (IGBT- enables the use of advanced PWM technology) by means of the improved new technologies in power electronics [2].

The main advantage of using PWM and IGBT is the capability of obtaining desired voltage output at several kHz (2-3 kHz). From the Fig 1, PWM provides a proper control of active and reactive power without coupling each together. That’s to say that independent control of real-reactive power can be an effective way of inherent HVDC control capability [13].

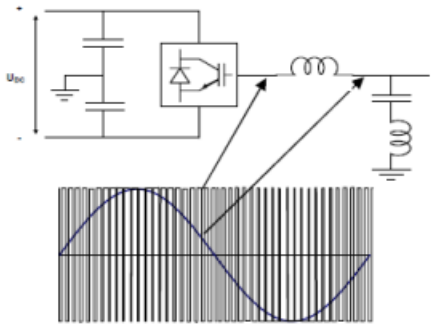

Fig 1. The PWM Pattern basic schematics and form [13].

Having defined what is meant by general knowledge, deeply analysis will now move on to discuss control and configuration aspect. When the difference between VSC-HVDC and classical HVDC is examined properly, the most significant one can be described as “Controllability”. As it is mentioned before, active and reactive power can be controlled independently from each other as if imitating an auxiliary service to the system and also no need any compensation component. This can be realised by fulfilling the active power requirement of the system acquired from the generators and supplying them with reactive power from the system. Therewith, this factor makes VSC an ideal component in the transmission networks which are isolated generation systems like offshore wind farms. Similarly reactive power can be regulated by employing an AC voltage control loop without analysing the DC section. In the case of fluctuating wind generation systems, this might be helpful [12].

The VSC-HVDC system can be coupled to AC networks which is called "weak" systems not having an adequate generation source. Hence, the short circuit level can be kept at a certain level [22, 23]. However, [14], [15] stressed that approaches of this kind carry with them various well known limitations especially when the DC system is connected to a very weak AC grid. According to [16], this situation can cause a complexity to provide necessary reactive power. That is, voltage distortion and failure might be come up with that. It is also worth noting that VSC based HVDC technology has the self-commutation leading to black start which results in available usage a balanced set of three phase voltages.[7].

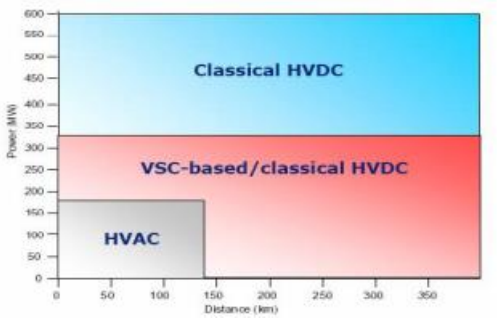

Fig 2. The transmission technologies regarding power and distance [12].

According to the Fig 2, returning briefly to the issue of availability of power transmission after sharing definitions and differences of VSC-HVDC, Classical HVDC and HVAC.

- For small capacity and short distances = HVAC;
- For medium capacity and long distances = VSC-based HVDC;
- For large capacity and long distances = Classical HVDC.

As it can be seen easily from Fig 2, for the small power networks HVAC is the best option. However, once the power and the distance reaches large amounts, the use of HVDC is more suitable. However, there are limits to how far the concept of VSC-based HVDC technology can be taken. It still have problems related to large power flow. Thus, classical HVDC method might be considerate as more preferable than VSC-HVDC [12].

On the other hand, it is likely that VSC-HVDC may have possible installation costs and high power losses with regard to equipment of all converters like power electronics on the offshore/onshore stations compared to classical HVDC and HVAC (Economic concerns).

The basic topology of VSC-HVDC systems can be depicted in Fig 3.

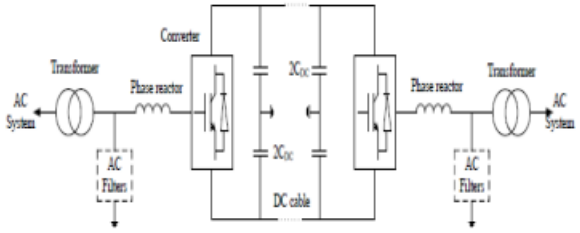

Fig 3. Simple configuration of a VSC-HVDC system [20].

The main components of transmission system of VSC-based HVDC can be basically stated that; voltage source converters, DC-link capacitors, DC cables, phase reactors, transformers and AC filters.

Voltage Source Converter

VSC-HVDC topology can be implemented by two converter parts. The basic configuration is the threephase two-level VSC system from Fig 4. IGBTs are connected series by including an anti-parallel diode. Also it can be added to this topology playing an important role of a higher blocking voltage delivering capability. Furthermore two voltage levels are obtained as -0.5 VDCn and +0.5 VDCn [1, 18].

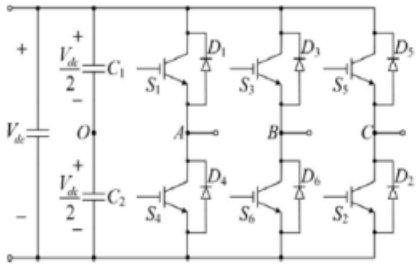

Fig 4. Conventional three-phase two-level VSC topology [17].

DC link Capacitors

Fig 4.3 have revealed that DC capacitors is located between two sides of arrangements. These dc link capacitors are not only responsible for creating a low inductive way to gain power transmission skill during the turned-off current state but also assisting to the system as an energy storage. One another reason of why DC capacitor is an option as a buffer between two side is due to the main benefit of attenuation on voltage ripple occurred in the dc side [13, 19,20].

DC Cables

In a VSC-HVDC, the choice of transmission cable, which is lighter in weight, can basically vary with its characteristics such as mechanical strength, flexibility, and low weight. There are 3 examples of what is meant by DC cable are; XLPE polymer extruded cables, solid cables and the self-contained fluid filled. Generally the first type cable is more popular than the others due to resistance specification to dc voltage [1,13,19].

Phase Reactors

Before proceeding to examine filter issue, it will be necessary to achieve control of active and reactive power transmission independently. And installing up a phase reactor can be considered as a key factor for this control mechanism thanks to its fundamental frequency through the AC and DC side. Similarly, it supplies a low-pass filter for the PWM model in order to obtain the desired voltage with fundamental frequency. Moreover, the harmonic currents that are excessively produced in the converter side can be suppressed by the phase reactor [12, 13].

AC Filters

Lack of linearity feature results in having non-linear system response. Semiconductor materials like an IGBT or MOSFETS in a power electronic circuit can have a profound harmonic contents in current or voltage by adding up to the power network. The purpose of these three-phase harmonic AC filters is to extract that emphasized unwanted harmonic contents. Therefore this filter can be located between phase reactors and a power transformer. If not considered, the ac power system may be extremely degraded and a telecommunication line disruption can even be come up against. On account of this, it is necessary that an AC filter should be tuned properly to multiples of switching frequency. This suggests a slight reduction on the harmonic content and prevention on dc voltage stresses in the transformer [11,20].

Transformers

In the VSC-HVDC link, transformers have a main function that ensures a practicable AC power transformation for maintaining the AC voltage between the network and the isolated loads as a compatible bridge.

VSC MODELLING AND DIFFERENT CONTROL ASPECTS

Designing of voltage source converter based on some available approaches and one of them can be called as average-value modelling (AVM) of farm side and grid side converters adopting controlled voltage and current sources[23].

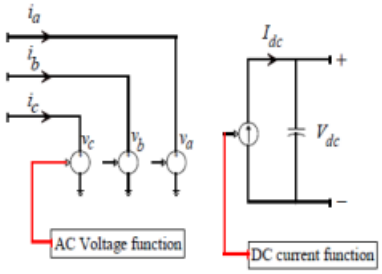

Fig 5. An Average-value modelling (AVM) basic schematic [19].

AVM Approach in phase and dq0 frames

Average value modelling can include voltagecontrolled and current-controlled sources on the ac side and dc side respectively as illustrated in Fig 5. From Fig 6 the reference voltages on the ac side are the output voltages obtained from the inner control system, in which the amplitude and phase are regulated separately and the harmonic contents in voltage and current waveforms are not represented. The ac side of the VSC is combined of three voltage controlled sources for the abc reference frame and a similar concept is also set for voltage inverter side [22, 43].

$$m_j = \frac{2V_i}{V_{dc}}, \qquad j = a, b, c \qquad (1.1)$$

In which, mj represents the modulation index and is obtained from the dq-abc conversion of the reference voltage VC*.

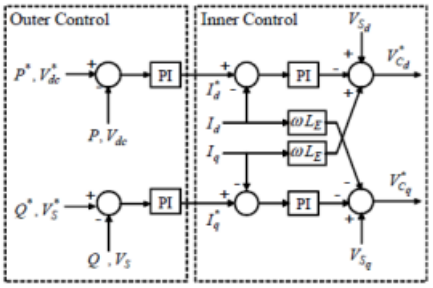

Fig 6. A basic methodology for VSC controls [21].

The dc side of the VSC is made up of utilising the operational principle of power conservation that means the power on the ac side must be equal to the power on the dc side including the converter losses as well [23].

Ignoring the converter losses, the controlled current Idc on the dc side is computed as follows from the Fig 5:

$$v_a i_a + v_b i_b + v_c i_c = V_{dc} I_{dc} \qquad (1.2)$$

$$I_{dc} = \frac{1}{2}(m_a i_a + m_b i_b + m_c i_c) \qquad (1.3)$$

Vector control and dq Transformation

Vector control topology consists of simplified figuration of three phase based systems known as dq transformations. “dq” transformation is the conversion of axis from the three-phase stationary axis to the d-q rotating axis. This transformation can be achieved by two stages [24]:

- abc transition from the three-phase based axis frame to the two-phase based α-β stationary axis frame,
- From the α-β axis frame to the d-q rotating axis frame

In order to transform the parameters into stationary αβ reference axis frame, Clark and Inverse-Clark conversion equations are utilised properly. Furthermore, in order to achieve the transformation from α-β reference axis frame to synchronously rotating d-q axis frame, Park and Inverse-Park conversion equations are used in a similar way corresponding to earlier equations. Accordingly, the given reference frames and conversion processes can be illustrated in Fig 7 [24].

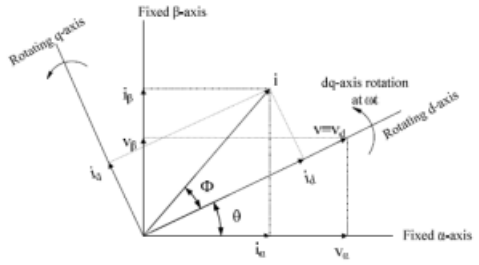

Fig 7. The basic conversion principle of axes for dq transformation [22]

The α-β axis frame is placed to be adjusted based on abc three phase axis for executing the analysis simplification. Afterwards, the d-q axis frame is rotated at a synchronous speed (ω) related to the α-β axis frame, and at any instant, the location of dq axis as regards α-β axis is created by θ=ωt.. In Fig 8, the conversion principles of abc-αβ-dq axes at the same configuration can be depicted in detail [24].

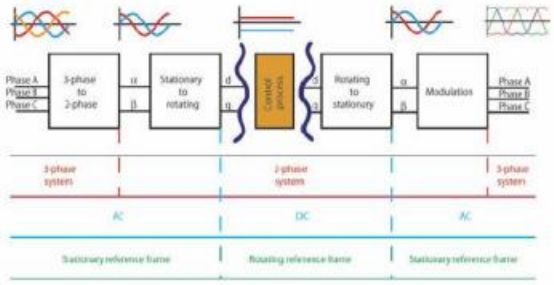

Fig 8. The Control structure and abc-dq-abc axis transformation topology [24]

In brief, due to the fact that the vector control with dq conversion principles represents the decoupled of all control process which might include active power, reactive power, DC-AC voltage and current controller with a fast dynamics, it makes the realization of system control in form of cascade structure possible, with two PI control loops in cascade, outer control loop and inner current control [24].

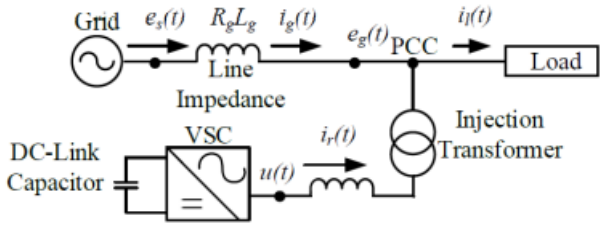

Fig 9. A shunt-connected VSC in single line [25]

From the previous discussion, it can be seen in Fig 9 that VSC converter produces reactive power once the amplitude of output voltage u(t) is lowered below the AC output voltage. Likewise, when the output voltage leads AC supply voltage, active power is injected by VSC converter [25]. Namely, phase is responsible for active power flow, while the amplitude of voltage is for reactive power flow. To have a leading lagging process on controlling reactive power, the phase angle between the converter and AC supply voltage is supposed to be considerate. Accordingly, the reactive power transportation can be implemented by examining the output voltage value.

As it is very well-known that a power rating of a converter can be calculated by the multiplication of the output voltage and the line current. If the converter gains a capability of controlling this power, there will not be necessary an extra energy storage or another VSC to supply that value. So voltage source converters uses four quadrant structure by managing the injected voltage to supply AC side [26].

Previously, [27] stressed out that using a direct control of phase angle controller and reactive power controller gives a non-complex and straightforward principle. However, in this "voltage controller (VC)" scheme, the phase angle (ρ) has such a problematic concern that means active and reactive power are not able to control independently. One another limitation with this concept that current flow to converter cannot be restricted due to the grid frequency dependency (overcurrent issue)

To deal with the problematic concerns in simple voltage control concept, the vector control methodology has been introduced about the role of independent control of active and reactive power. It has become commonplace to distinguish 'independent' from 'dependant' forms of control. Thanks to vector control, a transformation from three phase steady state into the d-q axis is implemented and subsequently a research environment is pronounced more aloud to decouple of active and reactive power.

From the previous discussion, it can clearly be seen that Fig 4.2 indicates two different control loop called as slow outer voltage control loop and fast inner current control loop. The d and q axis materials can have a separate control impact on active and reactive power between a supplier and a receiver end. Also, a Phase Locked Loop (PLL) component is injected to the system to synchronise grid and converter output. [44]

In this vector current controller (VCC) method, main advantage is to perform independent control by the help of the fast dynamic response. VCC gets better harmonic performance and fewer grid disturbance effect. Furthermore, the concept of VCC has been applied to situations where the current limitation problems exists in simple voltage control concept [28].

On the other hand, VCC is not suitable for the weak (2<SCR<3) and very weak (SCR<2) AC grid connection since a poor quality response is probably be achieved disorderly. Unstable case for outer loop and low-frequency resonance performance for the inner loop are considerate as main drawbacks of this concept. One another reason why VCC has some doubt to implement in the industry is that PLL

performance gives negative affect to the VSC-HVDC regarding unwanted frequency interference[29-30].

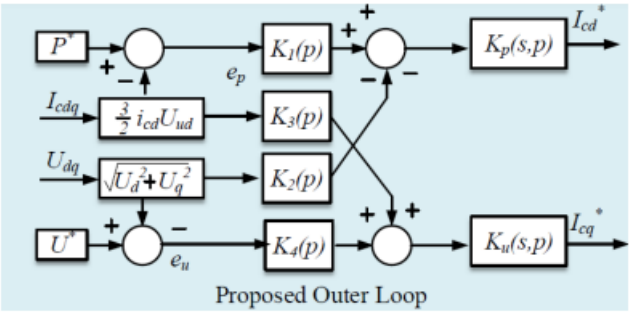

Fig 10. The control structure of advanced VCC [29]

Advanced Vector Control

A major criticism of classical current vector control is that the connection with very weak AC utility bring about a crucial synchronisation and degradation concerns. In [31], the key outcome with these main drawbacks has been improved by adding some nonlinear designs. In this comprehensive examination of advancement control, Fig 10 concluded that a slight novelty on the outer loop is achieved when it is compared to conventional version. Four new gains (K1(p), K2(p), K3(p), K4(p)) before the outer PI controller have been applied to forward side of the loop resulting in a proper regulation of the voltage and active power in an applicable range. The Research on [32] states that a parameter feasibility design towards varying parameters to deal with nonlinear effect can be observed. The aim of this method is to achieve a possible active power flow in an acceptable range by enhancing the interaction between voltage and active power control. Therefore, on very weak grid situations, non-linear degradations especially for the fault condition have been slightly improved as well as addressing high power demand. Nevertheless, on some occasions such as asymmetrical faults and grid sudden changes, this method does not involve expected response [33].

Adaptive Back Stepping and Adaptive Variation Controller

As described on the introduction part, DC connection unit forms one of the most critical component for VSC-HVDC unlike a HVAC technology. Because, it should have a straightforward bidirectional power flow and maintain constant DC bus voltage undertaking a duty as a buffer between two AC side. Regarding [34-35], a DC unit dynamic structure has been developed for the purpose of obtaining stability on the DC side voltage level [36].

Due to the important role of capacitors in providing power flow, fault current degradation can occur on capacitors. This delicate situation can be smoothed out to some extent with the cable model created in the form of pi (Π) as it can be seen from Fig.4.11. Each unit handles the accumulated error from the previous unit and contributes to its correction. These errors can be caused by parameter disorder and state errors.

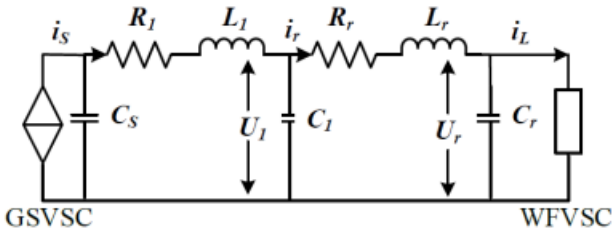

Fig. 4.11. The DC transmission line structure [34]

In [34], for every section, an imitating model is represented in the control loop. However, owing to the long cable in DC side, internal states examined by the help of a state observer considering measured voltage and current signal. From the Fig 12, results indicates that this control concept may reduce the DC voltage change and stabilization time under power step rise and fault when it is compared to conventional linear PI one.

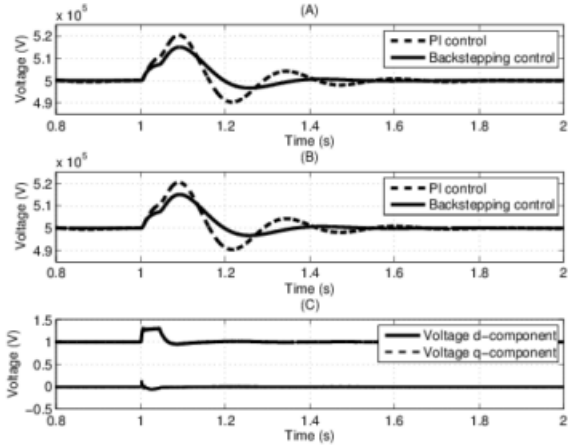

Fig. 12. System response under power step rise [34]

However, this kind of adaptive style method does not considering the parameter uncertainties which might affect the total system performance.

When it comes to parameter uncertainties, various adaptive control strategies have been studied [37], [38] and [39]. In [37], a well-designed adaptive strategy towards parameter uncertainties plus a resonant filter has been established on a unique synchronous reference frame. Having a slight elimination of the 2w ripple on the dc voltage arising during ac-side imbalances and an accurate and decoupled active and reactive power tracking when converter parameters are not perfectly known are the notable results based on varying parameter aspect.

In [38], another parameter uncertainty concept has been examined that the dynamics belonging to nonlinear environment converted to Linear Time Invariant (LTI) form. To do this, dc voltage of the third order VSC model is properly regulated to its LTI form. Results can also prove that an immune system to parameter variations in Rs, Rc and L with an adaptive control is enhanced in a robust manner.

The study on [39] is another good illustration of parameter uncertainty based adaptive control modelling that under unbalanced working conditions, an adaptive style variable-structure control scheme has been examined to a three-phase PWM converter. During the uncertainty in parameter values the controller take the role of the regulation processing DC output of converter. Afterwards, an adaptive control

scheme mentioned above is able to manage the output of the transformed system. Fig 13 shows the performance of the proposed controller on dc voltage value in the presence of reference changes

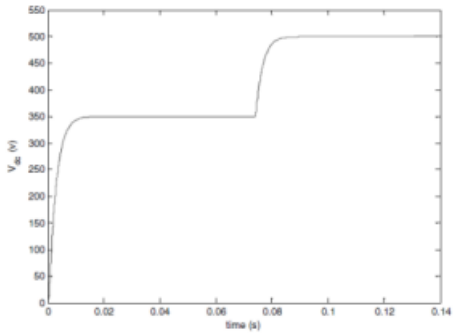

Fig.13. Output DC link voltage response during the possible change in reference value. [39].

Fuzzy Adaptive PI Controller

Turning now to the last adaptive concept control which is called fuzzy based adaptive PI controller is described in [41] and [40]. The network has a passive characteristic at the end. In the side of power delivery a DC voltage and a reactive power control is employed, while in the side of power receiving side an AC voltage control is used.

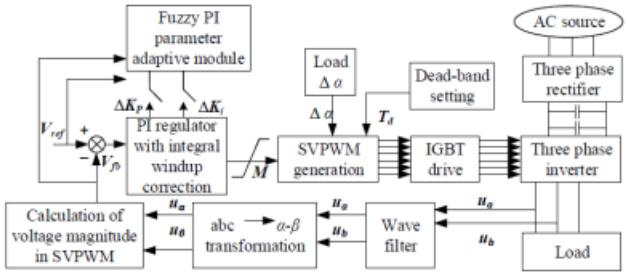

Fig.14. Fuzzy based PI control for VSC-HVDC system block diagram [42]

The detailed block diagram for the fuzzy based adaptive control can been from the Fig. 14. The main goal of this concept is to transform the abc three phase output voltages into the two phase α-β form to obtain a reference voltage vector. Using this reference vector the AC side voltage magnitude can be controllable.

It is also worth noting that fuzzy adaptive module can gain an auto-regulation mechanism by adaptively setting itself for the changed states and uncertainties during the system is on. Thereby, the supply side AC voltage can be systematically ruled. The binary system is constructed to have fuzzy definition and parameters are examined by Digital Signal Processing (DSP) [45]. This control concept has embraced not only adaptive module but also conventional current control in a double way. Nevertheless, the strategy has not escaped criticism from the researchers that the experimental results are rather controversial and there is no agreement about its robustness [42].

DISCUSSION AND CONCLUSION

In this paper, an overview of the HVDC technology especially for VSC based one and its recent developments has been detailed with control strategies. To do this, five different enhanced control strategies for HVDC power systems that have been reviewed are Conventional vector current control (VCC), Voltage Controller (VC), Advanced Vector Controller, Adaptive back-stepping Control, Adaptive variation Control and Fuzzy Adaptive PI Controller.

Among these controller schemes, having an independent control capability on active and reactive power gives great leading role for VCC in the industry. However, because of its restrictions to be able to manage overcurrent situation e.g. weak grid and some synchronisation concerns based on PLL structure, modern adaptive control concept has become more reasonable than previous one.

Modern Adaptive Controllers in VSC-based HVDC systems possess a correction of parameter uncertainty capability in overall performance and error measurement compensation capability in DC side. Ability to maintain dynamic stability and its robustness design to various faults make them best strategy in control area. At the same time, due to the nature of fluctuating wind farm, this specification has become a milestone characteristic to address parameter variation for wind farm based VSC-HVDC systems.

Although VSC-HVDC has some technical and economical limitations and a heavily dependent nature on the power electronic developments, it is still very promising and capable of breakthrough in the future. The need for high power demand and well designed transmission-distribution in the power industry is still to be necessary to employ HVDC systems. In terms of control perspective, “hybrid” solutions might be a good alternative in the market.

REFERENCES

[1] A.-I. Stan and D.-I. Store, "Control of VSCBASED HVDC Transmission System for Offshore Wind Power Plants," Master, Department of Energy Technology, Aalborg University, Denmark, 2010.

[2] V. K. Sood, HVDC and Facts Controllers: Applications of Static Converters in Power Systems. Boston, Dordrecht, New York, London: Kluwer Academic Publishers, 2004.

[3] C. Du, "The control of VSC-HVDC and its use for large industrial power systems," Doctor of Philosophy, Electric Power Engineering, CHALMERS UNIVERSITY OF TECHNOLOGY, Göteborg, Sweden, 2003.

[4] ABB. (2013) “The Gotland HVDC link,” http://www.abb.co.uk/industries/ap/db0003db004333/8e63373c2cdc1cdac125774a0032c5ed.aspx

[5] L. Xiao, Z. Xu, T. An, and Z. Bian, “Improved Analytical Model for the Study of Steady State Performance of Droop-Controlled VSC-MTDC Systems,” IEEE Trans. Power Syst., vol. 32, no. 3, pp. 2083–2093, May 2017.

[6] ABB. (2014) "Asynchronous interconnections," https://library.e.abb.com/public/fe162592ddb1d91dc1257cc3004307c3/IEEE_Black%20start.pdf, 10.1109/MPE.2013.2285592.

[7] M. P. Bahrman, "Overview of HVDC Transmission," in Power Systems Conference and Exposition, 2006. PSCE '06. 2006 IEEE PES, 2006, pp. 18- 23.

[8] Siemens. (July, 2012) “HVDC – High Voltage Direct Current Transmission” Available: http://www.energy.siemens.com/co/pool/hq/powertransmission/HVDC/HVDCClassic/HVDC_Transmission_EN.pd

[9] ABB, “Why HVDC economic and environmental advantages - why choose HVDC over HVAC abb.” 2019. [Online]. Available: https://new.abb.com/systems/hvdc/why-hvdc/economicand-environmental-advantages

[10] X. Lie, Y. Liangzhong, and C. Sasse, "Grid Integration of Large DFIG-Based Wind Farms Using VSC Transmission," Power Systems, IEEE Transactions on, vol. 22, pp. 976-984, 2007.

[11] M. P. Bahrman, J. G. Johansson, and B. A. Nilsson, "Voltage source converter transmission technologies: the right fit for the application," in Power Engineering Society General Meeting, 2003, IEEE, 2003, p. 1847 Vol. 3.

[12] E. Spahic and G. Balzer, "Offshore wind farms - VSC-based HVDC connection," in Power Tech, 2005 IEEE Russia, 2005, pp. 1-6.

[13] ABB, "Its time to connect – Technical description of HVDC Light technology," 2012.

[14] P. Mitra, L. Zhang, and L. Harnefors, "Offshore Wind Integration to a Weak Grid by VSC-HVDC Links Using Power-Synchronization Control: A Case Study," IEEE Trans. Power Deliv., vol. 29, no. 1, pp. 453–461, Feb. 2014.

[15] L. Huang, H. Xin, H. Yang, Z. Wang, and H. Xie, "Interconnecting Very Weak AC Systems by Multiterminal VSC-HVDC Links With a Unified Virtual Synchronous Control," IEEE J. Emerg. Sel. Top. Power Electron., vol. 6, no. 3, pp. 1041–1053, Sep. 2018.

[16] M. Ndreko, J. L. Rueda, M. Popov, and M. A. M. M. van der Meijden, "Optimal fault ride through compliance of offshore wind power plants with VSCHVDC connection by meta-heuristic based tuning," Electr. Power Syst. Res., vol. 145, pp. 99–111, Apr. 2017.

[17] Ağaçayak A.C., Terzioğlu H., Neşeli S., Yalçın G., "Small Power Wind Turbine Design," Acad. Studies in Eng., Gece Publishing, pp. 121-130, 2018.

[18] N. Flourentzou, V. G. Agelidis, and G. D. Demetriades, "VSC-Based HVDC Power Transmission Systems: An Overview," Power Electronics, IEEE Transactions on, vol. 24, pp. 592-602, 2009.

[19] J. Shri harsha, G. N. Shilpa, E. Ramesh, L. N. Dayananda, and C. Nataraja, "Voltage Source Converter Based HVDC Transmission," International Journal of Engineering Science and Innovative Technology (IJESIT), vol. 1, pp. 94-106, 2012.

[20] J. Peralta, H. Saad, S. Dennetiere, and J. Mahseredjian, "Dynamic performance of average-value models for multi-terminal VSC-HVDC systems," in Power and Energy Society General Meeting, 2012 IEEE, 2012, pp. 1-8.

[21] Ağaçayak A.C., Terzioğlu H., Analysis of Thermoelectric Cooler Used to Produce Electrical Energy in terms of Efficiency," Acad. Studies in Eng., Gece Publishing, pp. 111-120, 2018.

[22] S. Meier, "Novel Voltage Source Converter based HVDC Transmission System for Offshore Wind Farms," Doctor of Philosophy, Electrical Engineering / Electrical Machines and Power Electronics, Royal Institute of Technology, Stockholm, Sweeden, 2005.

[23] J. Peralta, H. Saad, S. Dennetiere, and J. Mahseredjian, "Dynamic performance of average-value models for multi-terminal VSC-HVDC systems," in Power and Energy Society General Meeting, 2012 IEEE, 2012, pp. 1-8.

[24] C. Bajracharya, "Control of VSC-HVDC for wind power," Master of Science, Electrical Power Engineering, Nowegian University of Science and Technology, Norway, 2008.

[25] M. Bongiorno and J. Svensson, "Voltage Dip Mitigation Using Shunt-Connected Voltage Source Converter," IEEE Trans. Power Electron., vol. 22, no. 5, pp. 1867–1874, Sep. 2007.

[26] H. F. Latorre, M. Ghandhari, and L. Söder, "Active and reactive power control of a VSC-HVdc," Electr. Power Syst. Res., vol. 78, no. 10, pp. 1756–1763, Oct. 2008

[27] Y. Li, L. Luo, C. Rehtanz, S. Rüberg, and F. Liu, "Realization of Reactive Power Compensation Near the LCC-HVDC Converter Bridges by Means of an Inductive Filtering Method," IEEE Trans. Power Electron., vol. 27, no. 9, pp. 3908–3923, Sep. 2012.

[28] M. A. Hannan et al., "Advanced Control Strategies of VSC Based HVDC Transmission System: Issues and Potential Recommendations," in IEEE Access, vol. 6, pp. 78352-78369, 2018, doi: 10.1109/ACCESS.2018.2885010.

[29] S. Luo, X. Dong, S. Shi, and B. Wang, “A Directional Protection Scheme for HVDC Transmission Lines Based on Reactive Energy,” IEEE Trans. Power Deliv., vol. 31, no. 2, pp. 559–567, Apr. 2016.

[30] Y. Xue and X.-P. Zhang, “Reactive Power and AC Voltage Control of LCC HVDC System With Controllable Capacitors,” IEEE Trans. Power Syst., vol. 32, no. 1, pp. 753–764, Jan. 2017.

[31] A. Egea-Alvarez, S. Fekriasl, F. Hassan, and O. Gomis-Bellmunt, “Advanced Vector Control for Voltage Source Converters Connected to Weak Grids,” IEEE Trans. Power Syst., vol. 30, no. 6, pp. 3072–3081, Nov. 2015.

[32] C. Guo, W. Liu, C. Zhao, and R. Iravani, “A Frequency-Based Synchronization Approach for the VSCHVDC Station Connected to a Weak AC Grid,” IEEE Trans. Power Deliv., vol. 32, no. 3, pp. 1460–1470, Jun. 2017.

[33] M. A. Hannan, N. N. Islam, A. Mohamed, M. S. H. Lipu, P. J. Ker, M. M. Rashid, and H. Shareef, “Artificial Intelligent Based Damping Controller Optimization for the Multi-Machine Power System: A Review,” IEEE Access, vol. 6, pp. 39574–39594, 2018.

[34] X. Zhao and Kang Li, “Control of VSC-HVDC for wind farm integration based on adaptive backstepping method,” in 2013 IEEE International Workshop on Inteligent Energy Systems (IWIES), 2013, pp. 64–69.

[35] O. P. Mahela and A. G. Shaik, “Comprehensive overview of grid interfaced wind energy generation systems,” Renew. Sustain. Energy Rev., vol. 57, pp. 260– 281, May 2016.

[36] C.-H. Lee and B.-R. Chung, “Adaptive backstepping controller design for nonlinear uncertain systems using fuzzy neural systems,” Int. J. Syst. Sci., vol. 43, no. 10, pp. 1855–1869, Oct. 2012.

[37] A. E. Leon, J. M. Mauricio, J. A. Solsona, and A. G´omez-Exp´osito, “Adaptive control strategy for vscbased systems under unbalanced network conditions,” Smart Grid, IEEE Transactions on, vol. 1, no. 3, pp. 311– 319, 2010.

[38] R. Milasi, A. F. Lynch, and Y. Li, “Adaptive control of a voltage source converter,” in Electrical and Computer Engineering (CCECE), 2010 23rd Canadian Conference on. IEEE, 2010, pp. 1–4.

[39] B. Khaki, A. Sharaf, S. Mousavi, N. Noroozi, and A. Seifi, “Adaptive control of dc link voltage of pwm vsc rectifier under unbalanced voltage source and uncertain parameters,” in Energy, Automation, and Signal (ICEAS), 2011 International Conference on. IEEE, 2011, pp. 1–6.

[40] A. Moharana, J. Samarabandu, and R. K. Varma, “Fuzzy supervised PI controller for VSC HVDC system connected to Induction Generator based wind farm,” in 2011 IEEE Electrical Power and Energy Conference, 2011, pp. 432–437.

[41] A. Fuchs, M. Imhof, T. Demiray, and M. Morari, “Stabilization of Large Power Systems Using VSC–HVDC and Model Predictive Control,” IEEE Trans. Power Deliv., vol. 29, no. 1, pp. 480–488, Feb. 2014.

[42] H. Liang, G. Li, M. Zhou, and C. Zhao, “The implementation of fuzzy adaptive PI controller in VSCHVDC systems,” in 2009 IEEE/PES Power Systems Conference and Exposition, 2009, pp. 1–5.

[43] Abbas, Ali M. and Peter W. Lehn. “PWM based VSC-HVDC systems — A review.” 2009 IEEE Power & Energy Society General Meeting (2009): 1-9.

[44] Sahoo, Aishwarya & Agarwal, Shobha & Sahu, M.M & Panigrahi, C.K. (2018). A review of recent control strategies for wind farm based HVDC systems. 1-8. 10.1109/ICSESP.2018.8376674.

[45] R. K. Mallick, "Adaptive sliding mode control of VSC-HVDC transmission links," 2011 International Conference on Energy, Automation and Signal, 2011, pp. 1-6, doi: 10.1109/ICEAS.2011.6147160

CHAPTER 14

MACHINABILITY OF MATERIALS USED IN THE MANUFACTURING INDUSTRY: A REVIEW

K. KAYA[1]
[1] Selcuk University, Konya/Turkey
ORCID: 0000-0002-9971-8826

O. KARATAY[2]
[2] Selcuk University, Konya/Turkey
ORCID: 0000-0001-9010-6973

Y.Ö. ERBAŞ [3]
[3] Selcuk University, Konya/Turkey
ORCID: 0000-0003-0858-3098

INTRODUCTION

Production stages in industry can be classified in two different ways as machining and chipless manufacturing processes. Both are important in the industry. Machining processes are used both as a finishing process from raw material and after chipless production. Therefore, machining is more important than other production methods. For this reason, although it has been used for many years, it continues to increase its popularity. Due to the chips removed from the material by the cutting tool during chip removal processes, temperature formation and cutting force occur on the cutting tool and workpiece material (Binali, Coşkun, & Neşeli, 2022; Binali, Kuntoğlu, et al., 2022; Mustafa Kuntoğlu et al., 2021). Therefore, it causes poor quality of the machined surface, wear of the cutting tool and workpiece material, and thus, material production with the desired efficiency is not achieved. For this reason, it is necessary to carry out machinability tests in order to increase productivity and to produce materials of desired quality and dimensions. The purpose of machinability experiments is to investigate the interaction between the cutting tool and workpiece material, ideal machining conditions, in order to increase the product quality and prevent the increase in machining costs. Workability studies are constantly popular. The reason for this is that new materials and cutting tools produced with the developing technology are constantly tested and included in the product production process. Machinability refers to the ability of materials to be easily machined as designed (surface quality and machining tolerance) in terms of tooling and machining processes. Machinability is affected by criteria such as selected machining parameters, material, cutting tool, machine tool, machining conditions (Korkmaz et al., 2022; Usca, Uzun, Kuntoğlu, Sap, & Gupta, 2021). Therefore, the optimum selection of these criteria during machining is important in machinability tests. In order to determine the machinability in machining processes, process outputs such as the life of the cutting tool, the ratio of the removed chip, the components of the cutting force, the consumed power and the quality and integrity of the machined surface are used, apart from the chip removed during the process. These process outputs are affected by input parameters such as machining parameters, conditions, workpiece and cutting tool material, and machine tool stiffness. The productivity of the materials and the cutting tools they are machined can be significantly improved by choosing the ideal combination of input parameters and output parameters (Binali, YALDIZ, & Neşeli, 2022; Demir, Ulas, & Binali, 2018; Rüstem, Süleyman, & Süleyman, 2021).

This study is intended to be a guide for people in the machining industry by evaluating some of the machinability studies done in the last two years and we hope it will be useful. The main purpose of the study is to be an information access article about the machining methods preferred in machinability studies and what is done for the machinability parameters of the materials processed with these methods. Within the scope of the article, machinability studies with turning, milling and drilling processes will be explained.

MACHINABILITY STUDIES WITH MILLING

The milling process can be expressed as the machining process on materials with generally prismatic geometry by means of the cutting tool rotating around its own axis. The cutting tool used in the milling process is called a pocket knife. The cutting mechanics are different from the turning process because the number of blades of the tool called the pocket knife is more than one. For this reason, it is a process that should be considered in machining operations and machinability tests. It can be said that the cutting force caused by the tool used in the milling process is not unidirectional but multidirectional. For this reason, the evaluations made in the machinability tests should first be evaluated on the cutting force and then other machining outputs (such as tool wear, temperature, roughness) due to the cutting force (Binali, YALDIZ, & Neşeli, 2021; Coşkun, Çiftçi, & Demir, 2021; Mustafa Kuntoğlu, Gupta, Aslan, Salur, &

Garcia-Collado, 2022; Salur, 2022; Usca, Şap, et al., 2022). Literature studies on milling are summarized below.

In his study, Fedai found that three different surface roughness and control factors are used to keep the machining time at the lowest level and to maximize the metal removal rate in the course of milling of AISI 4140 steel, which has the advantage of high machinability, easy heat treatment and low cost. examined the effect of these factors and determined the correct settings of these factors. In his study, Taguchi-Data Envelopment Analysis Based Sequencing technique multi-response optimization approach is used for optimization of multiple quality characteristics. As a result of his study, he stated that the cutting depth has the highest impact on the determination of performance measures due to its effect on the metal removal rate (FEDAİ). Karakılınç et al. studied the effect of cutting parameters (feed, cutting depth and rotation) on the burr formation and surface roughness of Ti6Al4V alloy in micromilling process. In the micromachinability tests, AlTiSiN coated two-edged micro cutting tools with a tool diameter of 0.5 mm were used. The surface roughness of the machined channels was measured with the Nanovea 3D optical surface profilometer. As a result, poor surface quality formation and excessive burring are seen due to the effective scraping mechanism at low feed rates. The cutting forces fluctuate with increasing feed rate. It has been determined that the cutting forces increase with increasing depth of cut, and finally, in case of an increase in the number of revolutions, the cutting forces decrease up to 20,000 rpm, and after this value, it tends to increase (Karakılınç, Ergene, Yalçın, & Aslantaş). Kuntoğlu investigated the machinability of Strenx 1100 structural steel, which is used in important engineering applications such as heavy and marine vehicles. The study includes flank wear analysis and experiments during MQL assisted milling of Strenx 1100 steel. Cutting speed, feed and cutting depth were included in the experimental plan and the Taguchi L9 design was applied. He stated that the cutting speed is the first parameter that affects the flank wear by approximately 53.2%, followed by the feed rate with approximately 35.77% (Mustafa KUNTOĞLU, 2021). Usca et al. investigated the machinability performance of AISI 5140 steel under different cooling/lubrication conditions. As a result, they determined that the use of Cryo-LN_2 cooling/lubrication tended to improve all studied machinability measures compared to the dry condition (Usca, Uzun, et al., 2022). Bektaş and Samtaş investigated the effects of machining parameters on cutting tool wear by performing face milling operations on aluminum 6051-T651 alloy with dimensions of 80x80x30 mm. Taguchi method was used for experimental design and optimization in the study. For experimental design, Taguchi L_9 orthogonal array was selected and 9 experiments were carried out. In the experiments, face milling was applied using three different inserts, three different feed and cutting speeds. After each test, the insert flank wear was measured. The results were interpreted using analysis of variance, three-dimensional graphics and regression method. Milling experiments were carried out on a DELTA SEIKI brand 1050A model 3-axis vertical milling machine with a maximum speed of 10000 RPM. As a result of the statistical analysis, the most important factor affecting the wear of the inserts was the inserts with 78.99%. This factor is followed by cutting speed with 19.83%. According to the experimental results, the lowest tool wear was measured in the verification experiments carried out with the optimum combinations obtained by the Taguchi method. TiN-TiCN-Al_2O_3 coated insert showed the best performance for minimal insert wear. They also stated that the effect of the feed rate on the insert wear was not according to the statistical analysis F ratio evaluation (BEKTAŞ & SAMTAŞ). Düzce and Samtaş investigated the effects of machining parameters on the cutting zone temperature in face milling processes applied to GG25 cast iron. For face milling, cutters with three different coatings, three different cutting speeds, three different feeds and three different depths of cut were used as cutting parameters. For the experimental design, Taguchi L27(3^4) orthogonal array was chosen and 27 experiments were performed, and the parameters were optimized by the Taguchi method. During each experiment, temperature measurements were made from the cutting zone with a thermal camera. Experimental results were evaluated with analysis of variance and three-dimensional graphics. When the variance analysis results were evaluated, the most important parameter

affecting the temperature was the depth of cut with 26.51%. The second most effective parameter was the insert with 6.15%. When the three-dimensional graphics are evaluated, the most suitable insert coating for minimum temperature is TiN-TiCN-AL203 coated insert, which is similar to Taguchi optimized parameters. They also stated that the type of insert coating directly affects the cutting zone temperature (DÜZCE & SAMTAŞ). Binali et al., in their study, made the machinability of S960QL structural steel material on power consumption. In their work, they used the milling method by means of finite element analysis. As a result of the finite element analysis, they stated that the power consumption increased with increasing depth of cut (Binali, YALDIZ, & Neşeli). In another study, Binali et al. studied the machinability of AISI P20 mold steel according to power consumption (Binali, Coşkun, et al., 2022). Şirin and Şirin studied the performance of ecological cooling/lubrication methods in milling AISI 316L stainless steel. For the machinability investigation, AISI 316L stainless steel was applied at three different cutting speeds (120, 150 and 180 m/min) with constant feed under three different cooling cooling/lubrication conditions (minimum amount of lubrication-MQL, LN_2 and MQL+LN_2). When the test results were evaluated in general, it was understood that the MQL+LN_2 hybrid cutting arm provided important improvements in all machining parameters compared to other conditions (Şirin & Şirin, 2021). Bayraktar and Uzun conducted an experimental study on the machinability of prehardened Toolox 44 and Nimax die steels. After examining the machined surface and subsurface conditions with optical microscope and scanning electron microscope, the machinability properties of these tool steels were detailed and it was revealed that the study results were affected. It has been stated that while the surface roughness of Nimax material is reduced with high cutting speed and low feed value, it increases at low cutting speed and high feed value. Looking at the machined surface images, it was determined that a small amount of progress traces were formed on the surface compared to Toolox 44 (Bayraktar & Gültekin, 2021). The evaluation of the literature study is given in Table 1.

Table 1: Machinability studies with milling.

Machining operations	Process	Workpiece	Aim	Ref.
CNC vertical machining	Milling	AISI4140	Investigation of the effects of cutting parameters on machining time and metal removal rate.	(FEDAİ)
Micro milling machine	Micro milling	Ti6Al4V	Experimental determination of minimum chip thickness in micro conditions.	(Karakılınç et al.)
CNC vertical machining	Milling	Strenx 1100	Investigate the tool flank wear progression.	(Mustafa KUNTOĞLU, 2021)
CNC vertical machining	Milling	AISI 5140	Investigate machinability performance of 5140 steel under different cooling/lubrication conditions.	(Usca, Uzun, et al., 2022)
CNC vertical machining	Milling	Al 6061-T651	Cutting conditions when milling with coated inserts investigation of its effect.	(BEKTAŞ & SAMTAŞ)
CNC vertical machining	Milling	GG25	Optimization of cutting parameters	(DÜZCE & SAMTAŞ)
FEM	Milling	S960QL	işlenebilirlik parametrelerinin güç tüketimi üzerindeki etkilerinin belirlenmesi	(Binali et al.)

FEM	Milling	AISI P20	Investigation of the amount of power consumed in the milling process	(Binali, Coşkun, et al., 2022)
CNC vertical machining	Milling	AISI 316 L	Examination of Ecological Cooling / Lubrication methods	(Şirin & Şirin, 2021)
CNC vertical machining	Milling	Toolox 44/Nimax	Cutting force, surface roughness of machining parameters and examining its effect on the machined subsurface form.	(Bayraktar & Gültekin, 2021)

MACHINABILITY STUDIES WITH TURNING

The turning process is called the process of removing chips from the material surface parallel to the material axis in each turn of the workpiece material by means of a cutting tool called a pencil. The cutting tool used is single-edged and the cutting mechanics are simpler than both milling and drilling. Machinability studies with turning process are more common than machining processes. This is because of linear machining and faster results in machinability output parameters. The summary of the literature research on the turning process is given below (Erçetin & Usca, 2016; M Kuntoğlu, 2016; Mustafa Kuntoğlu et al., 2020; Neşeli, Yalçın, & Yaldız, 2018).

Airao et al. have studied a new method that applies ultrasonic vibration along with lubrication (MQL) and cooling (LCO_2) to increase the machinability of Inconel 718. The aim of this study is to examine the machinability of Inconel 718 in conventional and ultrasonic assisted turning under dry, wet, MQL and LCO_2. LCO_2 indicated that nose wedge chipping, adhesion and vibration wear were significantly reduced in both processes. Compared to dry, wet and MQL techniques in conventional turning under LCO_2, a 32-60% reduction in blade wear and a reduction in power consumption by 4-41% and 5-31% was observed. Similarly, when applied in ultrasonic assisted turning, 32-53% reduction in blade wear and 11-40% and 32-53% reduction in power consumption were observed compared to dry, wet and MQL techniques. As a result, they stated that when Inconel 718 is machined with LCO2 technique in ultrasonic assisted turning, it significantly reduces tool wear and specific cutting energy without sacrificing surface quality, and that Inconel 718 is sustainable in machining (Airao, Nirala, & Khanna, 2022). Padhan et al., in their study, performed the turning of Nitronic 60 steel with SiAlON ceramic cutting tools under dry cutting, wet, minimal amount of lubricant (MQL) and compressed air conditions. They used the Taguchi L_{16} orthogonal index in their work. As a result of their experimental studies, they stated that the MQL system is more efficient than other processing conditions (Padhan et al., 2022). Yağmur and Pul have done their work on the investigation of tool wear behavior in the machining of Al6061/B4C/GNP hybrid composite. In the processing of Al6061 matrix, B4C and GNP reinforced composites, the B4C reinforcement element had the main effect on the tool wear amount. While the amount of wear increased depending on the B4C reinforcement ratio, it was revealed that the GNP added in the same composite structures showed the lubricating property and the tool wear decreased. It has been concluded that the B4C reinforcement element is more effective on tool wear than the feed and cutting speed in the machining of Al6061 matrix, B4C and GNP reinforced composites (YAĞMUR & Muharrem, 2022). Pul and Özerkan conducted their studies on the effects of depth of cut and cutting tool geometry on surface roughness and tool behavior in machining Al6061 alloy. In this experimental study on machinability, the effect of cutting depth and cutting tools of 4 different profiles on the roughness of the machined surface was investigated in turning of Al6061 aluminum alloy. As a result of visual inspection of the microscope images of the cutting tools, the least tool damage was obtained from the SNMA coded tools. However, it is generally concluded that all the cutting tools used may be suitable for machining such aluminum materials at lower depths of cut and higher cutting speeds. As a result of this study, it has been determined that the machining

performance of the SNMA series coated and negative stone angle tools is higher (Muharrem & Özerkan). Akgün and Demir made an experimental and numerical analysis of the effect of cutting parameters on the cutting force and chip formation in the turning process. Turning experiments were performed at five different cutting speeds (60,90,120,150 and 180 m/min), three different feed rates (0.12-0.18-0.24 mm/rev) and three different cutting depths (0.5-1-1, 5mm) on a CNC lathe under dry cutting conditions (AKGÜN & DEMİR). Demirer and Kayır analyzed the effect of cutting tool height adjustment on cutting forces in AISI304 stainless steel turning by Taguchi and Anova method. Experiments were carried out on CNC lathes using AISI304 stainless steel material, which is a reference material. KISTLER type-9272 multi-axis dynamometer was used to measure the shear force components in the experiments. The dynamometer is connected to the turret (ATC: Automated Tool Changer) on the CNC lathe with the designed and manufactured apparatus. For the cutting tool, an apparatus (tool holder) was designed and manufactured on the dynamometer. Depending on the analysis results, the feed rate should be kept at low levels (F:0.15 mm/rev) and the cutting tool height adjustment should be at or above the workpiece axis (H:0mm) (H:+0.5mm). It has been understood that the factors that have the greatest effect on the increase of the cutting force components are the cutting depth and the amount of feed (DEMiRER & KAYIR). Zeyrek and Er, in their study, investigated the effect of cutting fluid application on the machinability of the Ti-6Al-4V alloy using the minimum amount of lubrication (MMY) method. Ti-6Al-4V alloy was first turned without using cutting fluid with a TiAlN coated cutting tool, and then, for comparison, commercial vegetable-based cutting fluid was added into the MMY system with the same cutting parameters and subjected to turning. The test results were compared in terms of temperature and surface roughness, cutting force, and the performance differences of MMY machining method compared to dry machining were calculated. GLS-150 brand CNC machines were used for the turning process. In the experimental results, it was determined that the effects of machining variables on the cutting force changed with the use of MMY. It has been determined that the temperature is very high at high depth of cut values and MMY is more effective on the temperature drop rate. It has been stated that since the cutting fluid reduces the friction force with its lubricating feature, the heat generated decreases and the function of the compressed air in the MMY system to remove the chip also contributes to the removal of a large part of the heat with the sawdust (ER & ZEYREK). Deswal and Kant conducted experimental analyzes to investigate the machinability of aluminum 3003 alloy during conventional turning and Laser assisted turning processes. The effect of laser beam irradiation on machining performance was analyzed and compared with conventional turning in terms of chip morphology, cutting forces and surface roughness. As a result of their studies, it has been shown that cutting, pushing and feeding forces can be significantly reduced in Laser assisted turning compared to conventional turning. However, these forces were found to increase beyond the optimum laser power. It was also found that the surface roughness was higher in Laser assisted turning than in conventional turning. Chip morphology analysis showed that discontinuous and thick chips were observed at high laser power, while continuous and small chips were observed at low laser power, while continuous and long chips were obtained for conventional turning (Deswal & Kant, 2022). Mutlu et al. investigated the machinability of CoCrMo alloy used in biomedical applications according to cutting tool types (Mutlu, Binali, & Yaşar). The evaluation of the studies related to the literature research is given in Table 2.

Table 2. Machinability studies with turning

Machining operations	Process	Workpiece	Aim	Ref.
Conventional turning	UAT Turning	Inconel 718	Examination of ultrasonic assisted turning in combination with cryogenic and lubrication techniques	(Airao et al., 2022)
Lathe machine	Turning	Nitronic 60	Study of machinability under different Cooling/Lubrication conditions	(Padhan et al., 2022)
CNC Turning machine	Turning	Al 6061/B4C/GNP	Determination of the effect of B4C and GNP additive on tool wear	(YAĞMUR & Muharrem, 2022)
Lathe machine	Turning	Al6061	Investigation of the effect of different cutting depths and different cutting tools on the roughness value of the machined surface.	(Muharrem & Özerkan)
FEM and CNC turning machine	Turning	Inconel 625	Numerical and experimental analysis of the effect of cutting parameters	(AKGÜN & DEMİR)
CNC turning machine	Turning	AISI 304	Determination of the effect of cutting tool height adjustment on cutting forces	(DEMiRER & KAYIR)
CNC turning machine	Turning	Ti-6Al-4V	Investigation of the effects of cutting fluid application with minimum amount of lubrication on machinability	(ER & ZEYREK)
Lathe machine	Turning	Al 3003	Machinability analysis during laser assisted turning	(Deswal & Kant, 2022)
CNC turning machine	Turning	CoCrMo	Investigation of the effect of cutting tool type on machinability	(Mutlu et al.)

MACHINABILITY STUDIES WITH DRILLING

Drilling accounts for approximately 33% of the machining industry. Drilling is similar to both the cutting mechanics of milling and the cutting mechanics of turning. The reason for this can be attributed to both the fact that the tool used has more than one cutting edge and the cutting tool moves in a single axis direction while drilling. As in other machining processes, the drilling process starts the machining process directly on the part, that is, on the filled material, not on the part by moving empty. Therefore, it differs from other manufacturing methods (Al-Tameemi et al., 2021; Gunay, Yasar, & Korkmaz, 2016; Yaşar, 2019; Yaşar & Günay, 2019). The literature research on hole drilling processes is given below.

Yağmur and Pul investigated the effect of pre-drilling on the machinability properties of Ti6Al4V titanium alloy, which is widely used in the industry and applied machining operations. Hole drilling experiments were carried out on pre-drilled and non-drilled alloys by selecting single feed and five different cutting speed values. Surface roughness values, cutting moment, thrust force and drilling zone temperature were measured and recorded during and after the experiments. The obtained data were evaluated by comparison. Johnford VMC-550 CNC vertical machining centers were used in the experiment. There were no significant differences in the roughness values of the drilled surfaces with the change of cutting speed. Considering the machinability parameters discussed, lower cutting values were obtained from the pre-perforated samples. In this case, it was concluded that the pre-drilling process can be advantageous in terms of energy consumed, hole surface quality and indirectly tool life (YAĞMUR & Muharrem, 2021). The evaluation of the literature research is given in Table 3.

Table 3. Machinability studies with drilling.

Machining operations	Process	Workpiece	Aim	Ref.
CNC vertical machining	Drilling	Ti-6Al-4V	Investigation of the effect of front hole application on machinability	(YAĞMUR & Muharrem, 2021)

CONCLUSION

This review study includes details of the methods used for machinability studies and machining practices used in stock removal. With the application of machine tools and machinability parameters used in machining operations, the following results can be taken into account:

1) Machinability tests are very useful in machining operations.
2) Machinability tests can be done with more than one method in machining operations: These operations are mainly drilling, milling and turning.
3) Factors such as cutting parameters and cutting conditions are widely used in machinability input parameters.
4) In machinability tests, parameters such as cutting force, tool wear, temperature, surface roughness and tool life can be determined.
5) Further drilling should be studied as a recommendation for future machinability studies. In addition, more than one method can be compared for a material.

REFERENCES

Airao, J., Nirala, C. K., & Khanna, N. (2022). Novel use of ultrasonic-assisted turning in conjunction with cryogenic and lubrication techniques to analyze the machinability of Inconel 718. *Journal of Manufacturing Processes, 81*, 962-975.

AKGÜN, M., & DEMİR, H. Tornalama İşleminde Kesme kuvveti ve Talaş Oluşumu Üzerinde Kesme Parametrelerinin Etkisinin Deneysel ve Nümerik Analizi. *El-Cezeri, 8*(2), 897-908.

Al-Tameemi, H. A., Al-Dulaimi, T., Awe, M. O., Sharma, S., Pimenov, D. Y., Koklu, U., & Giasin, K. (2021). Evaluation of cutting-tool coating on the surface roughness and hole dimensional tolerances during drilling of Al6061-T651 alloy. *Materials, 14*(7), 1783.

Bayraktar, Ş., & Gültekin, U. (2021). Ön sertleştirilmiş Toolox 44 ve Nimax kalıp çeliklerinin işlenebilirliği üzerine deneysel çalışma. *Gazi Üniversitesi Mühendislik Mimarlık Fakültesi Dergisi, 36*(4), 1939-1948.

BEKTAŞ, B. S., & SAMTAŞ, G. Alüminyum 6061-T651 Alaşımının Kaplamalı Kesici Uçlarla Frezelenmesinde Kesici Takım Aşınmasının Optimizasyonu. *Düzce Üniversitesi Bilim ve Teknoloji Dergisi, 10*(2), 641-651.

Binali, R., Coşkun, M., & Neşeli, S. (2022). An Investigation of Power Consumption in Milling AISI P20 Plastic Mold Steel By Finite Elements Method. *Avrupa Bilim ve Teknoloji Dergisi*(34), 513-518.

Binali, R., Kuntoğlu, M., Pimenov, D. Y., Usca, Ü. A., Gupta, M. K., & Korkmaz, M. E. (2022). Advance monitoring of hole machining operations via intelligent measurement systems: A critical review and future trends. *Measurement*, 111757.

Binali, R., YALDIZ, S., & Neşeli, S. Investigation of Power Consumption in the Machining of S960QL Steel by Finite Elements Method. *European Journal of Technique (EJT), 12*(1), 43-48.

Binali, R., YALDIZ, S., & Neşeli, S. (2021). S960QL Yapı Çeliğinin İşlenebilirliğinin Sonlu Elemanlar Yöntemi ile İncelenmesi. *Avrupa Bilim ve Teknoloji Dergisi*(31), 85-91.

Binali, R., YALDIZ, S., & Neşeli, S. (2022). Investigation of Power Consumption in the Machining of S960QL Steel by Finite Elements Method. *European Journal of Technique (EJT), 12*(1), 43-48.

Coşkun, M., Çiftçi, İ., & Demir, H. (2021). AISI P20S Kalıp Çeliğinin İşlenebilirliğinin İncelenmesi. *İmalat Teknolojileri ve Uygulamaları, 2*(2), 1-9.

Demir, H., Ulas, H., & Binali, R. (2018). Investigation of the effects on surface roughness and tool wear in the toolox44 material. Technol. *Appl. Sci, 13*, 19-28.

DEMiRER, E., & KAYIR, Y. Analysis By Taguchi and ANOVA Methods For The Effect Of The Cutting Tool Height Adjustment On Cutting Forces In Turning AISI304 Stainless Steel Material.

Deswal, N., & Kant, R. (2022). Machinability analysis during laser assisted turning of aluminium 3003 alloy. *Lasers in Manufacturing and Materials Processing, 9*(1), 56-71.

DÜZCE, R., & SAMTAŞ, G. GG25 Dökme Demirin Frezelenmesinde Kesme Parametrelerinin Kesme Sıcaklığı Üzerine Etkisi ve Optimizasyonu. *İmalat Teknolojileri ve Uygulamaları, 2*(3), 20-33.

ER, A. O., & ZEYREK, K. Ti-6Al-4V Alaşımının Tornalanmasında Minimum Miktarda Yağlama (MMY) Yöntemi İle Kesme Sıvısı Uygulamanın İşlenebilirliğe Etkilerinin Araştırılması. *International Journal of Engineering Research and Development, 13*(2), 653-665.

Erçetin, A., & Usca, Ü. A. (2016). An experimental investigation of effect of turning AISI 1040 steel at low cutting speed on tool wear and surface roughness steel. *Turkish J. Nat. Sci., 5*(1), 29-36.

FEDAİ, Y. AISI 4140 ÇELİĞİNİN FREZLEMESİNİN TAGUCHİ-DEAR YÖNTEMİYLE OPTİMİZAYONU. *El-Cezeri, 9*(2), 882-897.

Gunay, M., Yasar, N., & Korkmaz, M. E. (2016). *Optimization of drilling parameters for thrust force in drilling of AA7075 Alloy.* Paper presented at the Proceedings of the International Conference on Engineering and Natural Sciences, Sarajevo, Bosnia and Herzegovina.

Karakılınç, U., Ergene, B., Yalçın, B., & Aslantaş, K. Tİ6AL4V ALAŞIMININ MİKRO FREZELEMESİNDE KESME KUVVETLERİ VE ÇAPAK OLUŞUMUNUN ARAŞTIRILMASI.

Korkmaz, M. E., Gupta, M. K., Li, Z., Krolczyk, G. M., Kuntoğlu, M., Binali, R., . . . Pimenov, D. Y. (2022). Indirect monitoring of machining characteristics via advanced sensor systems: a critical review. *The International Journal of Advanced Manufacturing Technology*, 1-36.

Kuntoğlu, M. (2016). Prediction of progressive tool wear and cutting tool breakageusing acoustic emission and cutting force signals in turning. *Msater's Thesis, Institute of Science and Technology, Selcuk University, Konya, Turkey*.

KUNTOĞLU, M. (2021). Tool flank wear analysis for MQL assisted milling of strenx 1100 structural steel. *Avrupa Bilim ve Teknoloji Dergisi*(25), 629-635.

Kuntoğlu, M., Acar, O., Gupta, M. K., Sağlam, H., Sarikaya, M., Giasin, K., & Pimenov, D. Y. (2021). Parametric optimization for cutting forces and material removal rate in the turning of AISI 5140. *Machines, 9*(5), 90.

Kuntoğlu, M., Aslan, A., Pimenov, D. Y., Usca, Ü. A., Salur, E., Gupta, M. K., . . . Sharma, S. (2020). A review of indirect tool condition monitoring systems and decision-making methods in turning: Critical analysis and trends. *Sensors, 21*(1), 108.

Kuntoğlu, M., Gupta, M. K., Aslan, A., Salur, E., & Garcia-Collado, A. (2022). Influence of tool hardness on tool wear, surface roughness and acoustic emissions during turning of AISI 1050. *Surface Topography: Metrology and Properties, 10*(1), 015016.

Muharrem, P., & Özerkan, H. B. Al 6061 alaşımının işlenmesinde kesme derinliği ve kesici takım geometrisinin yüzey pürüzlülüğüne ve takım aşınma davranışına etkisi. *Gazi Üniversitesi Mühendislik Mimarlık Fakültesi Dergisi, 37*(4), 2013-2024.

Mutlu, B., Binali, R., & Yaşar, N. Machinability of CoCrMo Alloy used in Biomedical applications: Investigation of Cutting Tool Type. *Gazi Mühendislik Bilimleri Dergisi, 8*(2), 215-227.

Neşeli, S., Yalçın, G., & Yaldız, S. (2018). Surface Roughness Estimation for Turning Operation Based on Different Regression Models Using Vibration Signals. *International Journal of Intelligent Systems and Applications in Engineering*.

Neşeli, S., Yalçın, G., Terzioğlu H., Ağaçayak A.C. (2019). Nano Yüzey Kalitesi Oluşturmak İçin Lepleme Makinesi Tasarımı. V Scıence Technology and Innovatıon Congress, 374-380. (Tam Metin Bildiri/Sözlü Sunum)(Yayın No:5601104)

Padhan, S., Das, S. R., Das, A., Alsoufi, M. S., Ibrahim, A. M. M., & Elsheikh, A. (2022). Machinability Investigation of Nitronic 60 Steel Turning Using SiAlON Ceramic Tools under Different Cooling/Lubrication Conditions. *Materials, 15*(7), 2368.

Rüstem, B., Süleyman, Y., & Süleyman, N. (2021). *Optimization of Machinability Parameters of S960QL Structural Steel by Finite Elements and Taguchi Method.* Paper presented at the Proceedings of the International Conference on Engineering Technologies (ICENTE'21)(Tam Metin Bildiri/Sözlü Sunum)(Yayın No: 7301857), Konya, Turkey.

Salur, E. (2022). Understandings the tribological mechanism of Inconel 718 alloy machined under different cooling/lubrication conditions. *Tribology International*, 107677.

Şirin, E., & Şirin, Ş. (2021). Investigation of the performance of ecological cooling/lubrication methods in the milling of AISI 316L stainless steel. *İmalat Teknolojileri ve Uygulamaları, 2*(1), 75-84.

Usca, Ü. A., Şap, S., Uzun, M., Kuntoğlu, M., Salur, E., Karabiber, A., . . . Wojciechowski, S. (2022). Estimation, optimization and analysis based investigation of the energy consumption in machinability of ceramic-based metal matrix composite materials. *journal of materials research and technology, 17*, 2987-2998.

Usca, Ü. A., Uzun, M., Kuntoğlu, M., Sap, E., & Gupta, M. K. (2021). Investigations on tool wear, surface roughness, cutting temperature, and chip formation in machining of Cu-B-CrC composites. *The International Journal of Advanced Manufacturing Technology, 116*(9), 3011-3025.

Usca, Ü. A., Uzun, M., Şap, S., Giasin, K., Pimenov, D. Y., & Prakash, C. (2022). Determination of machinability metrics of AISI 5140 steel for gear manufacturing using different cooling/lubrication conditions. *journal of materials research and technology, 21*, 893-904.

Yalçin G.,Neşeli S.,Terzioğlu H.,Ağaçayak A.C. (2019). Design and Construction of Compact CNC Router. International Conference on Engineering Technologies (ICENTE'19), 1(3), 474-478. (Tam Metin Bildiri/Sözlü Sunum)(Yayın No:5642081)

Yalçin G.,Neşeli S.,Terzioğlu H.,Ağaçayak A.C. (2018). Fatigue Tester Design and Frame Analysis for Estimation of Fatigue Life of Helical Compression Springs. International Conference on Engineering Technologies (ICENTE'1 8), 563-566. (Tam Metin Bildiri/Sözlü Sunum)(Yayın No:4509752)

YAĞMUR, S., & Muharrem, P. (2021). Ti-6Al-4V Titanyum Alaşımının Delinmesinde Ön Delik Uygulamasının İşlenebilirliğe Etkisinin İncelenmesi. *International Journal of Engineering Research and Development, 13*(1), 170-177.

YAĞMUR, S., & Muharrem, P. (2022). Al 6061/B4C/GNP Hibrit Kompozitin İşlenmesinde Takım Aşınma Davranışlarının İncelenmesi. *International Journal of Engineering Research and Development, 14*(2), 816-828.

Yaşar, N. (2019). Thrust force modelling and surface roughness optimization in drilling of AA-7075: FEM and GRA. *Journal of Mechanical Science and Technology, 33*(10), 4771-4781.

Yaşar, N., & Günay, M. (2019). Experimental investigation on novel drilling strategy of CFRP laminates using variable feed rate. *Journal of the Brazilian Society of Mechanical Sciences and Engineering, 41*(3), 1-12.

SELÇUK UNIVERSITY INTERNATIONAL

TECHNOLOGY AND INNOVATION

STUDENT SYMPOSIUM

24-27 NOVEMBER 2022 KONYA

Selçuk Üniversitesi Teknoloji Fakültesi Kampüs - KONYA
Selçuk Üniversitesi Müze Binası Kampüs - KONYA
Selçuk Üniversitesi Akşehir Mühendislik ve Mimarlık Fakültesi - Akşehir/KONYA

sutis.selcuk.edu.tr